Ground Improvement Design Services

Airport Way South Viaduct over
ARGO Railroad Yard
Seattle, Washington

for
City of Seattle Department of Transportation

August 15, 2012

GeoEngineers
Earth Science + Technology

Ground Improvement Design Services

Airport Way South Viaduct over ARGO Railroad Yard
Seattle, Washington

for
City of Seattle Department of Transportation

August 15, 2012

GeoEngineers

8410 154th Avenue NE
Redmond, Washington 98052
425.861.6000

Ground Improvement Design Services

Airport Way South Viaduct over ARGO Railroad Yard Project Seattle, Washington

File No. 0129-141-01

August 15, 2012

Prepared for:

City of Seattle Department of Transportation
c/o HNTB Corporation
600 108th Avenue NE, Suite 900
Bellevue, Washington 98004

Attention: Salima Hamlin, PE

Prepared by:

GeoEngineers, Inc.
8410 154th Avenue NE
Redmond, Washington 98052
425.861.6000

KING H. CHIN
STATE OF WASHINGTON
38761
REGISTERED
PROFESSIONAL ENGINEER

8/15/12

Heidi Disla

Heidi P. Disla, EIT
Geotechnical Engineer

Wenbin He, PE
Geotechnical Engineer

King H. Chin, PE
Associate

Shaun D. Stauffer, PE, LEEP AP
Principal

HPD:WBH:KHC:nlu

GEOENGINEERS

Table of Contents

Table of Contents (continued)

LIST OF FIGURES

Table of Contents (continued)

APPENDICES

INTRODUCTION

This report presents the results of our geotechnical design analyses completed to develop settlement mitigation ground improvement programs for the Airport Way South Viaduct over ARGO Railroad Yard project in Seattle, Washington.

The project site is located along Airport Way South between South Edmunds Street and South Lucile Street. The site is shown relative to surrounding physical features on the Vicinity Map, Figure 1. The project consists of replacing the north and south timber trestle approach structures with additional bridge spans and mechanically stabilized earth (MSE) fill approaches. The new bridge spans are currently designed to be supported on deep foundations.

The MSE fill approaches (North and South Approach) up to about 25 feet in height were designed to be supported on improved ground with compaction grouting techniques to mitigate the settlement induced by soil liquefaction during a design earthquake event. Construction associated with compaction grouting was started and completed within the eastern two-thirds of the North Approach area. Early return of the compaction grout occurred at depths ranging from less than 5 feet to more than 20 feet, resulting in highly variable and lower than expected grout volumes injected in the ground. In addition, excessive ground movements caused by the compaction grouting also posed a high risk of damaging the existing sensitive utilities at the project site. In order to achieve a more consistent ground improvement effect and to reduce the risk of damaging the existing sensitive utilities nearby, deep soil mixing (DSM) was identified as a more suitable method for the remaining area at the North Approach and the entire South Approach area.

The design of the DSM program was completed concurrently with the construction in order to minimize delays to the project schedule. This report presents the results of our engineering analyses completed and our recommendations of the alternate ground improvement program consisting of DSM columns with load transfer structural slabs. A separate as-built supplemental report that provides an evaluation of the as-built DSM columns was prepared to document the deviation from the design recommendations and the mitigation measures implemented.

REVIEW OF PREVIOUS GEOTECHNICAL REPORTS

We reviewed the geotechnical reports prepared for this project as presented below:

- Final Geotechnical Report, Plans, Specifications and Estimates Phase, Airport Way South Viaduct Over ARGO Railroad Yard, Seattle, Washington, prepared by Shannon & Wilson dated June 8, 2010.
- Supplemental Geotechnical Explorations and Geotechnical Report prepared by GeoEngineers dated May 18, 2012.

SUBSURFACE SOIL AND GROUNDWATER CONDITIONS

The subsurface soil conditions at the site were evaluated by reviewing the logs of exploratory borings and cone penetration test (CPT) probes completed near the existing North and South Approaches, and by reviewing the USGS geologic map of the area. The locations of the borings and CPTs completed at the North and South Approaches are shown on the Site Plans, Figures 2 and 3, respectively. We provided a detailed description of the subsurface soil and groundwater conditions in our May 18, 2012 report and will not present the information in this report for brevity.

Subsurface soils encountered at the site generally consisted of fill, alluvium, estuarine, beach and colluvium deposits overlying the Blakely formation (bedrock). The sections below present the generalized soil profiles developed for use in the design analysis for both the North and South Approaches.

North Approach

Figures 4 and 5 present the generalized subsurface soil profiles developed along the east and west sides of the North Approach embankment, respectively. Based on the CPT and boring information, the subsurface soils at the North Approach generally consist of 20 to 25 feet of loose to medium dense sand overlying 8 to 20 feet of medium stiff to stiff clayey silt. Bedrock was encountered at depths ranging from 22 feet to 42 feet. The bedrock was found to be dipping from east to west and from north to south within the North Approach embankment footprint. Groundwater was interpreted at depths ranging from 4 to 9 feet below the ground surface.

South Approach

Figures 6 and 7 present the generalized subsurface soil profiles developed along the east and west sides of the South Approach embankment, respectively. Based on the CPT and boring information, the subsurface soils at the South Approach generally consist of 25 to 40 feet of loose to medium dense sand overlying 20 to 45 feet of medium stiff to stiff clayey silt. Bedrock was encountered at depths ranging from 55 feet to 80 feet. The bedrock was found to be dipping from north to south within the South Approach embankment footprint. Groundwater was interpreted at depths ranging from 8 to 9 feet below the ground surface.

CONCLUSIONS AND RECOMMENDATIONS

Based on the results of our analyses, it is our opinion that the proposed DSM column with load transferring structural slab system can significantly lower the static settlement and mitigate liquefaction induced settlement under the design earthquake event. Figures 8 and 9 show the layout of the DSM columns developed for both the North and South Approaches, respectively.

The design of the DSM columns was completed to meet the design criteria developed by the project team, shown in Appendix A of this report. A summary of the results of the design analyses completed for the North and South Approaches is presented below:

North Approach

Static Conditions:

Embankment global stability factor of safety >	1.5
Embankment total static settlement =	0.6 inches
Embankment post-construction settlement =	0.3 inches
Unconfined compressive strength factor of safety >	3.0
End bearing capacity factor of safety >	3.0

Seismic Conditions:

Embankment global stability factor of safety >	1.1
Embankment post-liquefaction settlement =	1.1 inches
DSM Column unconfined compressive strength factor of safety >	2.0
End bearing capacity factor of safety >	2.0

South Approach

Static Conditions:

Embankment global stability factor of safety >	1.5
Embankment total static settlement =	1.4 inches
Embankment post-construction settlement =	0.7 inches
Unconfined compressive strength factor of safety >	3.0
End bearing capacity factor of safety >	3.0

Seismic Conditions:

Embankment global stability factor of safety >	1.1
Embankment post-liquefaction settlement =	1.4 inches
DSM Column unconfined compressive strength factor of safety ~	2.0
End bearing capacity factor of safety >	2.0

The results of our analyses show that all the design criteria, as presented in Appendix A, were fulfilled except the post-liquefaction settlement of both the North and South Approaches which exceed 1 inch, and the DSM column unconfined compression strength factor of safety at the South Approach is slightly less than 2.0. The total post-construction settlement (static plus post-liquefaction) was estimated to be about 2 inches; which fulfills the total post-construction settlement performance objective specified by City of Seattle Department of Transportation (SDOT). In addition, the seismic performance estimated for the North and South Approaches fulfills the collapse prevention objective per American Association of State Highway and Transportation Officials (AASHTO) design criteria. These results were discussed with the project team and third party peer reviewer during the design meetings and was concluded that no additional DSM columns were needed to reduce the post-liquefaction settlement to less than 1 inch.

The DSM column unconfined compressive strength factor of safety was computed to be slightly lower than 2.0. This factor of safety was calculated based on the average unconfined compressive strength of 300 psi. Based on the actual unconfined compressive strength test results, the average unconfined compressive strength achieved ranges from 537 psi to 677 psi, which is higher than 300 psi; hence, the actual factor of safety will exceed 2.0.

The following presents the details of our analyses completed for design of the DSM columns for both the North and South Approaches.

DSM COLUMNS DESIGN CONCEPT

The recommended DSM ground improvement system is similar to the conventional ground improvement system used for embankment on soft ground. The only difference is that the recommended DSM ground improvement system utilizes a reinforced concrete slab as the load distribution platform instead of a gravel layer. The design concept of the system is to utilize the reinforced concrete slab to distribute the load from the MSE walls to the DSM columns in a uniform manner and to more effectively engage the load resisting capacity of the DSM columns. This results in a more optimized design that requires less DSM columns and reduces the impact to the construction schedule.

Another important feature of the recommended DSM ground improvement system is the use of a load transfer gravel layer between the reinforced concrete slab and the DSM columns. One of the key functions of this load transfer gravel layer is to isolate the DSM columns from the reinforced concrete slab to minimize the transfer of shear forces from the MSE wall to the DSM columns, especially under seismic conditions. The high friction resistance of the gravel layer will also prevent the MSE wall from sliding under seismic conditions.

DSM COLUMNS DESIGN ANALYSES

General Approach

The DSM column design was completed by performing simplified engineering analyses and numerical modeling using the computer programs PLAXIS three-dimensional (3D) Foundation (PLAXIS b.v., 2012) and Fast Lagrangian Analysis of Continua (FLAC) 3D (Itasca, 2009). GeoEngineers modeled the DSM columns using the program PLAXIS 3D Foundation to evaluate the settlement induced by the embankment loads under static conditions. PLAXIS 3D Foundation is a 3D finite element program that can analyze the soil response and soil-structure interaction, including soil deformations and the 3D behavior of the transfer slab and embankment with the proposed DSM columns. We used the FLAC 3D V4.0 computer program to evaluate the performance of the North and South Approach embankments under the seismic (pseudo-static) conditions. FLAC 3D is a 3D explicit finite-difference program that can analyze the large strain, nonlinear soil response and soil-structure interaction during a seismic event.

The following outlines the DSM column design procedure used for both the North and South Approach embankments:

1. Develop PLAXIS 3D and FLAC 3D models that are representative of the soil profiles and embankments at the North and South Approaches.
2. Calibrate the soil parameters such that the associated settlement computed by the PLAXIS 3D and FLAC 3D models are consistent with the results of the simplified analysis for the unimproved ground conditions. The calibration process ensures that the DSM columns are designed to the appropriate loading conditions.
3. Calculate the anticipated settlement of the approach embankment by modeling the DSM column layout and concrete slab under both the static and seismic conditions using the computer programs PLAXIS 3D and FLAC 3D, respectively.
4. Complete LPILE analysis to check that the shear and moment sustained by the DSM columns does not exceed the shear and moment capacity of the DSM columns.
5. Complete bearing capacity analysis to check that the end bearing factor of safety meets the specified value in the design criteria.
6. Complete global stability analyses to verify that the required factor of safety under both the static and seismic conditions is met.

Simplified Engineering Analyses for Unimproved Conditions

Elastic and Consolidation Settlement

The elastic settlement analysis was completed based on the procedure developed by Schmertmann (1970). Based on the results of the analysis, the elastic settlement within the improved zone with the compaction grouting at the north approach is about ¼ inch, and within the unimproved zone is estimated to be about ⅜ inch. The elastic settlement within the proposed ground improvement limits for the unimproved conditions at the south approach is estimated to range between 1 to 2 inches.

The soft to medium stiff clayey silt layers (alluvium and estuarine deposits) are prone to consolidation settlement. These soils were encountered at depths ranging from 30 to 70 feet below the ground surface. Based on our consolidation settlement analyses and the planned roadway profiles, we estimate that the long term post-construction consolidation settlement due to the new embankment weights will be up to 2 inches at the south approach and less than 1 inch at the north approach. These estimates are for the unimproved conditions at both approaches.

The results of our analyses indicate that the total static settlement (elastic and consolidation) under the proposed embankment loads for the unimproved conditions is less than 1.5 inches for the north approach and up to 4.0 inches for the south approach.

Liquefaction Analyses

Soil liquefaction refers to the condition by which vibration or shaking of the ground, such as from earthquake forces, results in the development of excess pore pressure in saturated soils with subsequent loss of strength. In general, soils that are susceptible to liquefaction at this site include very loose to medium dense, clean to silty sands and non-plastic silts that are below the water table. The evaluation of liquefaction potential is complex and dependent on numerous parameters, including soil type, grain-size distribution, soil density, depth to groundwater, in-situ static ground stresses, earthquake-induced ground stresses and excess pore water pressure generated during seismic shaking.

We evaluated liquefaction potential of the site soils for the 2009 AASHTO design earthquake event using the supplemental subsurface data and information obtained from the CPTs. We evaluated liquefaction potential using the simplified method proposed by Youd et al (2001). The seismic design parameters used in our liquefaction analyses are consistent with that recommended and developed by Shannon & Wilson (2010) and are provided in Table 1 below.

TABLE 1. SEISMIC DESIGN PARAMETERS FOR LIQUEFACTION ANALYSIS

Design Earthquake	Magnitude	Ground Surface Peak Ground Acceleration (g)
AASHTO Event (975-year return period)	6.8	0.47

Based on our analyses, the site soils are highly susceptible to liquefaction under the AASHTO design earthquake event. The results of our analysis indicate that at the south approach approximately 6 to 12 inches of liquefaction-induced settlement may occur after a design earthquake, and approximately 4 to 6 inches of liquefaction-induced settlement may be expected at the north approach. These estimates are for no ground improvement below the approach areas, which can be expected for the areas without ground improvement.

We also completed engineering analyses to estimate the downdrag forces on the DSM columns as a result of liquefaction. Based on the boring and CPT data, we estimated that the average residual strength of the liquefied soils is about 500 pounds per square foot (psf); this results in an average downdrag force of 4.7 kips per foot of DSM column within the liquefiable soil zone.

Soil Profiles and Design Parameters

Based on the CPT data we collected within the approach embankments, we interpret general subsurface conditions at the North and South Approaches as summarized in Tables 2 and 3 below. These interpreted soil profiles were used in our engineering analyses and numerical modeling completed for this project.

TABLE 2. INTERPRETED SUBSURFACE SOIL PROFILE – NORTH APPROACH

Thickness (feet)	Soil Type	Consistency
8 - 9	Silty Sand with occasional gravel	Loose to Medium Dense
20 - 25	Silty Sand	Loose to Medium Dense
8 - 20	Clayey Silt	Medium Stiff to Stiff
-	Bedrock (Blakely Formation)[a]	Very Dense

Notes:

a. The Bedrock is encountered at depths ranging from 25 feet to 42 feet dipping from east to west and north to south within the North Approach embankment footprint.

TABLE 3. INTERPRETED SUBSURFACE SOIL PROFILE – SOUTH APPROACH

Thickness (feet)	Soil Type	Consistency
8 - 9	Silty Sand with occasional gravel	Loose to Medium Dense
25 - 40	Silty Sand	Loose to Medium Dense
20 - 45	Clayey Silt	Medium Stiff to Stiff
4 - 5	Silty Sand/Stiff Sandy Silt	Dense to Very Dense
-	Bedrock (Blakely Formation)[a]	Very Dense

Notes:

a. The Bedrock is encountered at depths ranging from 55 feet to 80 feet dipping north to south within the South Approach embankment footprint.

Based on the subsurface data collected and the results of our simplified engineering analysis, we developed the representative engineering properties of the soil units under the static and seismic conditions. Tables 4 and 5 provide the soil properties used in the slope stability analyses and numerical modeling completed for the project for the North and South Approaches, respectively.

TABLE 4. SOIL PARAMETERS – NORTH APPROACH

Soil Unit	Unit Weight (pcf)	Shear Strength	Modulus of Elasticity (ksf)
Sand (above GWT)	125	$\phi=38^o$, c=0 psf	800
Sand (below GWT)	120	$\phi=36^o$, c=0 psf (Static) $\phi=0^o$, c=500 psf (Liquefied)[a]	600 (Unimproved) 1,000 (Improved)[d] 120 (Liquefied)[e]
Clayey Silt	100	$\phi=0^o$, c=750 psf (Unimproved)[b] $\phi=0^o$, c=1400 psf (Improved)[c]	1,200 (Unimproved) 1,500 (Improved)[d]
Rock	135	$\phi=0^o$, c=10,000 psf	–

Notes:

a. The residual shear strength of the liquefiable layer is determined using the correlation between equivalent clean sand SPT blowcounts (N1)60-CS and residual undrained shear strength (Seed and Harder, 1990).

b. The undrained shear strength of the clay is determined using the correlation: $(q_t - \sigma_{vo}) / N_{kt}$, where q_t = cone tip penetration resistance, σ_{vo} = vertical stress and N_{kt} = 15.

c. The improved (compaction grouting) shear strength was calculated based on undrained shear strength of the compaction grout = 50 psi.

d. The improved (compaction grouting) modulus of elasticity was calculated as the weighted average value of the modulus of elasticity of the compaction grout of 300 x q_u = 4320 ksf, and the modulus of elasticity of the soil.

e. The liquefied Modulus of Elasticity was backcalculated using the liquefaction induced settlement simplified method analysis results.

TABLE 5. SOIL PARAMETERS – SOUTH APPROACH

Soil Unit	Unit Weight (pcf)	Shear Strength	Modulus of Elasticity (ksf)
Sand (above GWT)	125	ϕ=38°, c=0 psf	1,000
Sand (below GWT)	120	ϕ=36°, c=0 psf (Static) ϕ=0°, c=500 psf (Liquefied)[a]	800 (Static) 120 (Liquefied)[c]
Clayey Silt	100	ϕ=0°, c=750 psf[b]	250
Silty Sand	115	ϕ=36°, c=0 psf	1,300
Rock	135	ϕ=0°, c=10,000 psf	–

Notes:

a. The residual shear strength of the liquefiable layer is determined using the correlation between equivalent clean sand SPT blowcounts (N1)60-CS and residual undrained shear strength (Seed and Harder, 1990).

b. The undrained shear strength of the clay is determined using the correlation: $(q_t - \sigma_{vo}) / N_{kt}$, where q_t = cone tip penetration resistance, σ_{vo} = vertical stress and N_{kt} = 15.

c. The liquefied Modulus of Elasticity was backcalculated using the liquefaction induced settlement simplified method analysis results.

DSM Columns and Structural Slab

The DSM column properties were determined using the results of the unconfined compressive strength laboratory tests and the plate load test. Filz et al (2005) presents the relationship between Young's Modulus, E, and the unconfined compression strength, q_u, to range between 75 and 1,000. Based on the results of the unconfined compressive strength tests performed on the DSM column core samples, we estimated the DSM column stiffness to be about 190 q_u. Two plate load tests were also completed, one at each approach, and the DSM column stiffness was back-calculated to be range from 500 to 1,000 q_u. Based on the results of the laboratory tests and plate load tests, we completed our numerical modeling assuming a DSM column stiffness of 150 q_u and 500 q_u to account for the uncertainties associated with the DSM column stiffness.

The structural slab properties were determined using the ACI semi-empirical equations for static conditions, this assumes that the slab remains elastic (uncracked conditions). For seismic conditions, we used 50 percent of the static modulus (cracked conditions) based on discussions with the project team. Table 6 below presents the DSM column and structural slab properties used in our analyses.

TABLE 6. DSM COLUMN AND STRUCTURAL SLAB PROPERTIES

Element	Unit Weight - γ (pcf)	Unconfined Compressive Strength - q_u (psi)	Modulus of Elasticity – E (ksf)
DSM Columns	125	300	6,480[a] – 21,600[b]
Structural Slab	150	4,000	519,119.5[c]

Notes:

a. The modulus of elasticity for the DSM columns was calculated based on the results of the unconfined compressive strength tests and the plate load test. The lower bound was assumed as $150q_u$.

b. The modulus of elasticity for the DSM columns was calculated based on the results of the unconfined compressive strength tests and the plate load test. The upper bound was assumed as $500q_u$.

c. The structural slab modulus was calculated based on the ACI semi-empirical equation: $57000\sqrt{q_u}$.

Traffic Surcharge

The traffic surcharge is modeled as 250 psf in our slope stability analysis and numerical modeling. We included the traffic surcharge in the design analysis for both the static and seismic conditions, which is conservative for the seismic conditions.

NORTH APPROACH

PLAXIS 3D Model – Static Conditions

Numerical analysis was completed to evaluate the performance of the ground improvement system under the static conditions using the computer PLAXIS 3D. Figure 10 shows the PLAXIS 3D model developed for the North Approach, with DSM columns within the ground improvement limits. As shown in Figure 10, all DSM columns at the North Approach will be tipped into the bedrock.

PLAXIS 3D Model Calibration

The Plaxis 3D model for the north approach was calibrated using the results of our simplified analysis. The embankment load and traffic surcharge were applied directly on the unimproved soils. Figure 11 shows the static settlement computed under the dead load plus traffic surcharge load for the north approach. As shown in Figure 11, the maximum computed total settlement under the static conditions generally ranges from 1 to 1.2 inches, and is consistent with the estimated total static settlement calculated using the simplified engineering analysis.

PLAXIS 3D Results

Figure 12 shows the settlement contours of the slab under the static loading conditions with the proposed DSM columns installed. The results show that the proposed DSM columns and slab system reduces the maximum total static settlement from 1.2 inches to 0.6 inch, which is less than the specified 1-inch criteria. We estimated that half of the total static settlement would occur right after the embankment is constructed, hence, the expected post-construction static settlement at the North Approach is estimated to be less than 0.3 inches. Figures 13 through 18 present the slab forces calculated under the static loading conditions for use in the structural design completed by HNTB, the project structural engineer.

Figure 19 presents the resultant lateral deflection (vector sum of the lateral deflection in transverse and longitudinal directions) of the DSM columns under the static loading conditions for Zones 1 and 2. Figure 20 presents the calculated axial forces at the top of the DSM columns under the static loading conditions. As presented in Figure 20, the average axial force of the DSM columns under the static loading conditions is computed to be about 80 kips. The average factor of safety under the static loading conditions is at least 3.0. The maximum axial force of the DSM columns under the static loading conditions is computed to be about 155 kips.

FLAC 3D Model

Numerical analysis was completed to evaluate the performance of the ground improvement system under the pseudo-static conditions using the computer FLAC 3D. Figure 21 shows the FLAC 3D model developed for the North Approach, with DSM columns within the ground improvement limits.

FLAC 3D Model Calibration – Liquefied Conditions

The FLAC 3D model for the north approach was calibrated using the results of our simplified liquefaction analysis. The embankment load and traffic surcharge were modeled as a soil mass applied directly on the unimproved soils. Figure 22 shows the settlement contours calculated by FLAC 3D for the liquefied conditions (no ground improvement). As shown in Figure 22, the maximum computed total settlement under the liquefied conditions generally ranges from 2 to 6.5 inches, and is consistent with the estimated liquefaction induced settlement calculated using the simplified engineering analysis.

FLAC 3D Results

Liquefied Conditions

Figure 23 shows the settlement contours of the slab under the liquefied conditions (DSM Young's Modulus=150q_u and 500q_u). The results show that the proposed DSM columns and slab system reduces the maximum liquefied induced settlement from 6.5 inches to about 1.1 inches. The post-earthquake settlement is higher than the specified 1 inch criteria. However, the total post-construction settlement (static plus liquefied) is estimated to be about 1.4 inches, which is lower that the total specified post-construction settlement of 2.0 inches.

Figures 24 and 25 present the resultant lateral deflection (vector sum of the lateral deflection in transverse and longitudinal direction) of the DSM columns under the liquefied conditions for Zones 1 and 2, respectively. Figure 26 presents the maximum calculated axial forces in the DSM columns under the liquefied loading conditions for various zones. As presented in Figure 26, the average maximum axial force of the DSM columns for DSM Young's Modulus of 150q_u and 500q_u under the liquefied conditions is computed to be about 100 kips and 150 kips, respectively. The average factor of safety of the compressive strength of the DSM columns under the liquefied conditions is about 2.1 to 3.0. The maximum value of the maximum axial force of the DSM columns for DSM Young's Modulus of 150q_u and 500q_u under the liquefied loading conditions is computed to be about 140 kips and 230 kips, respectively.

Earthquake Conditions

The effect of the seismic load to the DSM axial load is evaluated by multiplying the maximum static axial load by an amplification factor calculated based on the applied normal foundation force and the overturning moment resulting from the earthquake loading. Table 7 below presents the calculated adjustment factors for different seismic coefficients for the highest embankment section and the estimated maximum axial force of the DSM columns.

TABLE 7. ADJUSTMENT FACTOR BY OVERTURNING MOMENT AND ESTIMATED MAXIMUM DSM AXIAL FORCES

Seismic Coefficient	Load Amplification Factor (1+6e/B, e = M/P)	Estimated Maximum Axial Load (kips)	Estimated Adjusted Max Axial Load (kips)
0.23g	1.35	155	209

We also completed pseudostatic analyses using the computer program FLAC 3D with a design seismic coefficient of 0.23 g, which was the seismic coefficient used in design of the compaction grouting program. Figure 27 present the maximum axial forces calculated for DSM columns located in various zones within the North Approach. As shown in Figure 27, the FLAC analyses results are generally consistent with the results calculated using the simplified analysis method as presented in Table 7 above.

LPile Results

In order to evaluate the shear and moment of the DSM columns, LPILE analyses were completed to induce the maximum deflected shape presented in Figure 28 for the static loading conditions and in Figure 29 for the earthquake conditions. The results indicate that the maximum shear and moment calculated is less than the shear and moment capacity of the DSM columns.

DSM Column End Bearing Factor of Safety

The most critical case in terms of DSM column end bearing factor of safety is identified to be the liquefied case where additional downdrag loads will need to be resisted by the side friction of the DSM columns within the non-liquefiable silt and by the end bearing of the DSM columns on the bedrock. As presented in Table 2 above, the average thicknesses of liquefiable soils and the nonliquefiable silt are 22 and 14 feet, respectively. Using the residual strength of liquefiable soils of 500 psf and the undrained shear strength of the silt of 750 psf, we estimate that the downdrag forces will mostly be resisted by the side friction of the DSM columns within the silt. The axial force that results from the weight of the approach embankment under the liquefied conditions (shown in Figure 26) will need to be resisted by the end bearing of the DSM columns on bedrock. Based on our analyses, the factor of safety of the DSM columns end bearing capacity is at least 3.0.

Global Stability Analyses

Global stability analyses were completed using the computer program SLOPE/W (GEO-SLOPE International, Ltd., 2005). SLOPE/W evaluates the stability of the critical failure surfaces identified using vertical slice limit-equilibrium methods. This method compares the ratio of forces driving slope movement with forces resisting slope movement for each trial failure surface, and presents the result as the FS. Based on our analyses, we conclude that the factor of safety of global stability is significantly higher than 1.5 and 1.1 for the static and seismic conditions, respectively.

SOUTH APPROACH

PLAXIS 3D Model – Static Conditions

Numerical analysis was completed to evaluate the performance of the ground improvement system under the static conditions using the computer PLAXIS 3D. Figure 30 shows the PLAXIS 3D model developed for the South Approach, with DSM columns within the ground improvement limits. As shown in Figure 30, the DSM columns within approximately the northern 2/3 of the ground improvement footprint at the South Approach will be tipped into the bedrock. The DSM columns within approximately the southern ⅓ of the ground improvement footprint will be limited to 75 feet long and will not be embedded in the bedrock.

PLAXIS 3D Model Calibration

The Plaxis 3D model for the south approach was calibrated using the results of our simplified analysis. The embankment load and traffic surcharge were applied directly on the unimproved soils. Figure 31 shows the static settlement computed under the dead load plus traffic surcharge load for the south approach. As shown in Figure 31, the maximum computed total settlement under the static conditions is approximately 4.7 inches, and is generally consistent with the estimated total static settlement calculated using the simplified engineering analysis.

PLAXIS 3D Results

Figure 32 shows the settlement contours of the slab under the static loading conditions with the proposed DSM columns installed (DSM Young's Modulus=150q_u and 500q_u). The results show that the proposed DSM columns and slab system reduces the maximum total static settlement from 4.7 inches to 1.4 inches. We estimated that half of the total static settlement would occur immediately after the embankment is constructed, hence, the expected post-construction static settlement at the South Approach is estimated to be less than 0.7 inches. Figures 33 through 38 present the slab forces calculated under the static loading conditions for use in the structural design completed by HNTB, the project structural engineer.

Figures 39 through 44 present the resultant lateral deflection (vector sum of the lateral deflection in transverse and longitudinal directions) of the DSM columns under the static loading conditions for various zones. Figure 45 presents the calculated axial forces at the top of the DSM columns under the static loading conditions for various zones. As presented in Figure 45, the average axial force of the DSM columns for DSM Young's Modulus of 150q_u and 500q_u under the static loading conditions is computed to be about 70 kips and 120 kips, respectively. The average factor of safety under the static loading conditions is at least 3.0. The maximum axial force of the DSM columns for DSM Young's Modulus of 150q_u and 500q_u under the static loading conditions is computed to be about 125 kips and 220 kips, respectively.

FLAC 3D Model

Numerical analysis was completed to evaluate the performance of the ground improvement system under the seismic conditions using the computer FLAC 3D. Figure 46 shows the FLAC 3D model developed for the South Approach, with DSM columns within the ground improvement limits.

FLAC 3D Model Calibration – Liquefied Conditions

The FLAC 3D model for the south approach was calibrated using the results of our simplified liquefaction analysis. The embankment load and traffic surcharge were applied directly on the unimproved soils and attached Figure 47 shows the settlement contours calculated by FLAC 3D for the liquefied conditions (no ground improvement). As shown in Figure 47, the maximum computed total settlement under the liquefied conditions generally ranges from 5 to 10.8 inches, and is consistent with the estimated liquefaction induced settlement calculated using the simplified engineering analysis.

FLAC 3D Results

Liquefied Conditions

Figure 48 shows the settlement contours of the slab under the liquefied conditions (DSM Young's Modulus=150q_u and 500q_u). The results show that the proposed DSM and slab system reduces the maximum liquefied induced settlement from 10.8 inches to about 1.4 inches.

Figures 49 and 54 present the resultant lateral deflection (vector sum of the lateral deflection in transverse and longitudinal direction) of the DSM columns under the liquefied conditions for various zones. Figure 55 presents the maximum calculated axial forces in the DSM columns under the liquefied loading conditions in various zones. As presented in Figure 55, the average maximum axial force of the DSM columns for DSM Young's Modulus of 150q_u and 500q_u under the liquefied conditions is computed to be about 165 kips and 200 kips, respectively. The average factor of safety of the compressive strength of the DSM columns under the liquefied conditions is about 1.6 to 1.9. The maximum value of the maximum axial force of the DSM columns for DSM Young's Modulus of 150q_u and 500q_u under the liquefied loading conditions is computed to be about 230 kips and 280 kips, respectively.

Earthquake Conditions

The effect of the seismic load to the DSM axial load is evaluated by multiplying the maximum static axial load by an amplification factor calculated based on the applied normal foundation force and the overturning moment resulted from the earthquake loading. Table 8 below presents the calculated adjustment factors for different seismic coefficients and the highest embankment section and the estimated maximum axial force of the DSM columns.

TABLE 8. ADJUSTMENT FACTOR BY OVERTURNING MOMENT AND ESTIMATED MAXIMUM DSM AXIAL FORCES

Seismic Coefficient	Load Amplification Factor (1+6e/B, e = M/P)	Estimated Maximum Axial Load (kips)	Estimated Adjusted Max Axial Load (kips)
0.23g	1.35	125 (150q_u) 220 (500q_u)	169 (150q_u) 297 (500q_u)

We also completed pseudostatic analyses using the computer program FLAC 3D with a design seismic coefficient of 0.23 g, which was the seismic coefficient used in design of the compaction grouting program. Figure 56 presents the maximum axial forces calculated for DSM columns located in various zones within the South Approach. As shown in Figure 56, the FLAC analyses results are generally consistent with the results calculated using the simplified analysis method as presented in Table 8 above.

LPile Results

In order to evaluate the shear and moment of the DSM columns, LPILE analyses were completed to induce the maximum deflected shape presented in Figure 57 for the static loading conditions and in Figure 58 for the earthquake conditions. The results indicate that the maximum shear and moment calculated is less than the shear and moment capacity of the DSM columns.

DSM Column End Bearing Factor of Safety

The most critical case in terms of DSM column end bearing factor of safety is identified to be the liquefied case where additional downdrag loads will need to be resisted by the side friction of the DSM columns within the non-liquefiable silt and by the end bearing of the DSM columns on the bedrock. As presented in Table 3 above, the average thicknesses of liquefiable soils and the nonliquefiable silt are about 33 feet. Using the residual strength of liquefiable soils of 500 psf and the undrained shear strength of the silt of 750 psf, we estimate that the downdrag forces will be resisted by the side friction of the DSM columns within the silt. A portion of the axial force that results from the weight of the approach embankment under the liquefied conditions (shown in Figure 55) will need to be resisted by the end bearing of the DSM columns on bedrock. Based on our analyses, the factor of safety of the DSM columns end bearing capacity is at least 3.0.

Global Stability Analyses

Global stability analyses were completed using the computer program SLOPE/W (GEO-SLOPE International, Ltd., 2005). SLOPE/W evaluates the stability of the critical failure surfaces identified using vertical slice limit-equilibrium methods. This method compares the ratio of forces driving slope movement with forces resisting slope movement for each trial failure surface, and presents the result as the FS. Based on our analyses, we conclude that the factor of safety of global stability is significantly higher than 1.5 and 1.1 for the static and seismic conditions, respectively.

LIMITATIONS

We have prepared this report for SDOT, HNTB, their authorized agents and regulatory agencies for the Airport Way South Viaduct over ARGO Railroad Yard project.

Within the limitations of scope, schedule and budget, our services have been executed in accordance with generally accepted practices for geotechnical engineering in this area at the time this report was prepared.

Any electronic form, facsimile or hard copy of the original document (email, text, table, and/or figure), if provided, and any attachments should be considered a copy of the original document. The original document is stored by GeoEngineers, Inc. and will serve as the official document of record.

Please refer to Appendix B titled “Report Limitations and Guidelines for Use” for additional information pertaining to use of this report.

REFERENCES

Baez, J. I. and Martin, G. R. (1993). “Advances in the Design of Vibro Systems for the Improvement of Liquefaction Resistance,” *Proceedings of the 7th Annual Symposium of Ground Improvement*, 1-16.

Filz, Dr. G.M., Duncan, Dr. J.M., Gutierrez, Dr. M.S., Kriz, Dr. R.D., Singh, Dr. M.P. 2005. "Stability of Embankments Founded on Soft Soil Improved with Deep-Mixing-Method Columns." Navin, M.P. *Dissertation submitted to the faculty of the Virginia Polytechnic and State University in partial fulfillment of the requirements for the degree of Doctor of Philosophy in Civil and Environmental Engineering.*

GeoEngineers, Inc (2012). "Supplemental Geotechnical Explorations and Geotechnical Report, Airport Way South Viaduct over ARGO Railroad Yard, Seattle, Washington."

GEO-SLOPE International, Ltd. (2005). "Slope/W" Version 6.17.

Itasca, 2009. Itasca Consulting Group, Inc. Fast Lagrangian Analysis of Continua (FLAC).

Idriss, I.M., and Boulanger R.W. (2008). "Soil Liquefaction During Earthquakes," Earthquake Engineering Research Institute EERI Monograph MNO-12, Oakland, California.

Imai, T. and Tonouchi, K. (1982). "Correlation of N-value with S-wave velocity and shear modulus," Proceedings, 2nd European Symposium on Penetration Testing, Amsterdam, pp. 57-72.

International Building Code (2009): International Code Council, Sec. 1613, 2006.

Mayne, P. (2007). "Cone Penetration Testing, A Synthesis of Highway Practice," National Cooperative Highway Research Program, NCHRP Synthesis 368, Washington D.C.

Plaxis bv, 2012. Plaxis. PLAXIS 3D software package.

Schmertmann, J. 1970. Static cone to compute static settlement over sand. *Journal of Soil Mechanics and Foundation Division*, American Society for Civil Engineers, vol. 96, pp 1011–1043.

Seed, H. B., Wong, R.T., Idriss, I.M., and Tokimatsu, K. (1986). "Moduli and Damping Factors for Dynamic Analysis of Cohesionless Soils," Journal of Geotechnical Engineering, ASCE, Vol. 112, No. 11, November, pp. 1016-1032.

Shannon & Wilson (2010). "Final Geotechnical Report, Plans, Specifications and Estimates Phase, Airport Way South Viaduct Over ARGO Railroad Yard, Seattle, Washington."

Washington State Department of Transportation Geotechnical Design Manual (2012). April 2012 revision package M 46-03.07.

Youd, T.L., Idriss, I.M., Andrus R.D., Arango, I., Castro, G., Christian, J.T., Dobry, R., Finn, W.D.L., Harder, L.F. Jr., Hynes, M.E., Ishihara, K., Koester, J.P., Liao, S.S.C., Marcuson, W.F. III., Martin, G.R., Mitchell, J.K., Moriwaki, Y., Power, M.S., Robertson, P.K., Seed, R.B., and Stokoe, K.H. II. 2001. "Liquefaction Resistance of Soils: Summary Report from the 1996 NCEER and 1998 NCEER/NSF Workshops on Evaluation of Liquefaction Resistance of Soils." J. Geotech. Geoenviron. Eng. 127, 817.

FIGURES

GeoEngineers

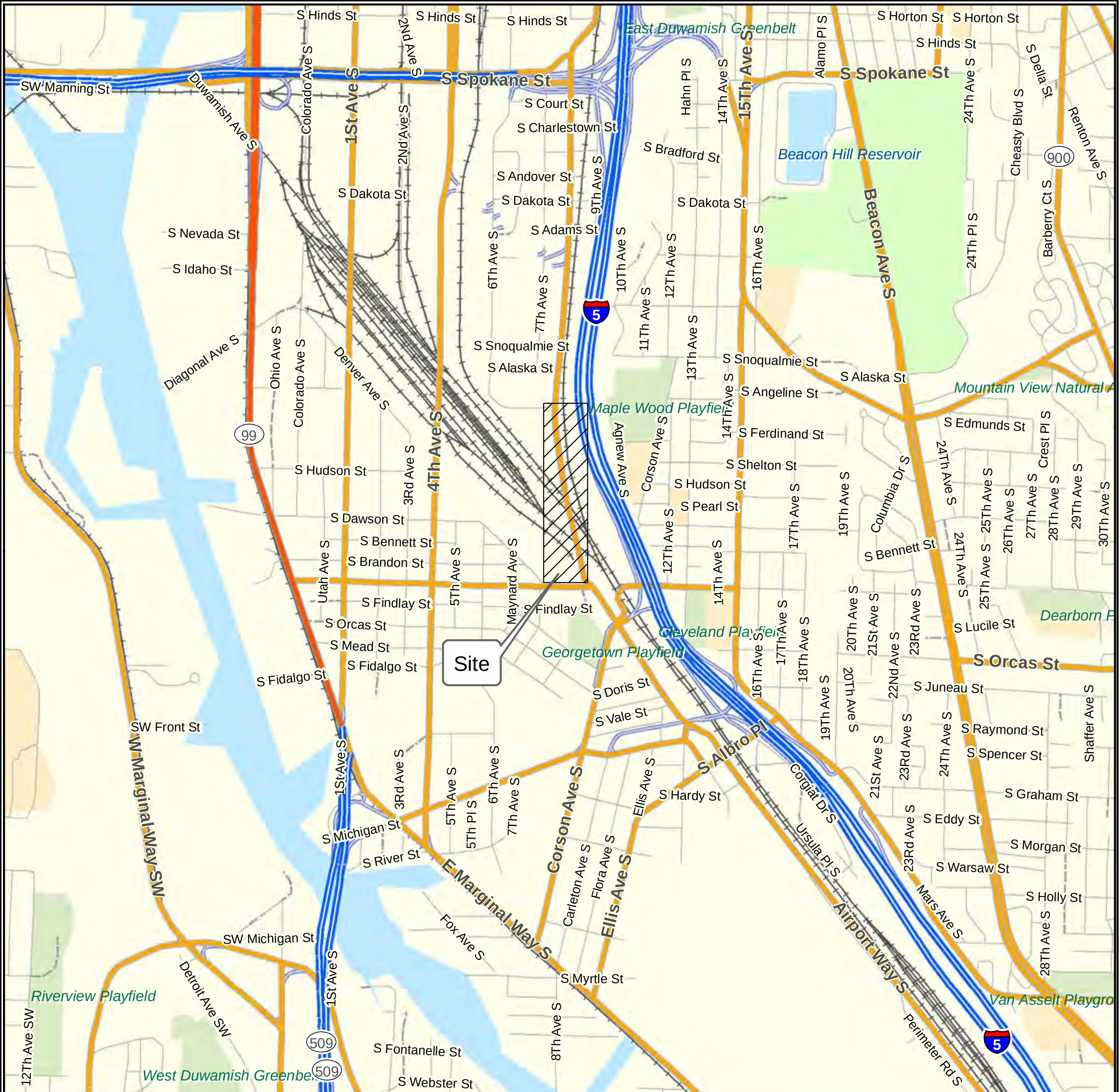

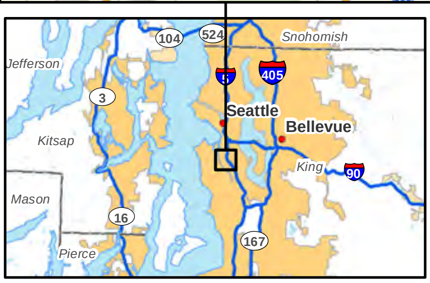

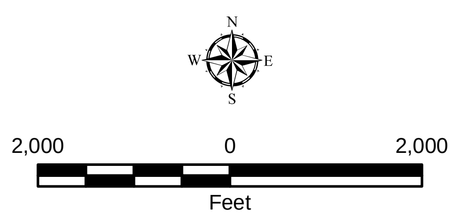

Notes:
1. The locations of all features shown are approximate.
2. This drawing is for information purposes. It is intended to assist in showing features discussed in an attached document. GeoEngineers, Inc. cannot guarantee the accuracy and content of electronic files. The master file is stored by GeoEngineers, Inc. and will serve as the official record of this communication.
3. It is unlawful to copy or reproduce all or any part thereof, whether for personal use or resale, without permission.

Data Sources: ESRI Data & Maps, Street Maps 2005

Transverse Mercator, Zone 10 N North, North American Datum 1983
North arrow oriented to grid north

Vicinity Map

Airport Way South Viaduct over ARGO Railroad Yard
Seattle, Washington

GeoEngineers

Figure 1

Office: Redmond Path: \\red\projects\0\0129141\GIS\012914100_F1_VicinityMap.mxd Map Revised: April 25, 2012 EL

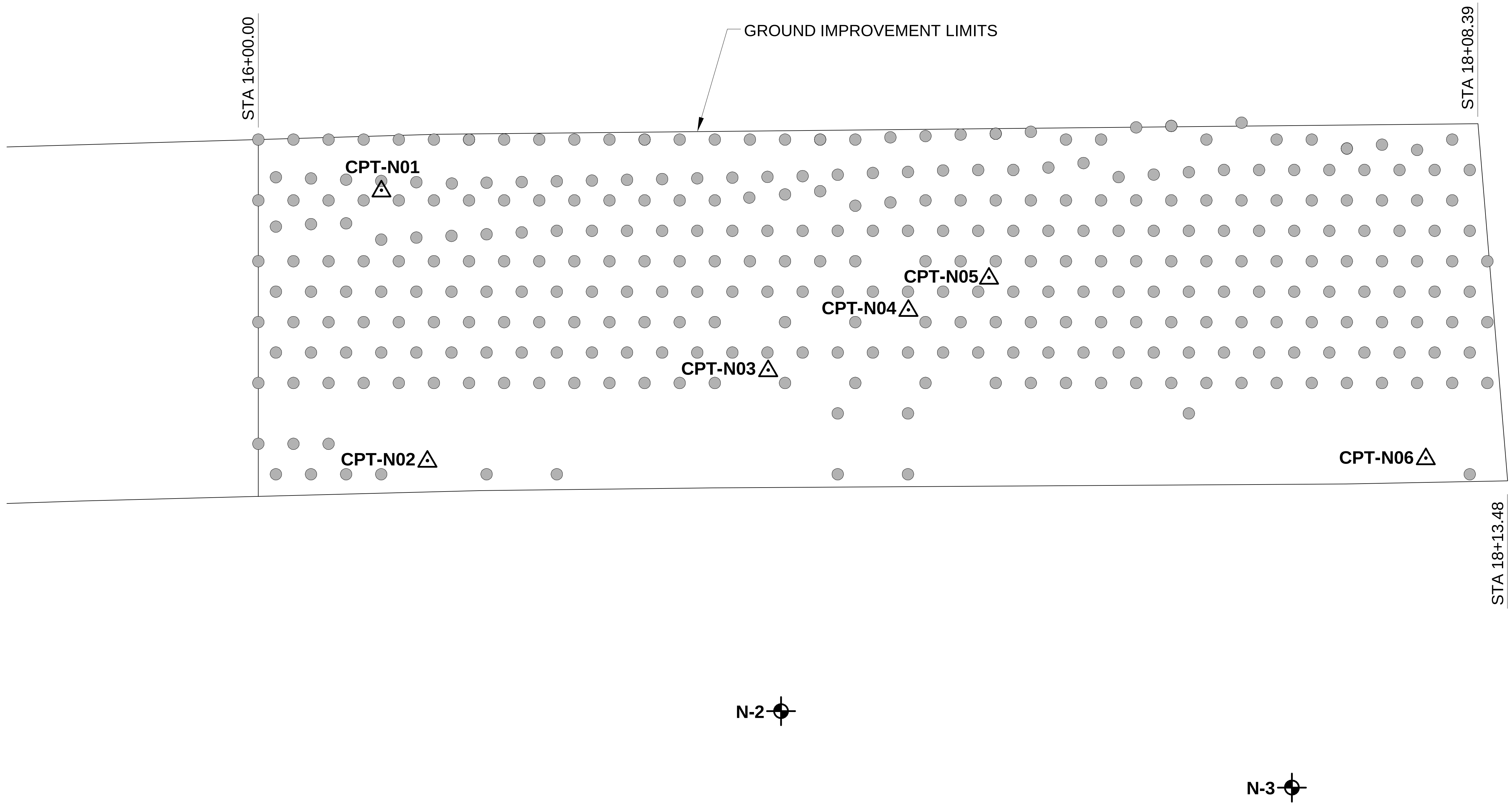

Notes

1. The locations of all features shown are approximate.
2. This drawing is for information purposes. It is intended to assist in showing features discussed in an attached document. GeoEngineers, Inc. cannot guarantee the accuracy and content of electronic files. The master file is stored by GeoEngineers, Inc. and will serve as the official record of this communication.

Reference: GeoEngineers staff sketch.

Legend

Compaction Grouting Column Installed

CPT-N01 Cone Penetration Test by GeoEngineers, April 2012

N-2 Boring by Shannon & Wilson, June 2010

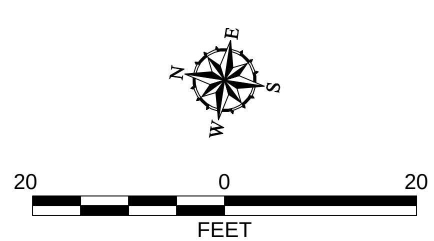

Site Plan - North Abutment

Airport Way South Viaduct
over ARGO Railroad Yard
Seattle, Washington

GEOENGINEERS

Figure 2

W:\REDMOND\PROJECTS\0\0129141\00\CAD\0129141-00 SITE PLAN.DWG\TAB:NORTH ABUTMENT MODIFIED BY TMICHAUD ON APR 30, 2012 - 15:42

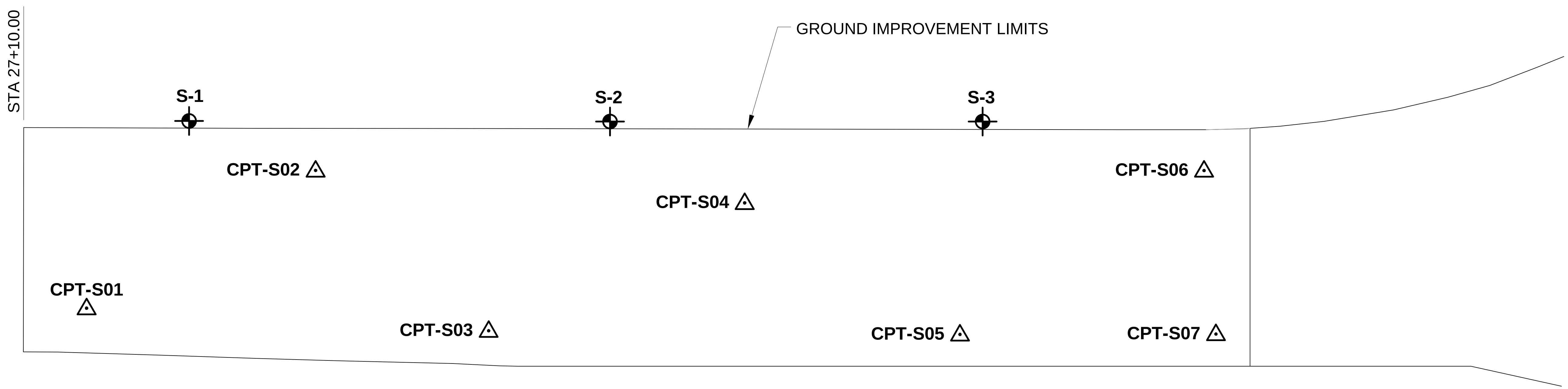

Notes

1. The locations of all features shown are approximate.
2. This drawing is for information purposes. It is intended to assist in showing features discussed in an attached document. GeoEngineers, Inc. cannot guarantee the accuracy and content of electronic files. The master file is stored by GeoEngineers, Inc. and will serve as the official record of this communication.

Reference: GeoEngineers staff sketch.

Legend

CPT-S01 — Cone Penetration Tests by GeoEngineers, April 2012

S-1 — Boring by Shannon & Wilson, June 2010

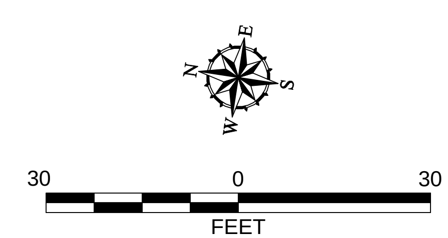

Site Plan - South Abutment

Airport Way South Viaduct
over ARGO Railroad Yard
Seattle, Washington

GEOENGINEERS

Figure 3

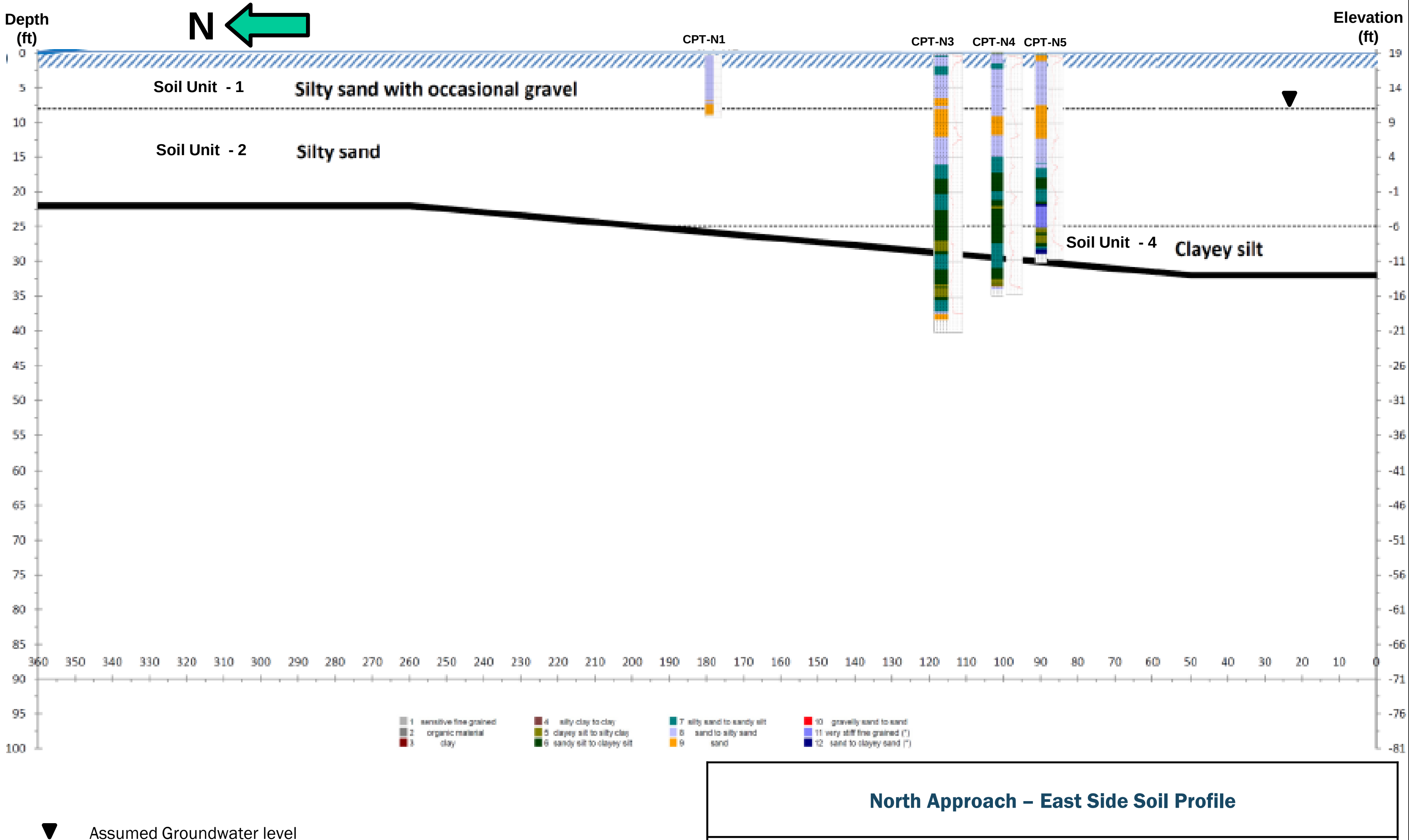

North Approach – East Side Soil Profile

Airport Way South Viaduct over ARGO Railroad Yard project
Seattle, Washington

GeoEngineers

Figure 4

http://projects/sites/0012914101/Draft\0129-141-01_DSM_Design_Figures.ppt WBH:hpd:khc:sds 07/05/2012

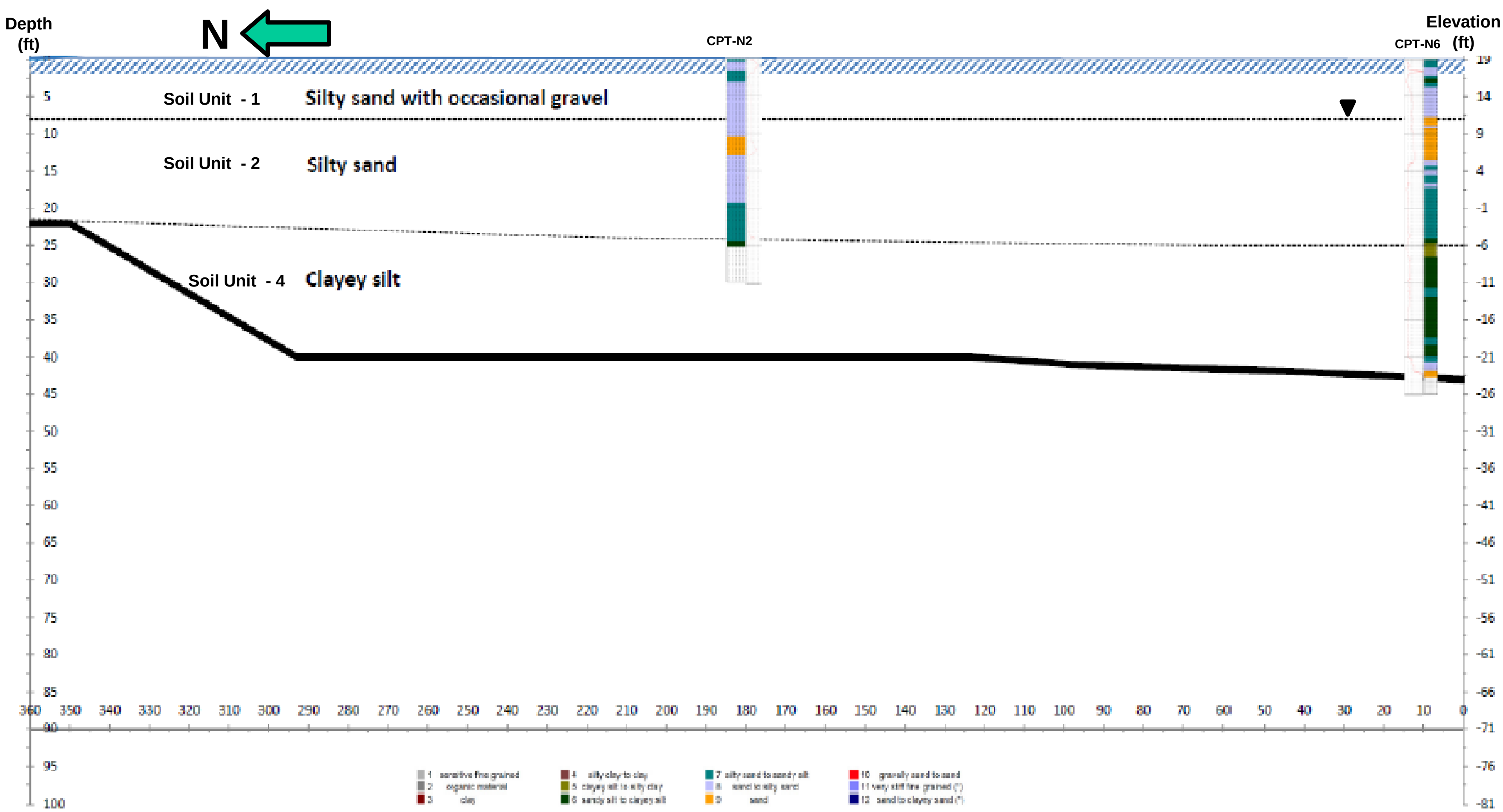

▼ Assumed Groundwater level

North Approach – West Side Soil Profile

Airport Way South Viaduct over ARGO Railroad Yard project
Seattle, Washington

GEOENGINEERS

Figure 5

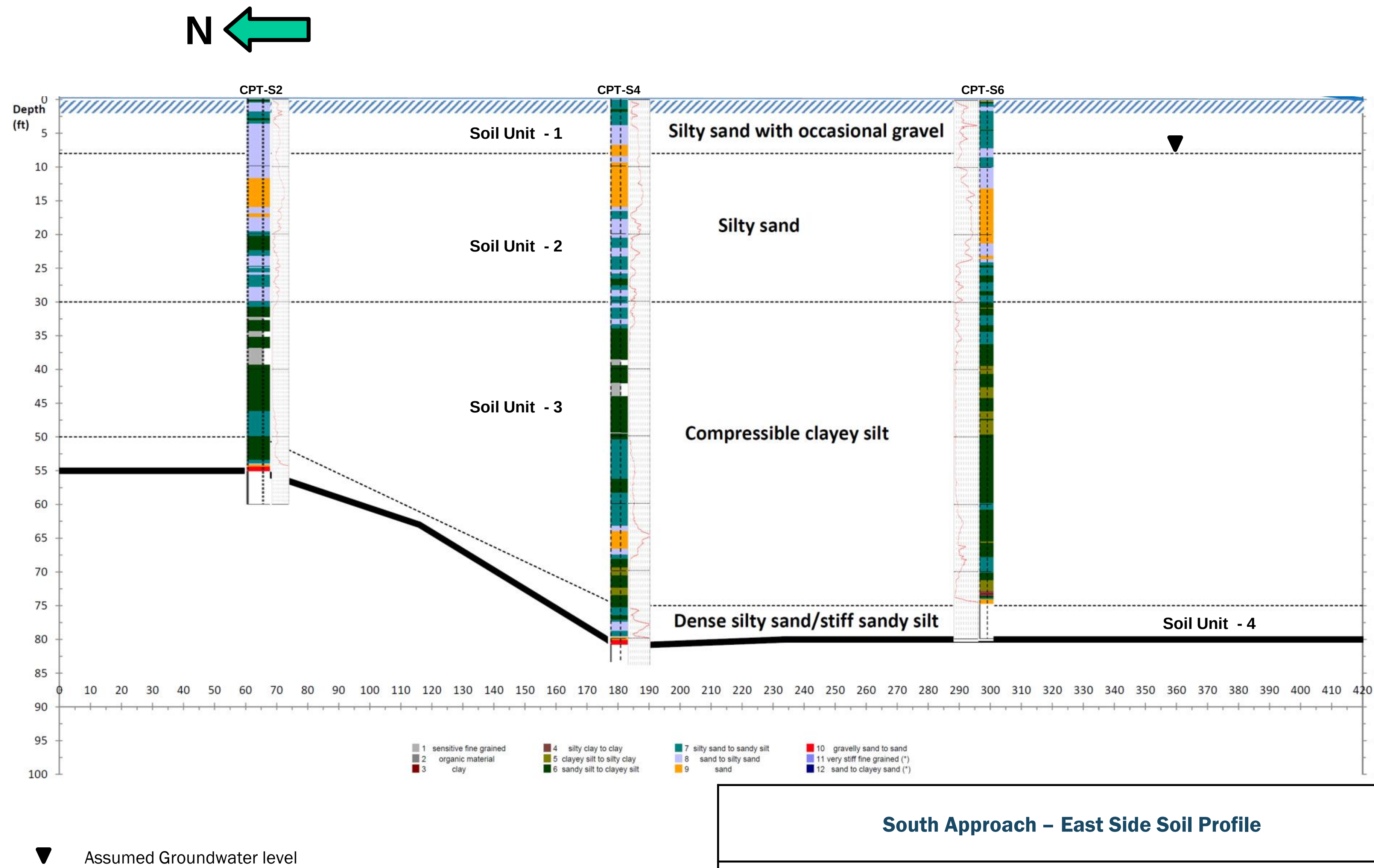

South Approach – East Side Soil Profile
Airport Way South Viaduct over ARGO Railroad Yard project Seattle, Washington

GeoEngineers

Figure 6

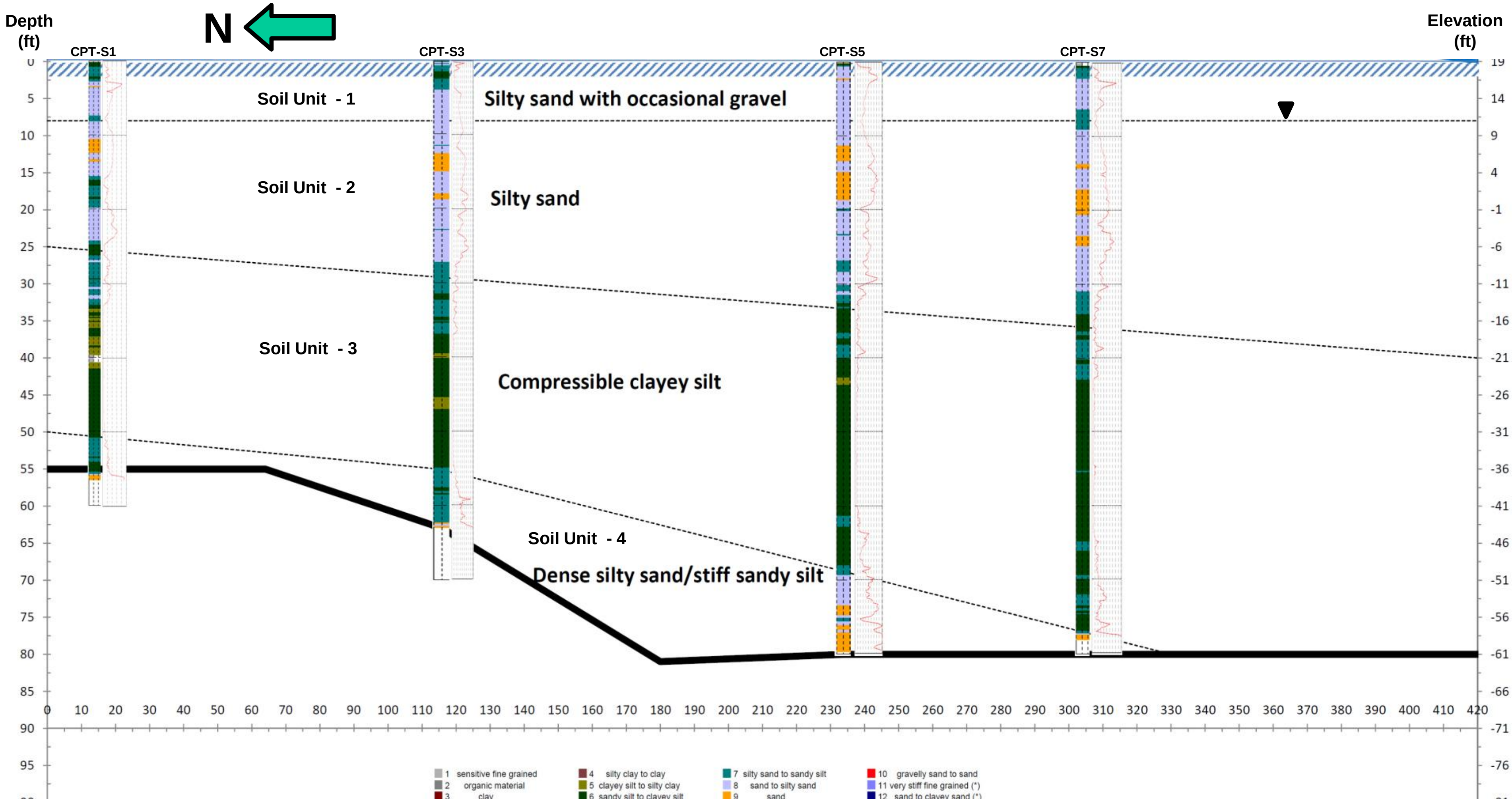

▼ Assumed Groundwater level

South Approach – West Side Soil Profile

Airport Way South Viaduct over ARGO Railroad Yard project
Seattle, Washington

GeoEngineers

Figure 7

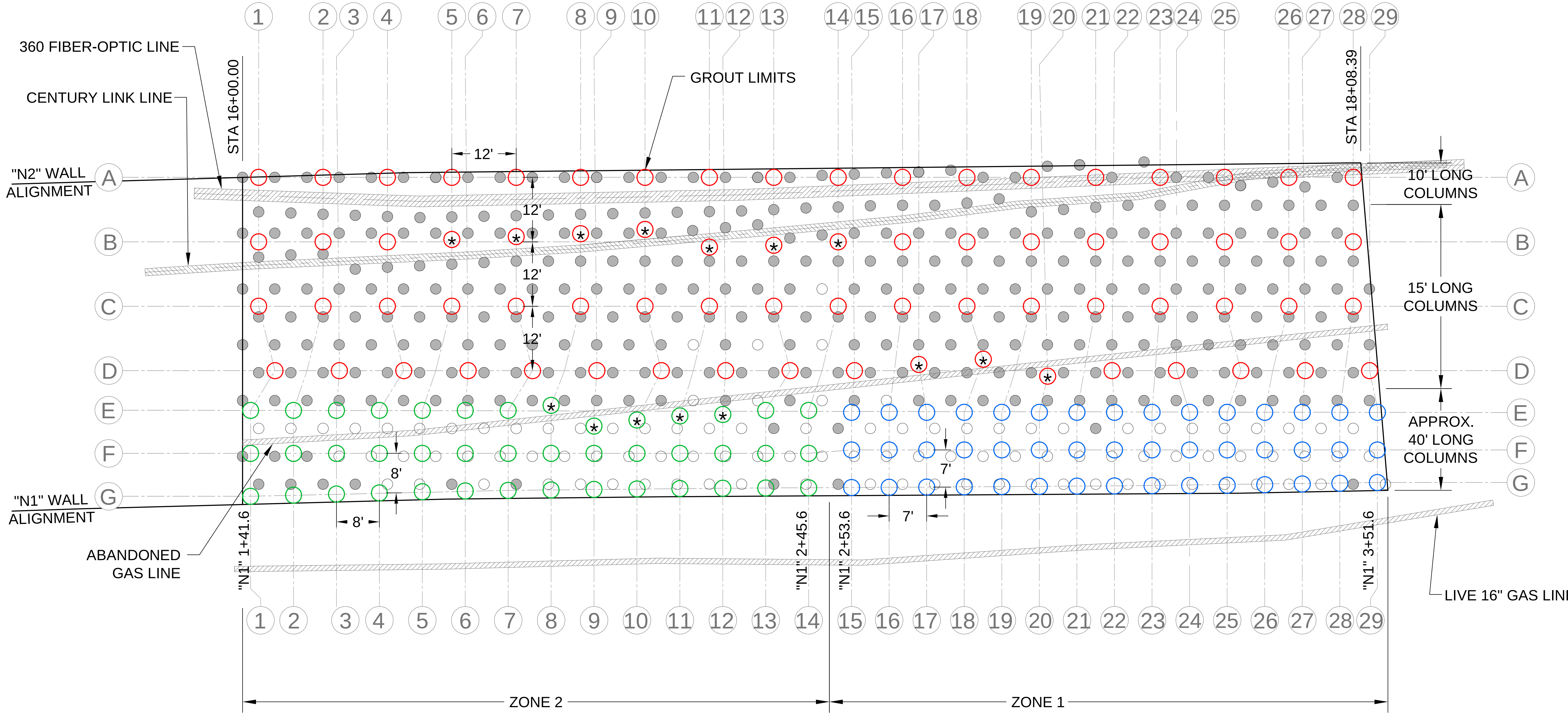

AREA REPLACEMENT RATIO = 10%

Notes

1. The locations of all features shown are approximate.
2. This drawing is for information purposes. It is intended to assist in showing features discussed in an attached document. GeoEngineers, Inc. cannot guarantee the accuracy and content of electronic files. The master file is stored by GeoEngineers, Inc. and will serve as the official record of this communication.
3. "A" Line column alignment to match compaction grout column "A" Line. Center new "A" Line columns between compaction grout columns.

Reference: GeoEngineers staff sketch.

Legend

- 36" Grout Column - 12' Spacing (72 Columns)
- 36" Grout Column - Zone 1 (42 Columns)
- 36" Grout Column - Zone 2 (45 Columns)
- Compaction Grouting Column Installed
- * Adjust columns to miss utility as required. Utility must be exposed or potholed prior to installing column.

20 0 20
FEET

North Approach - DSM Column Layout

Airport Way South Viaduct
over ARGO Railroad Yard
Seattle, Washington

GEOENGINEERS

Figure 8

W:\REDMOND\PROJECTS\0\0129141\01\CAD\0129141-01 SOILCRETE LAYOUTS.DWG\TAB:NORTH ABUTMENT MODIFIED BY TMICHAUD ON AUG 15, 2012 - 9:44

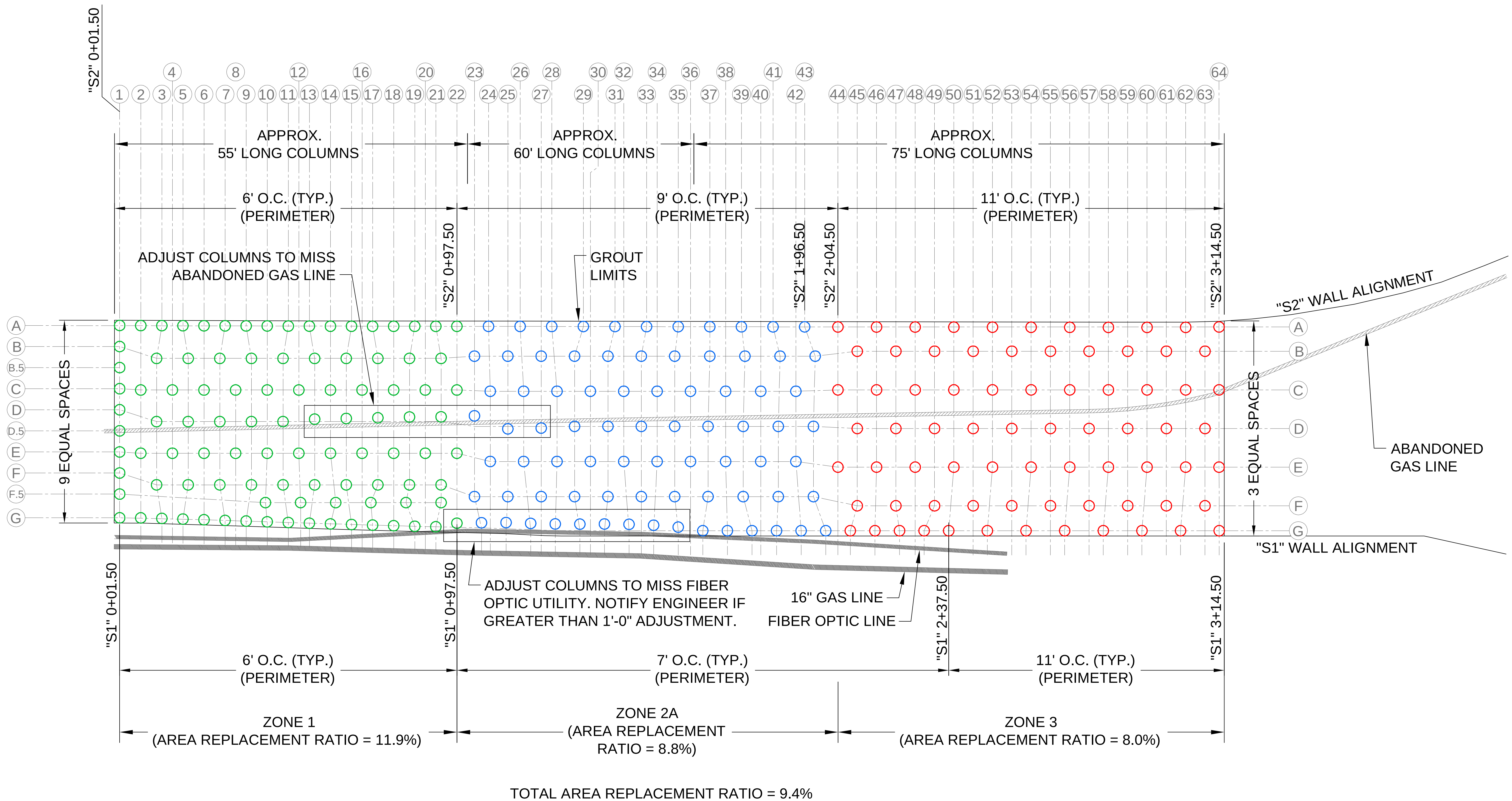

Notes

1. The locations of all features shown are approximate.
2. This drawing is for information purposes. It is intended to assist in showing features discussed in an attached document. GeoEngineers, Inc. cannot guarantee the accuracy and content of electronic files. The master file is stored by GeoEngineers, Inc. and will serve as the official record of this communication.

Reference: GeoEngineers staff sketch.

Legend

- 36" Grout Column - Zone 1 (100 Columns)
- 36" Grout Column - Zone 2 (79 Columns)
- 36" Grout Column - Zone 3 (75 Columns)

30 0 30
FEET

South Approach - DSM Column Layout

Airport Way South Viaduct
over ARGO Railroad Yard
Seattle, Washington

GEOENGINEERS

Figure 9

W:\REDMOND\PROJECTS\0\0129141\00\CAD\012914100 SOILCRETE LAYOUTS.DWG\TAB:SOUTH ABUTMENT (CONCRETE PAD OPTION) MODIFIED BY TMICHAUD ON JUL 16, 2012 - 13:22

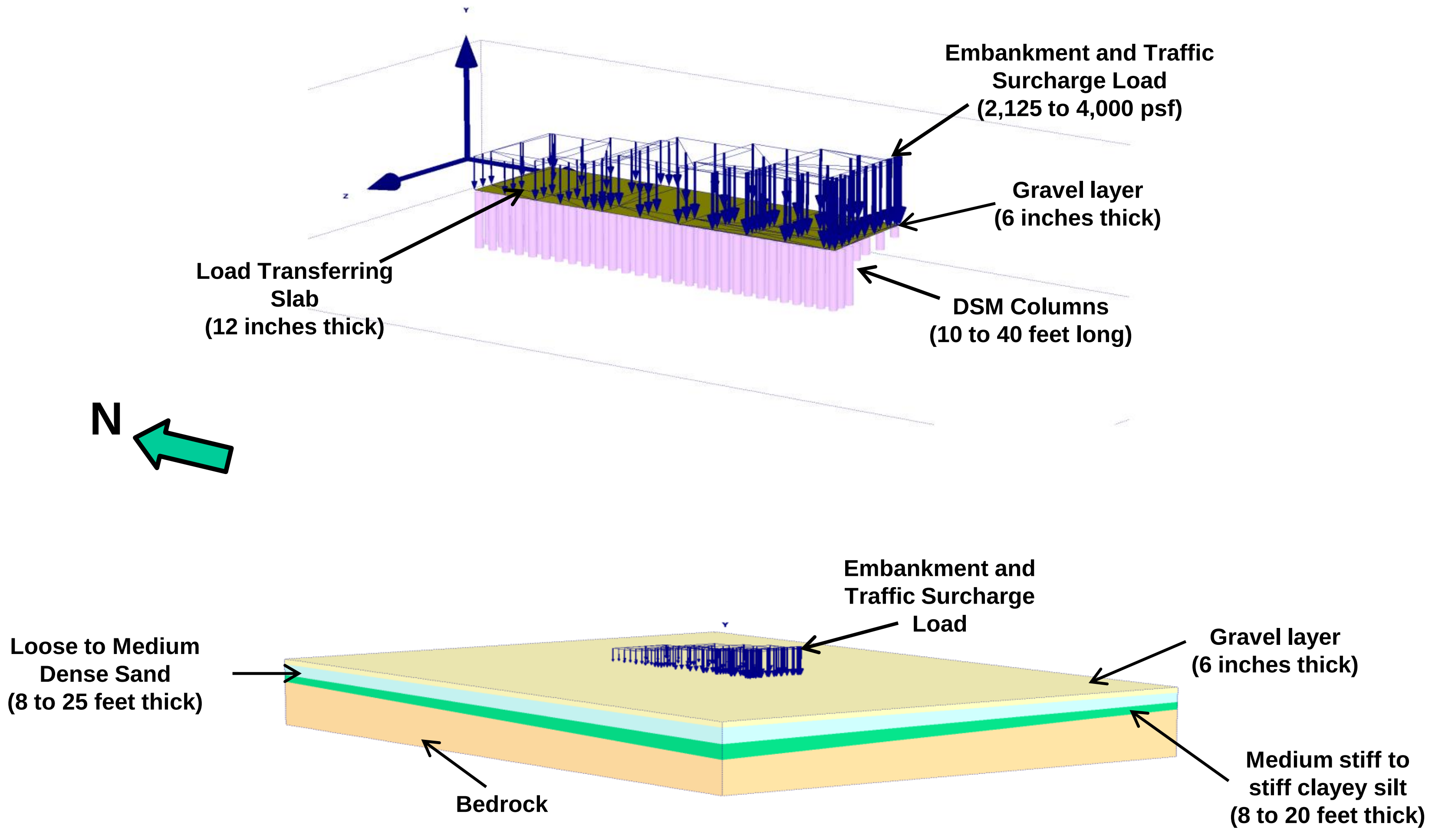

PLAXIS 3D Model – North Approach (DSM columns and Soil Profile)

Airport Way South Viaduct over ARGO Railroad Yard project
Seattle, Washington

GeoEngineers

Figure 10

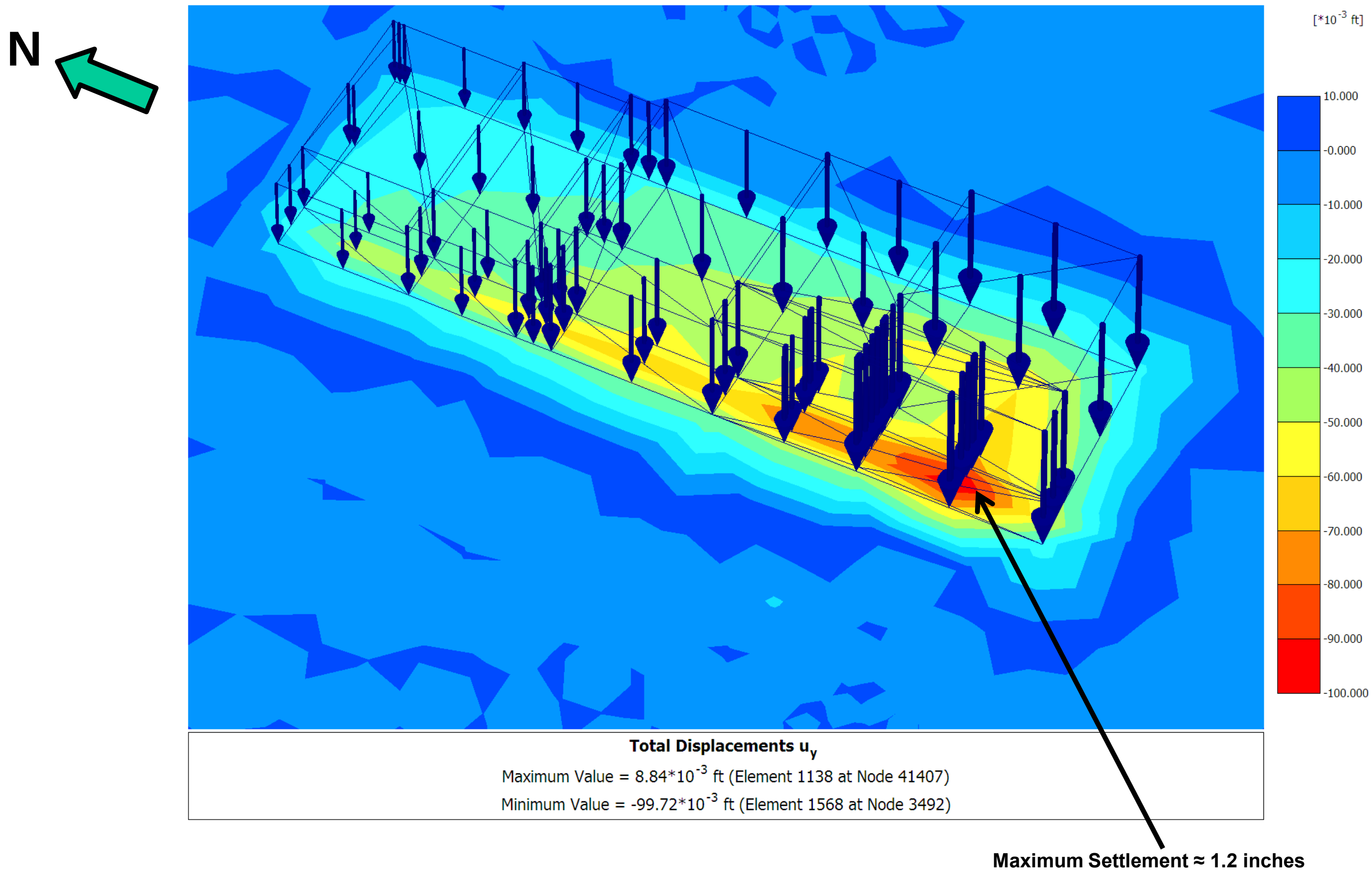

PLAXIS 3D Model – North Approach Static Settlement (Existing Conditions)	
Airport Way South Viaduct over ARGO Railroad Yard project Seattle, Washington	
GeoEngineers	**Figure 11**

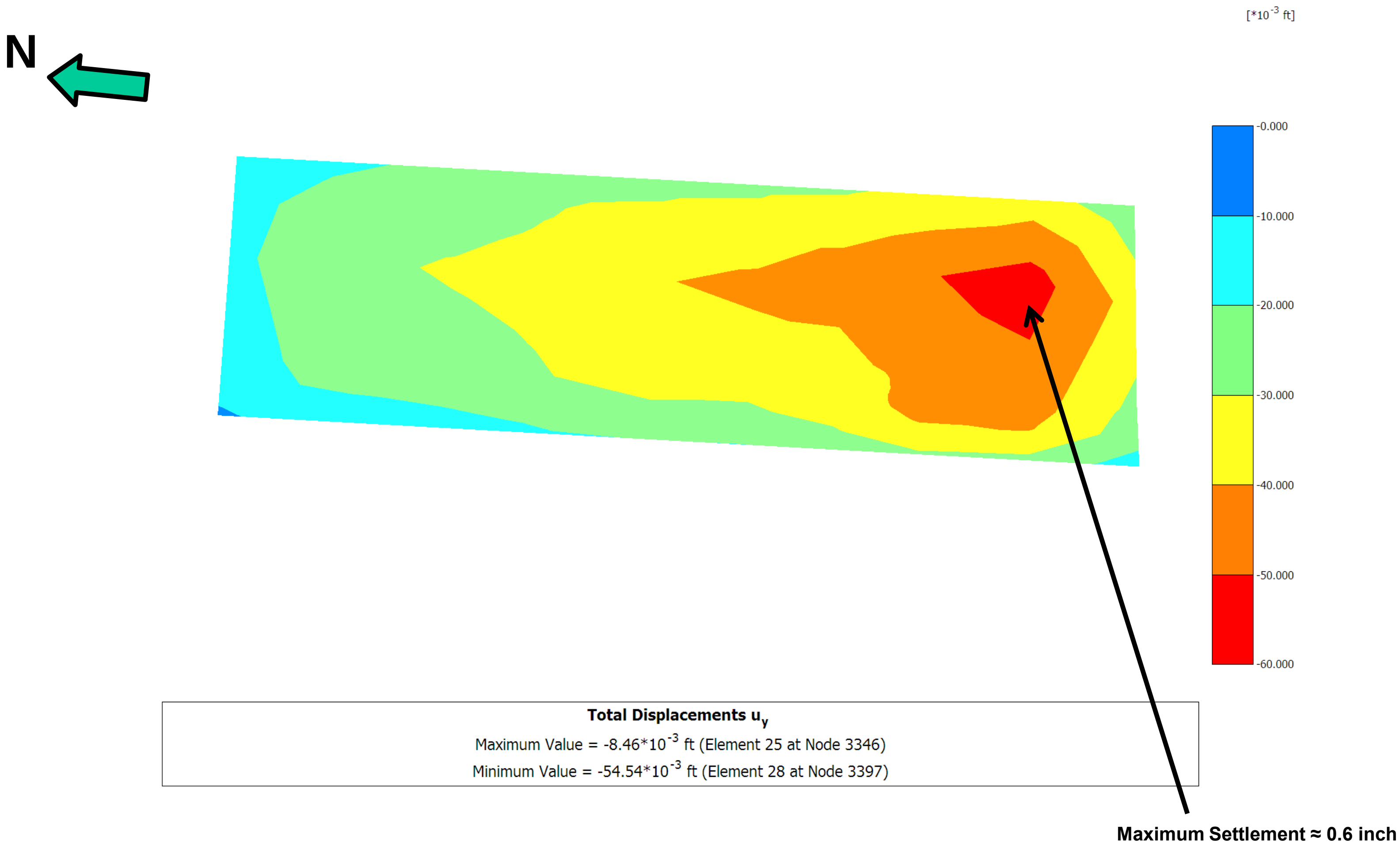

PLAXIS 3D Model – North Approach
Static Settlement (Improved Conditions)

Airport Way South Viaduct over ARGO Railroad Yard project
Seattle, Washington

GEOENGINEERS

Figure 12

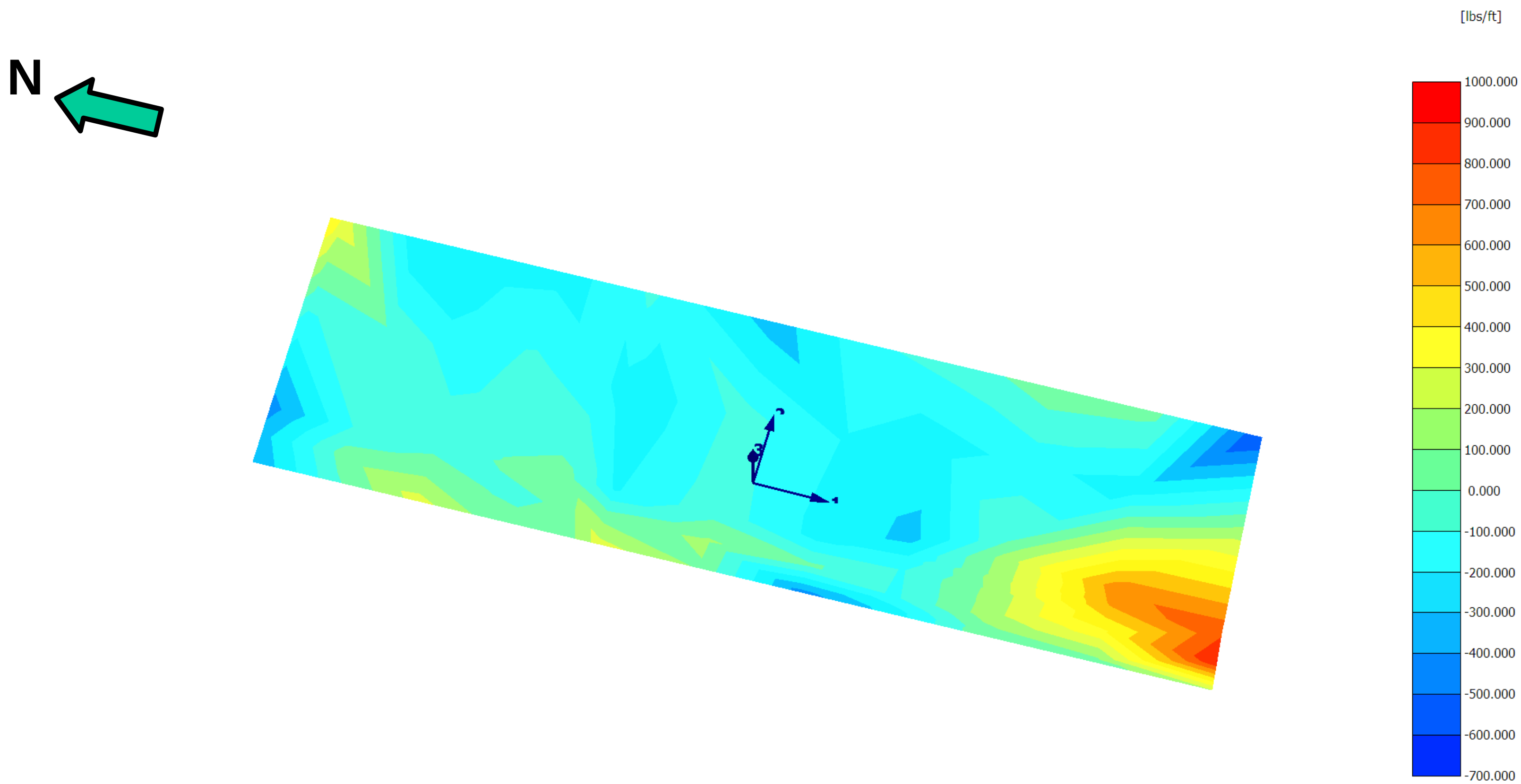

Shear Forces Q_{12}

Maximum Value = 907.69 lbs/ft (Element 33 at Node 3495)

Minimum Value = -603.09 lbs/ft (Element 28 at Node 3476)

PLAXIS 3D Model – North Approach **Slab Forces (Static Conditions)**	
Airport Way South Viaduct over ARGO Railroad Yard project Seattle, Washington	
GEOENGINEERS	**Figure 13**

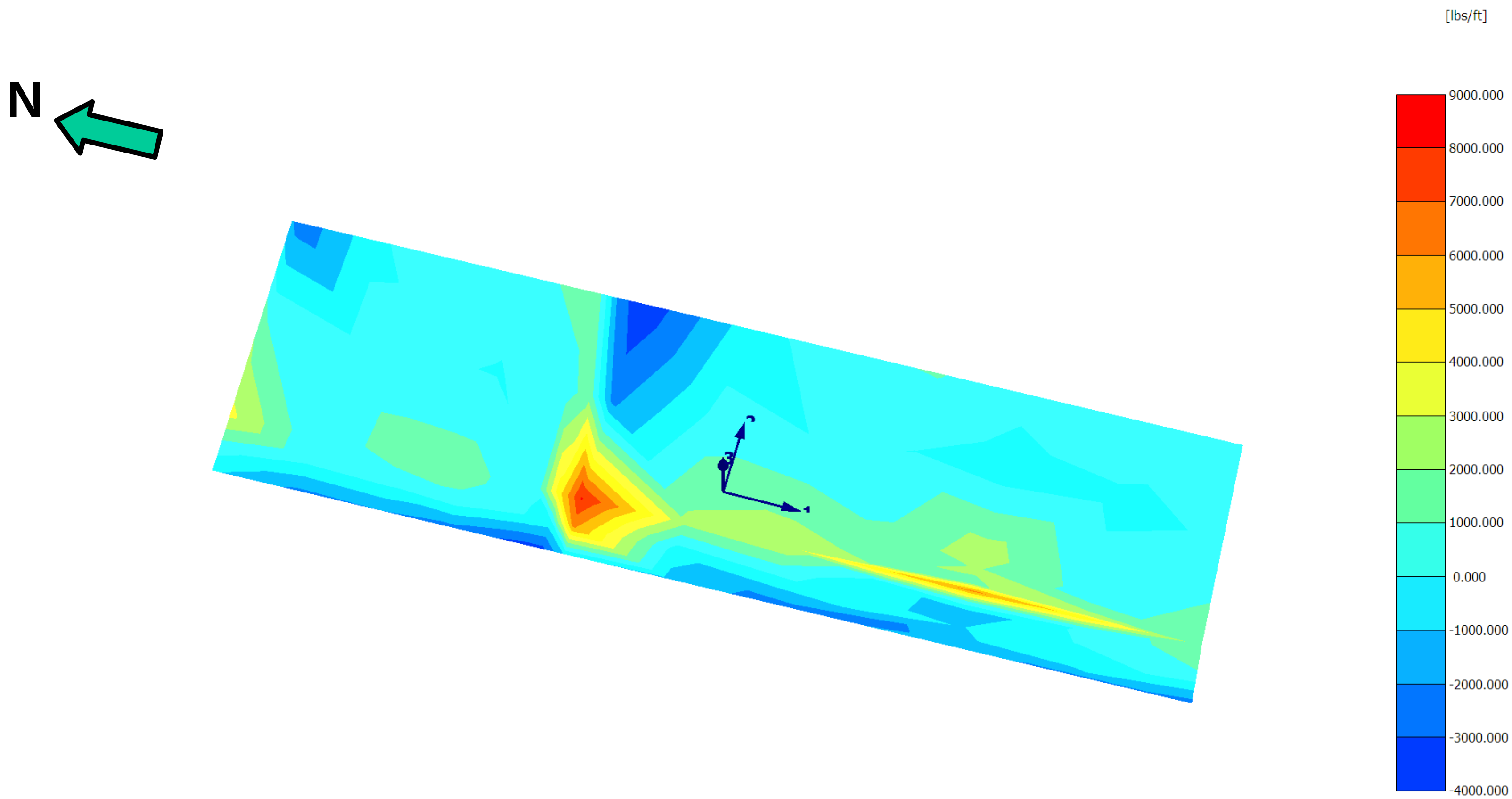

Shear Forces Q_{23}

Maximum Value = $8.12*10^3$ lbs/ft (Element 10 at Node 3358)

Minimum Value = $-3.86*10^3$ lbs/ft (Element 20 at Node 3231)

PLAXIS 3D Model – North Approach Slab Forces (Static Conditions)	
Airport Way South Viaduct over ARGO Railroad Yard project Seattle, Washington	
GeoEngineers	**Figure 14**

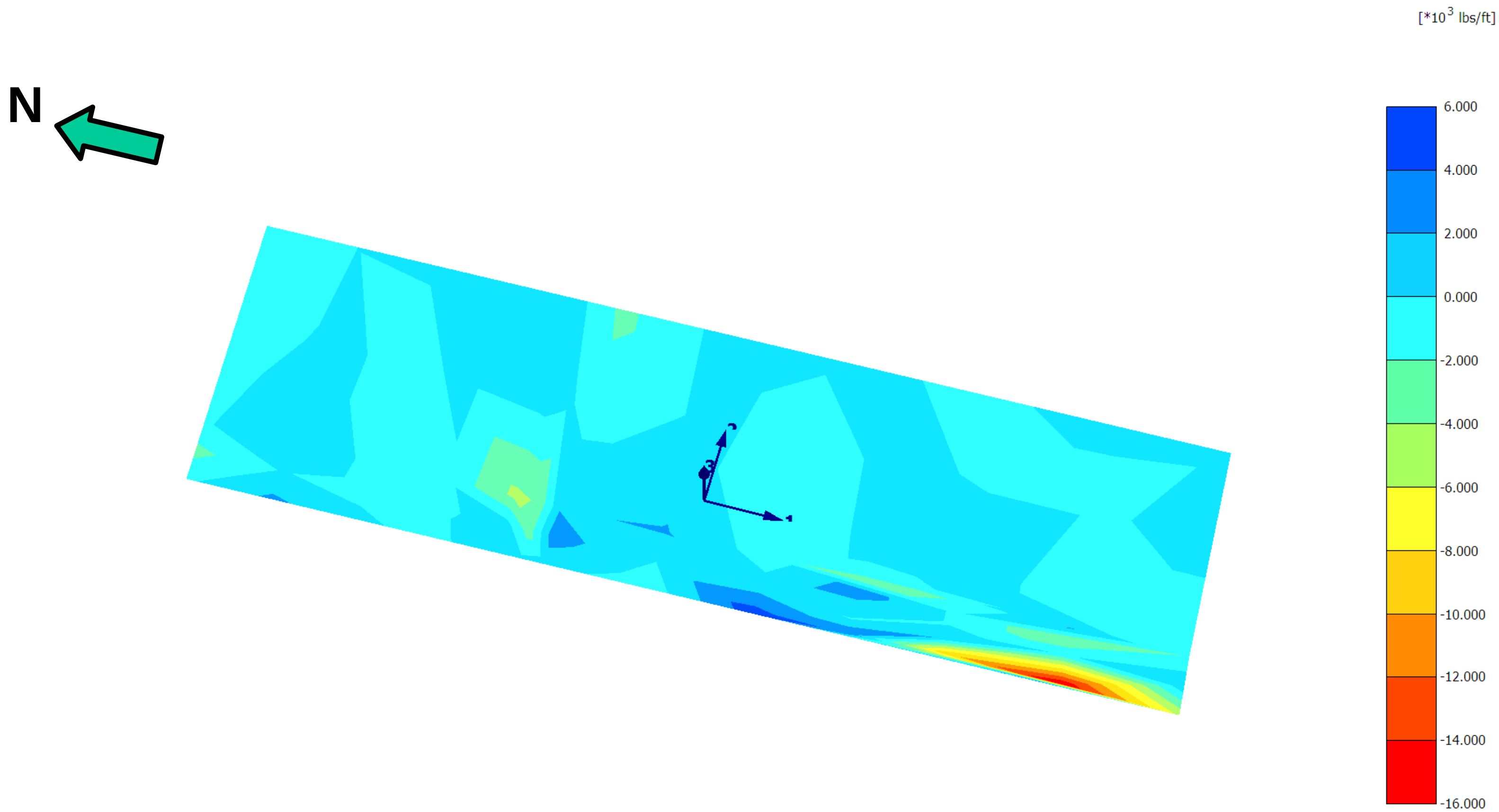

Shear Forces Q_{13}

Maximum Value = $5.16*10^3$ lbs/ft (Element 6 at Node 3517)

Minimum Value = $-15.87*10^3$ lbs/ft (Element 30 at Node 3498)

PLAXIS 3D Model – North Approach
Slab Forces (Static Conditions)

Airport Way South Viaduct over ARGO Railroad Yard project
Seattle, Washington

GEOENGINEERS

Figure 15

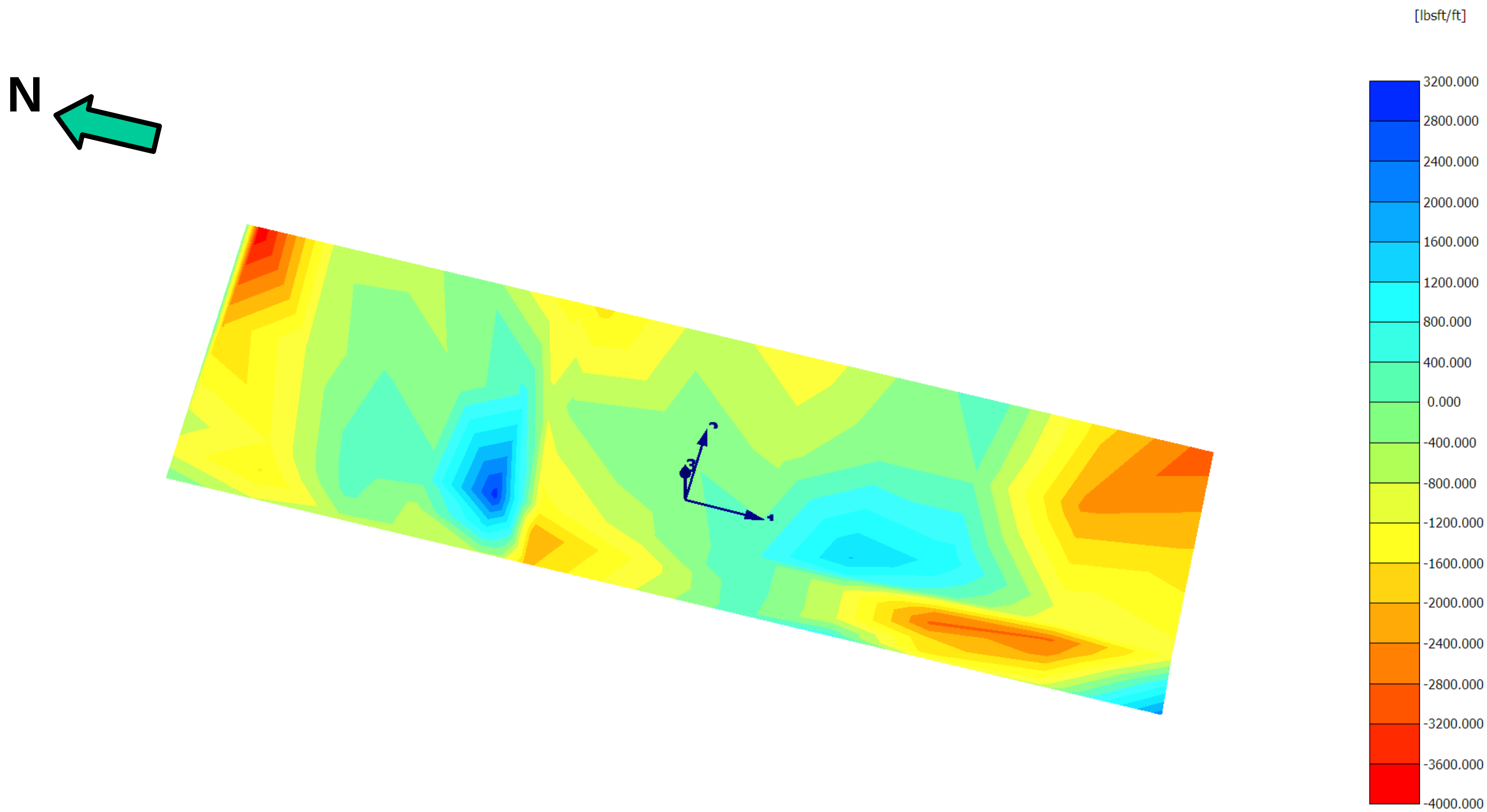

Bending Moments M_{11}

Maximum Value = $2.98*10^{3}$ lbsft/ft (Element 4 at Node 3335)

Minimum Value = $-3.95*10^{3}$ lbsft/ft (Element 1 at Node 3223)

PLAXIS 3D Model – North Approach
Slab Forces (Static Conditions)

Airport Way South Viaduct over ARGO Railroad Yard project
Seattle, Washington

GeoEngineers

Figure 16

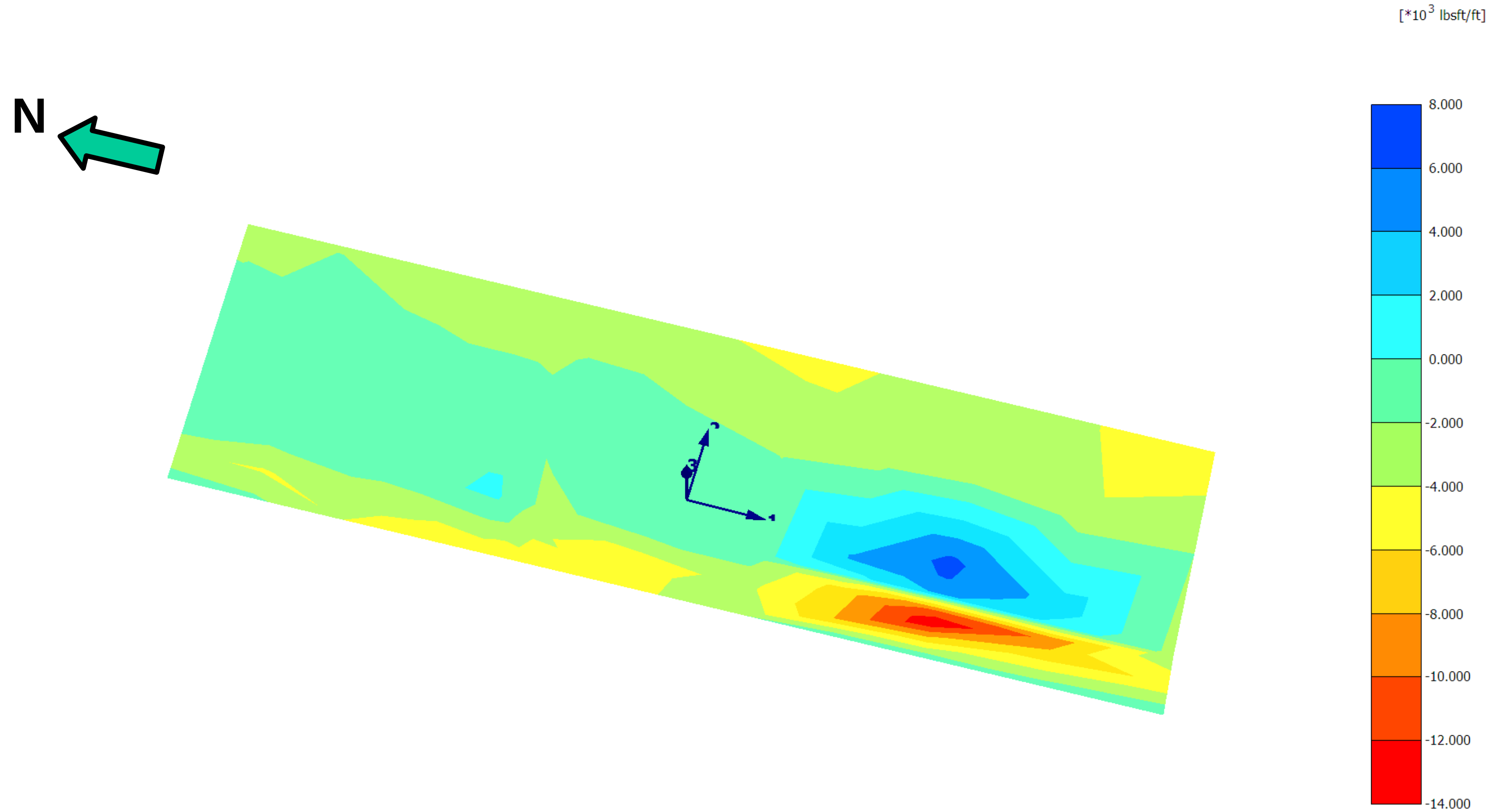

Bending Moments M_{22}

Maximum Value = 6.44×10^3 lbsft/ft (Element 13 at Node 3396)

Minimum Value = -13.52×10^3 lbsft/ft (Element 7 at Node 3403)

PLAXIS 3D Model – North Approach
Slab Forces (Static Conditions)

Airport Way South Viaduct over ARGO Railroad Yard project
Seattle, Washington

GeoEngineers

Figure 17

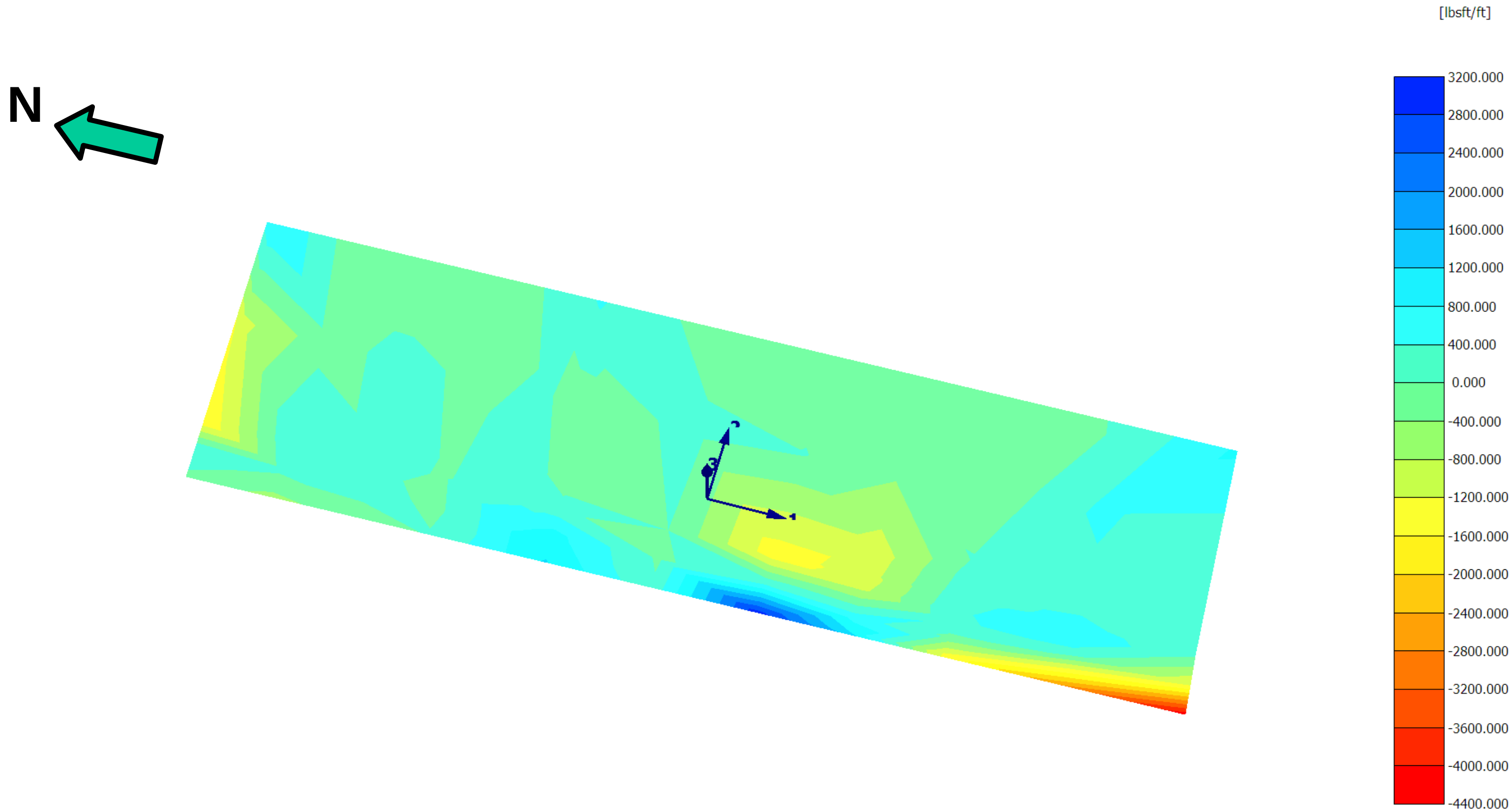

Torsion Moments M_{12}

Maximum Value = $3.03*10^3$ lbsft/ft (Element 6 at Node 3517)

Minimum Value = $-4.27*10^3$ lbsft/ft (Element 30 at Node 3629)

PLAXIS 3D Model – North Approach
Slab Forces (Static Conditions)

Airport Way South Viaduct over ARGO Railroad Yard project
Seattle, Washington

GeoEngineers

Figure 18

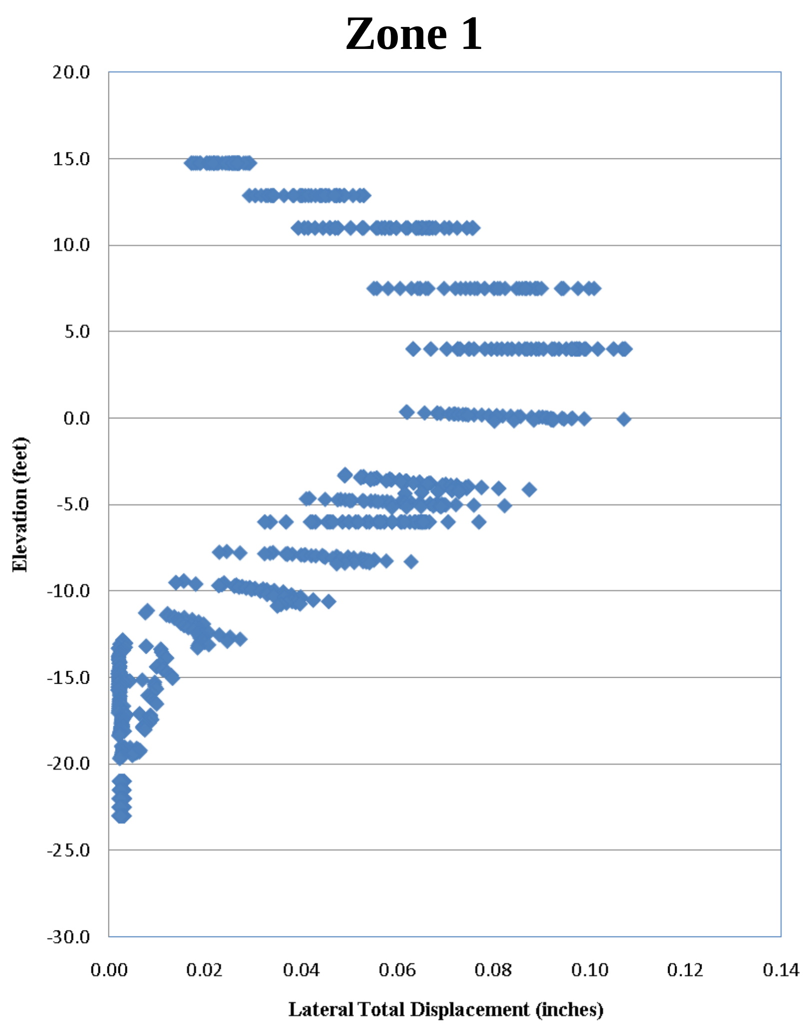

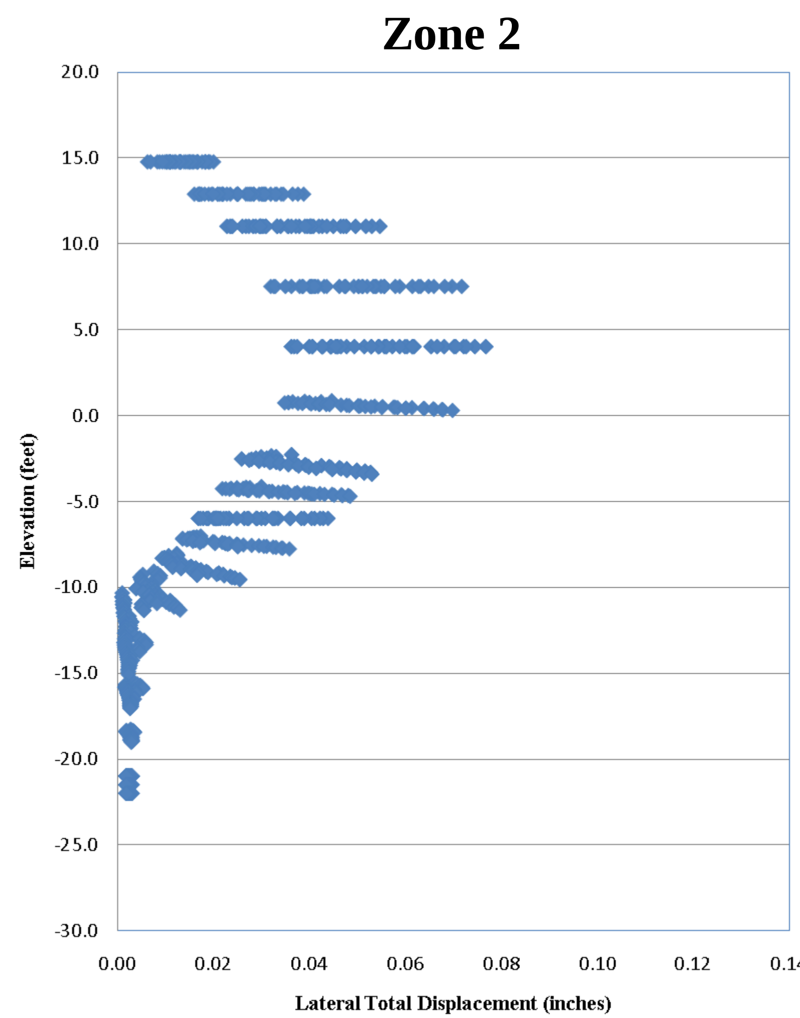

PLAXIS 3D Model – North Approach
DSM Lateral Displacement (Static Conditions)

Airport Way South Viaduct over ARGO Railroad Yard project
Seattle, Washington

GeoEngineers

Figure 19

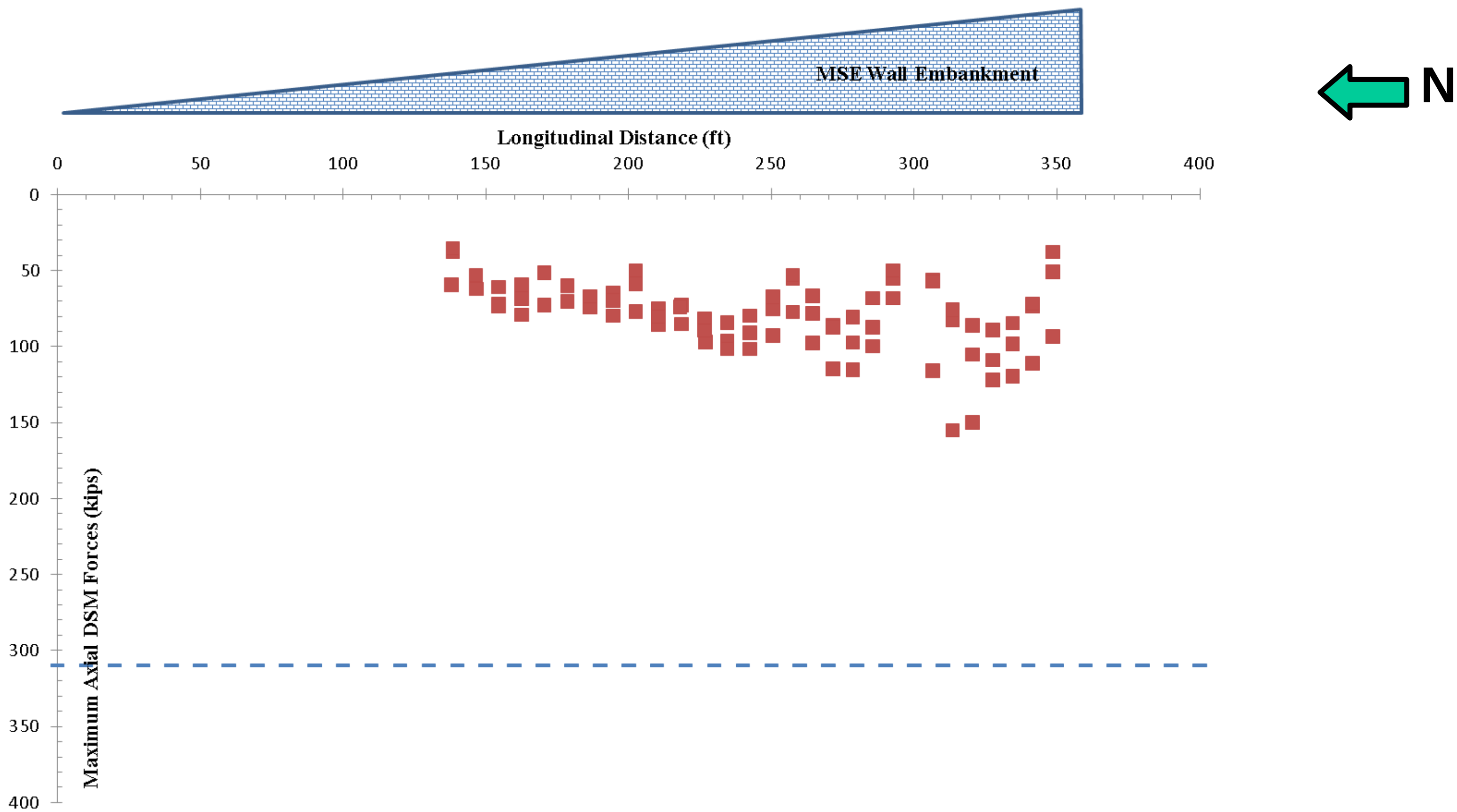

PLAXIS 3D Model – North Approach
DSM Maximum Axial Forces (Static Conditions)

Airport Way South Viaduct over ARGO Railroad Yard project
Seattle, Washington

GeoEngineers

Figure 20

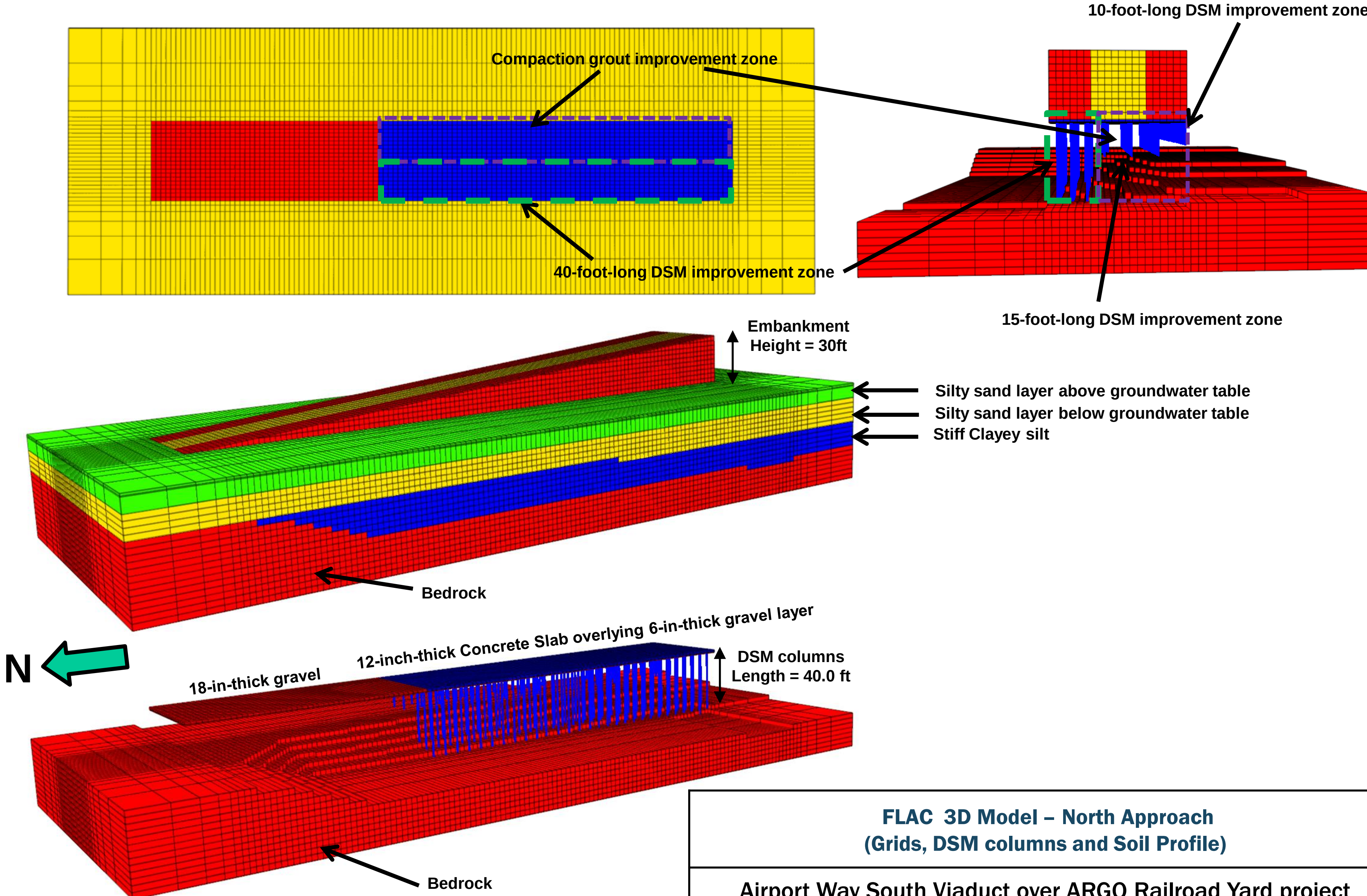

FLAC 3D Model – North Approach
(Grids, DSM columns and Soil Profile)

Airport Way South Viaduct over ARGO Railroad Yard project
Seattle, Washington

GeoEngineers

Figure 21

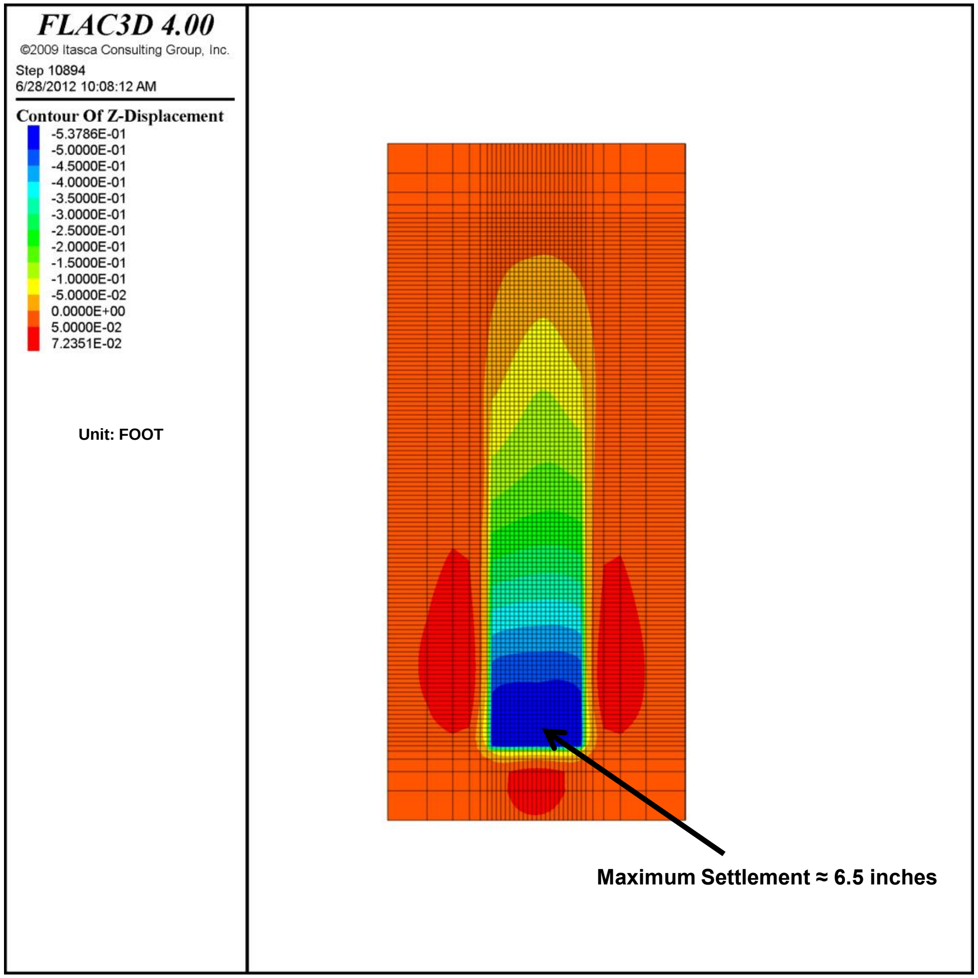

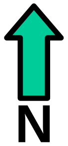

FLAC 3D Model – North Approach
Liquefaction-Induced Settlement (Existing Conditions)

Airport Way South Viaduct over ARGO Railroad Yard project
Seattle, Washington

GeoEngineers

Figure 22

N

Young's Modulus of DSM=150 x f'c

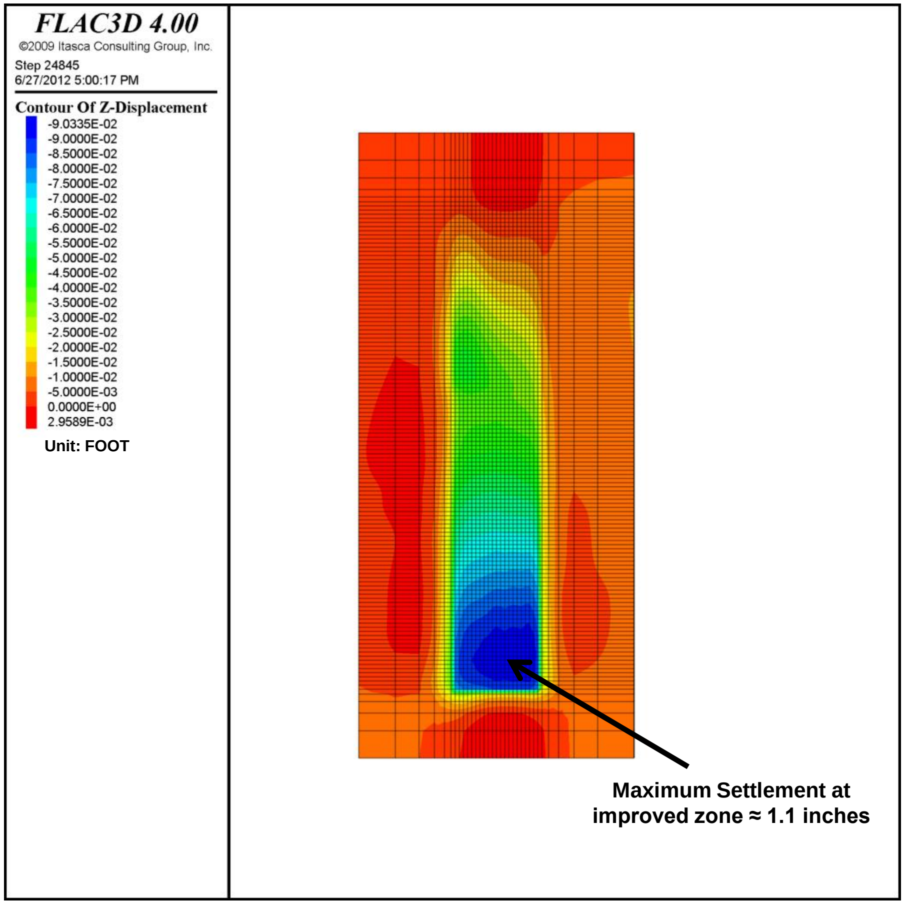

Young's Modulus of DSM=500 x f'c

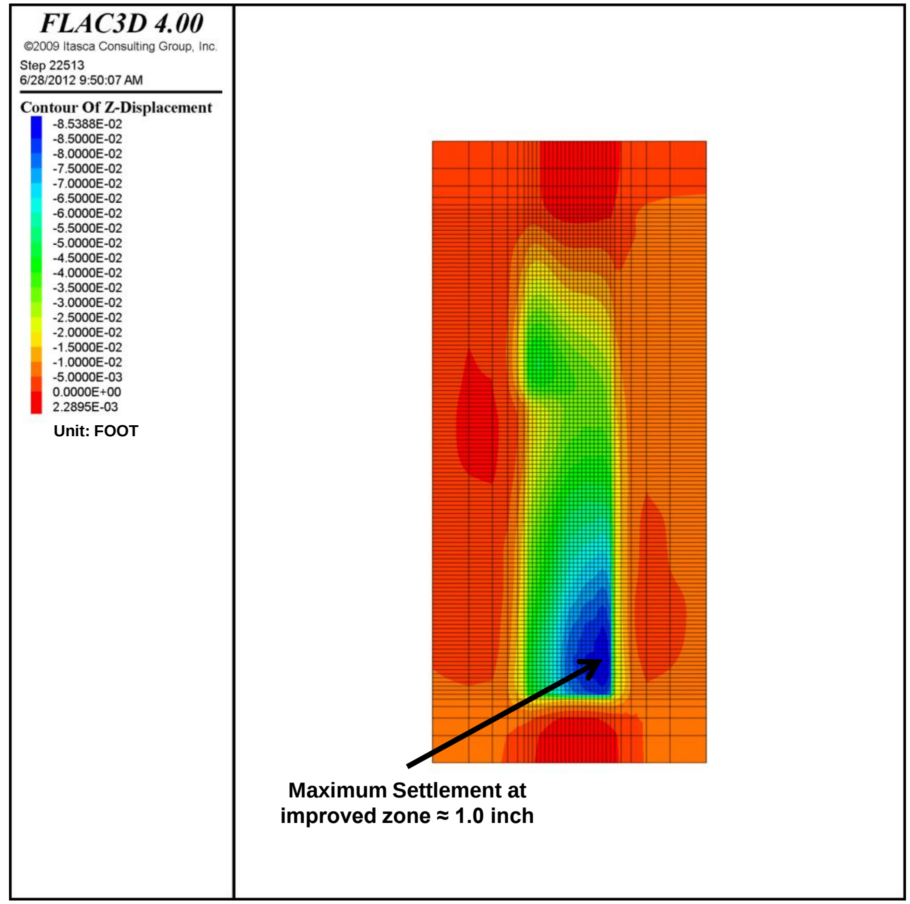

FLAC 3D Model – North Approach
Liquefaction-Induced Settlement (Improved Conditions)

Airport Way South Viaduct over ARGO Railroad Yard project
Seattle, Washington

GeoEngineers

Figure 23

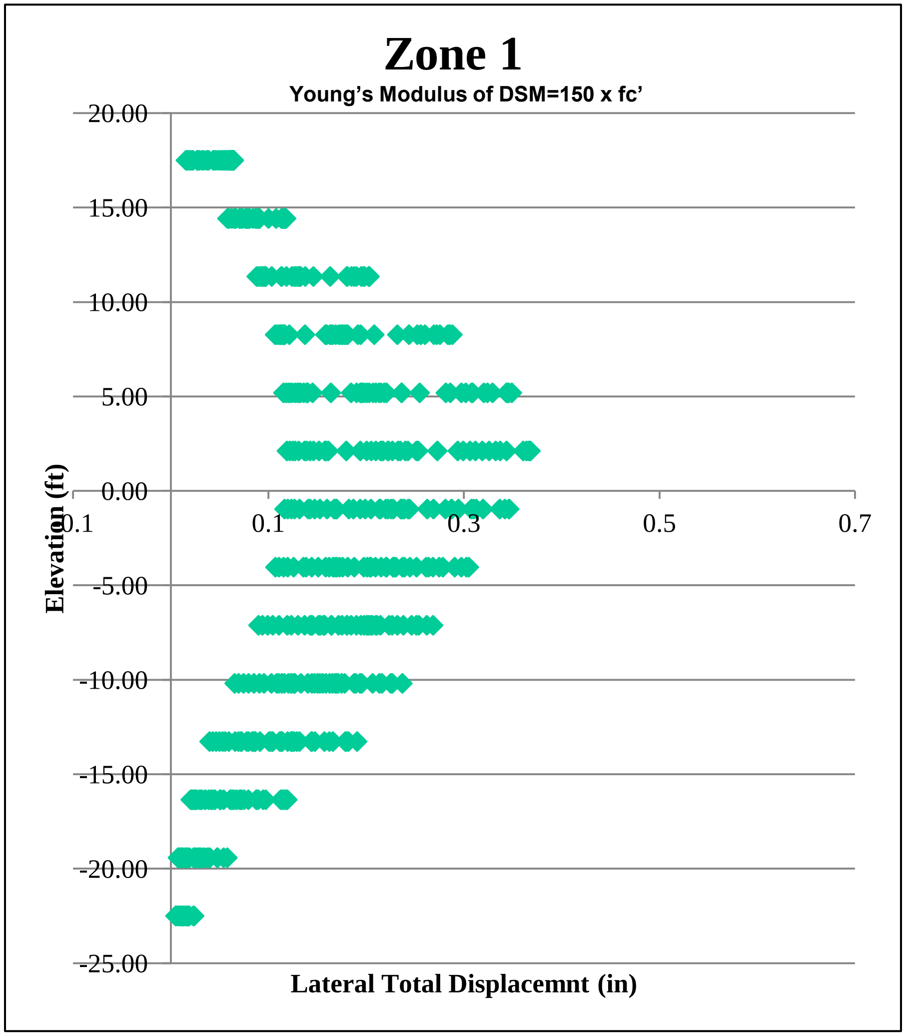

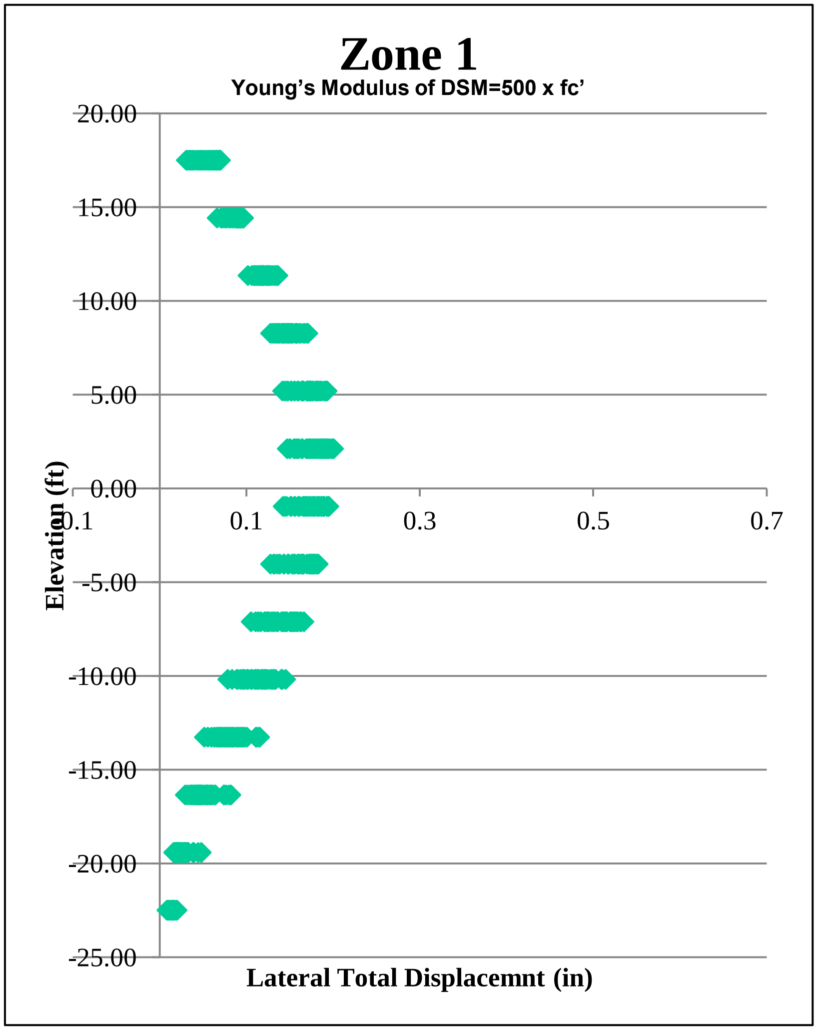

FLAC 3D Model – North Approach (Zone 1)
DSM Lateral Displacement (Liquefied Conditions)

Airport Way South Viaduct over ARGO Railroad Yard project
Seattle, Washington

GeoEngineers

Figure 24

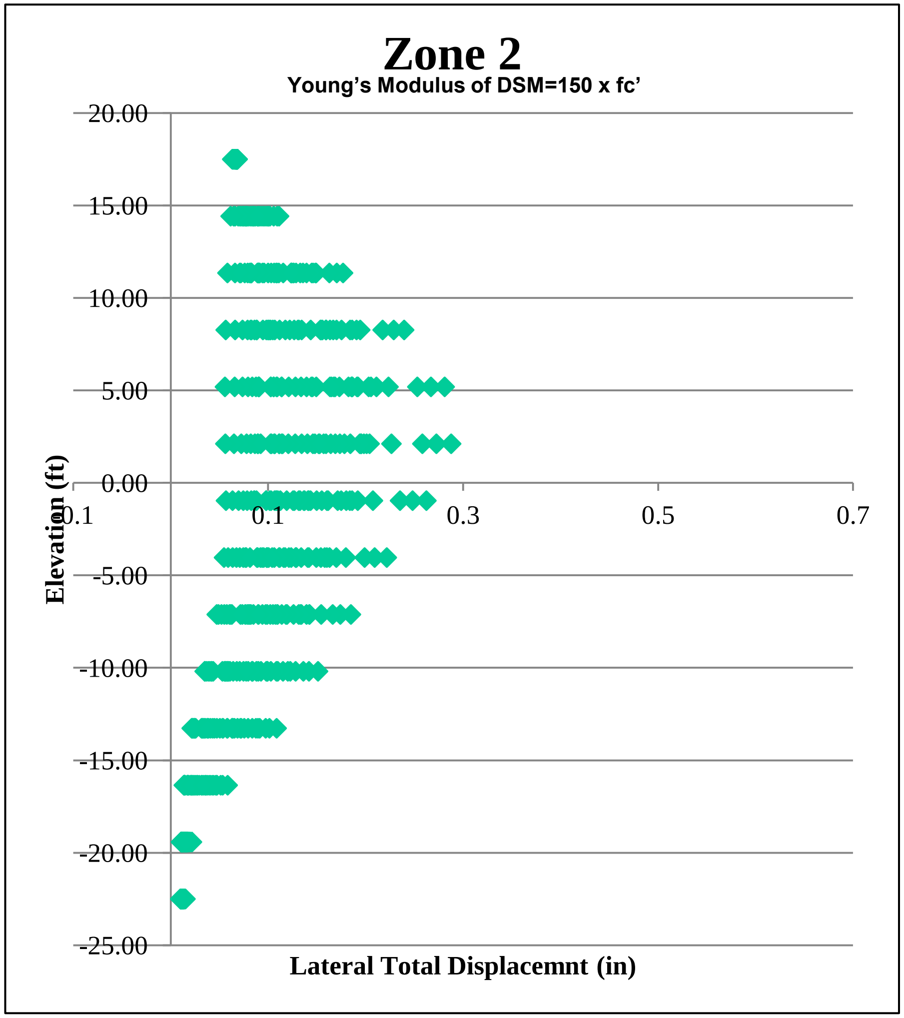

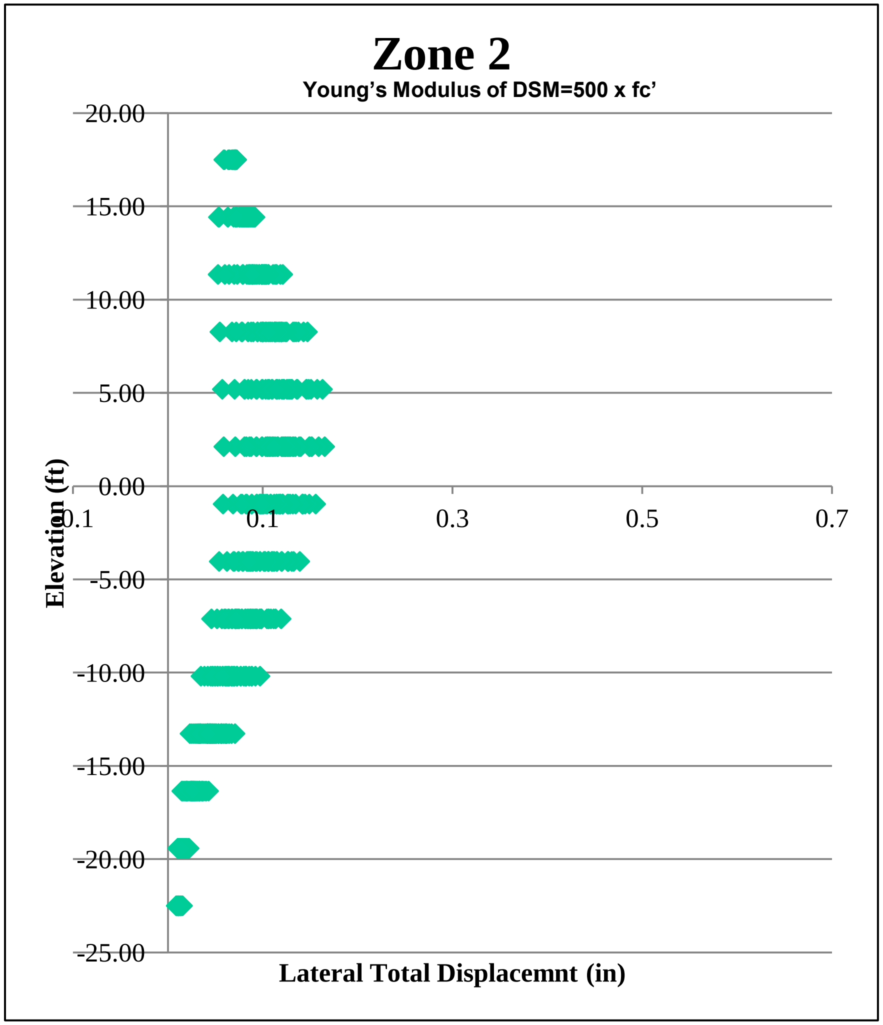

FLAC 3D Model – North Approach (Zone 2)
DSM Lateral Displacement (Liquefied Conditions)

Airport Way South Viaduct over ARGO Railroad Yard project
Seattle, Washington

GEOENGINEERS

Figure 25

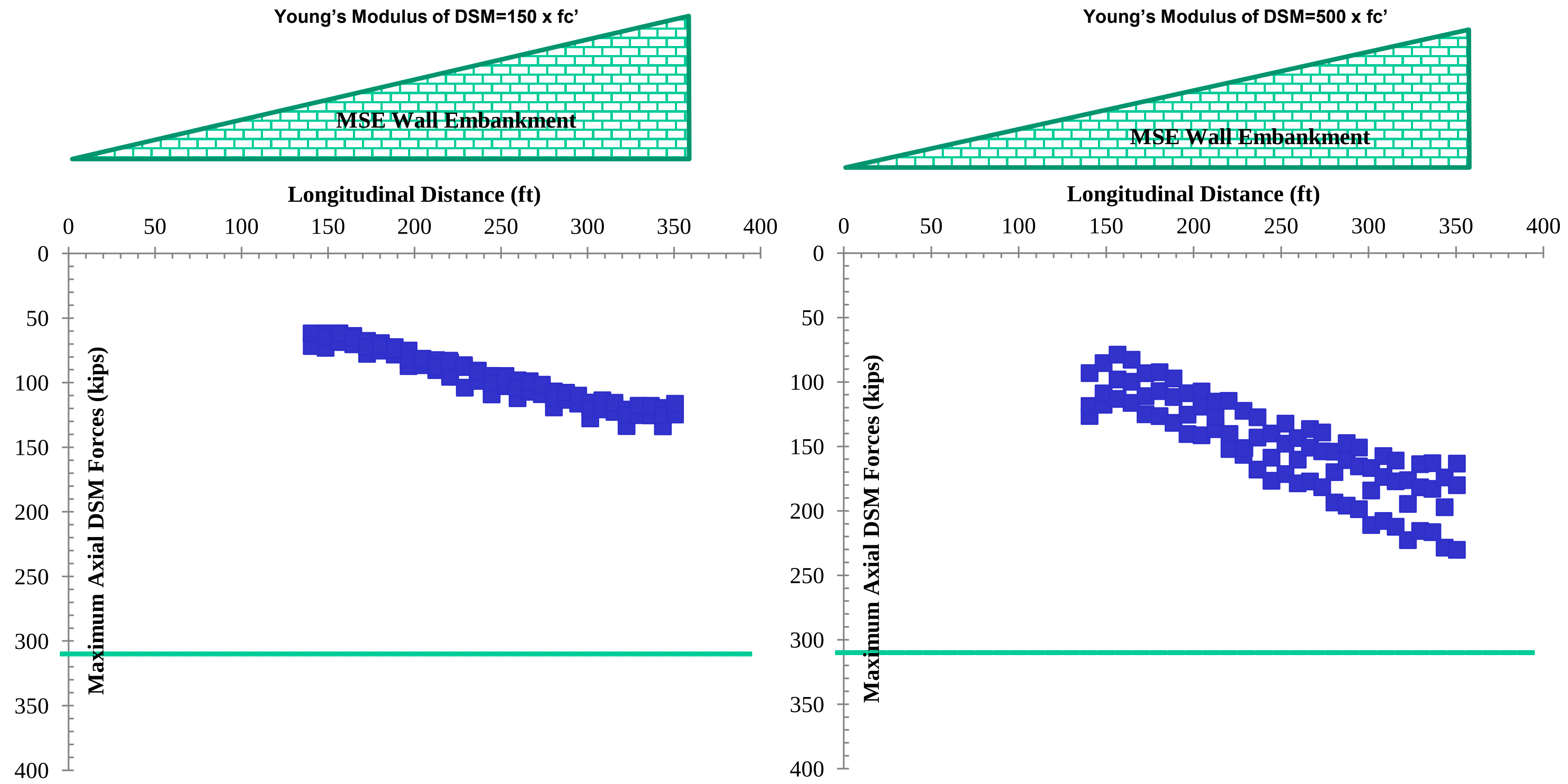

FLAC 3D Model – North Approach
DSM Maximum Axial Forces (Liquefied Conditions)

Airport Way South Viaduct over ARGO Railroad Yard project
Seattle, Washington

GeoEngineers

Figure 26

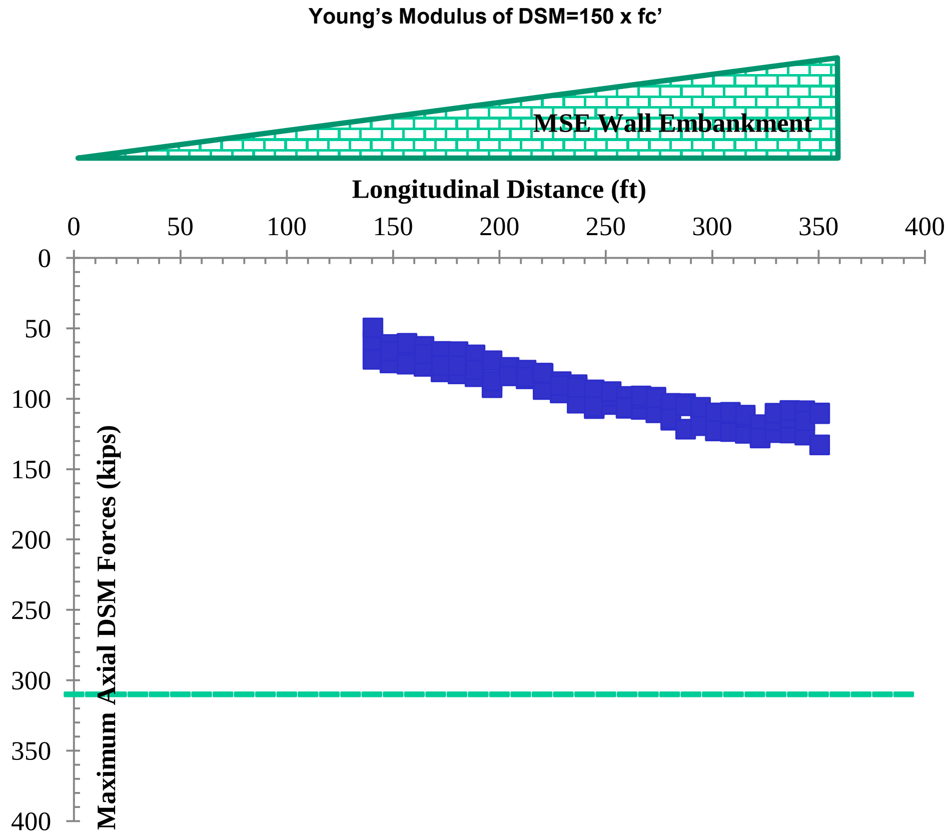

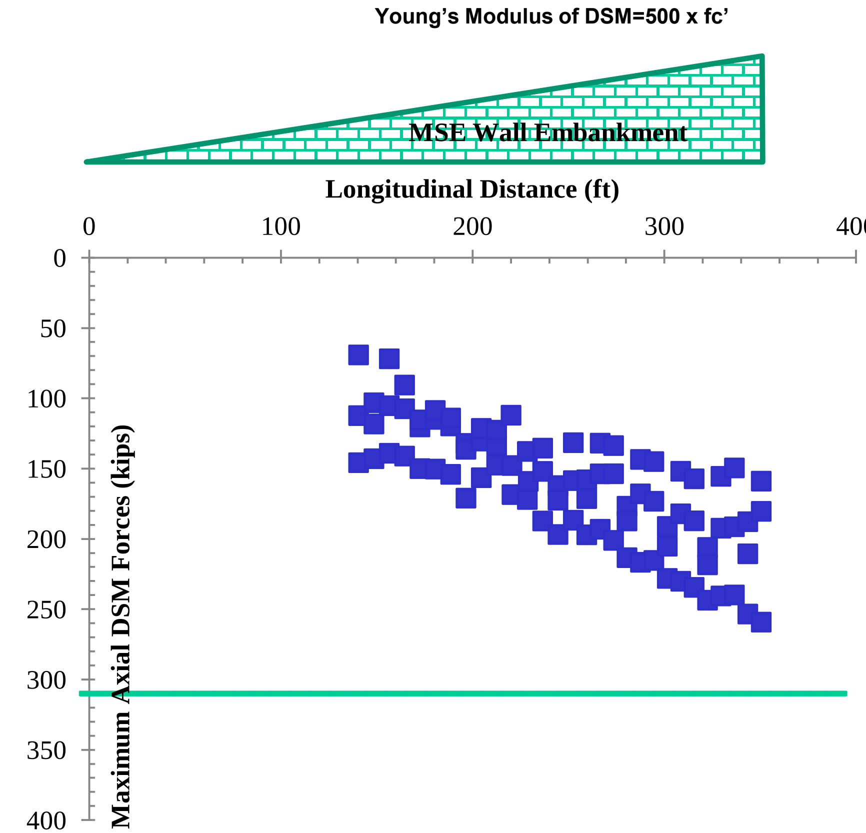

FLAC 3D Model – North Approach
DSM Maximum Axial Forces (Pseudo-static Conditions)
0.23g – ½ of design PGA

Airport Way South Viaduct over ARGO Railroad Yard project
Seattle, Washington

GeoEngineers

Figure 27

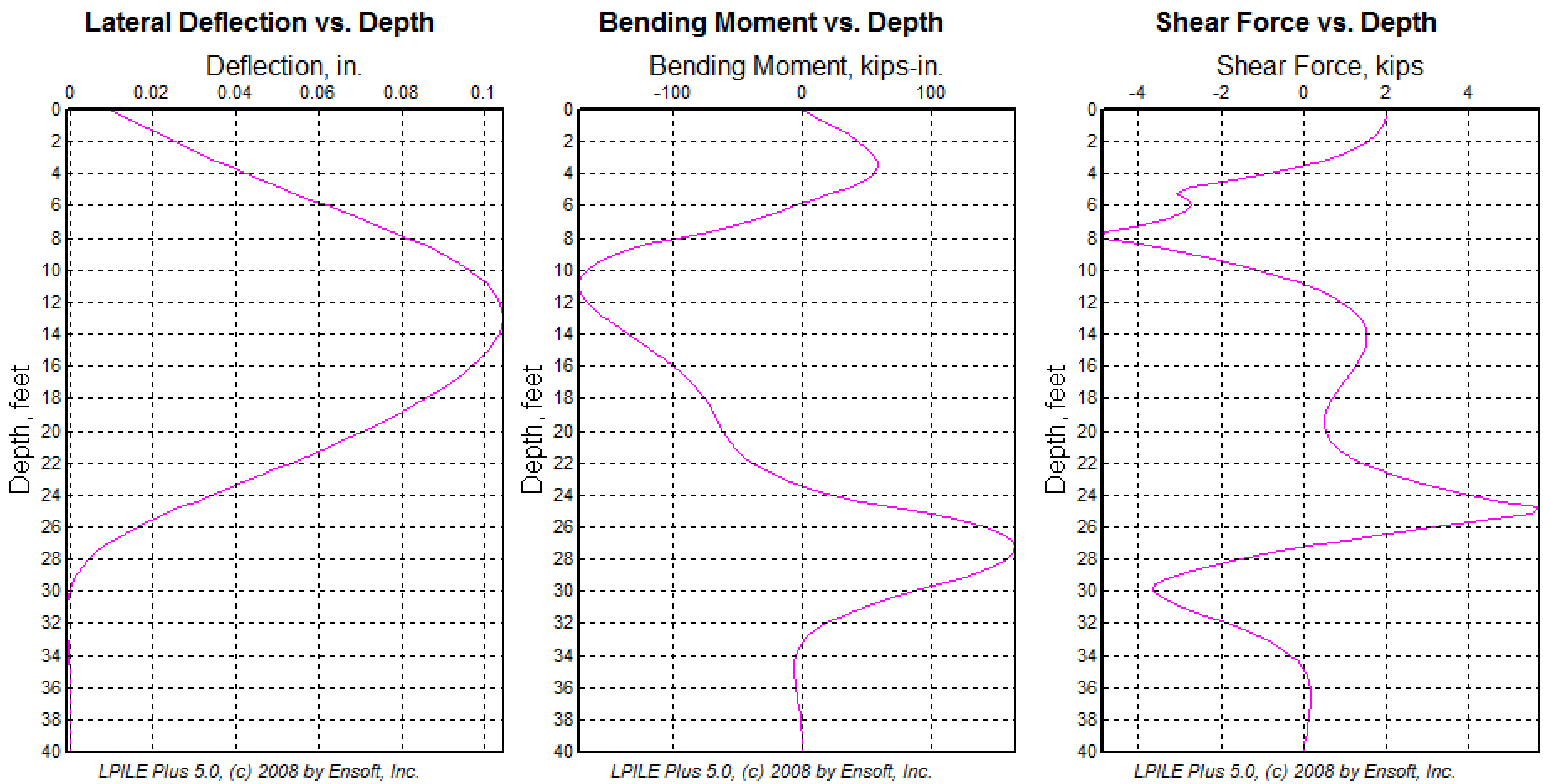

LPILE Analysis – North Approach
DSM Column Shear and Moment (Static Conditions)

Airport Way South Viaduct over ARGO Railroad Yard project
Seattle, Washington

GeoEngineers

Figure 28

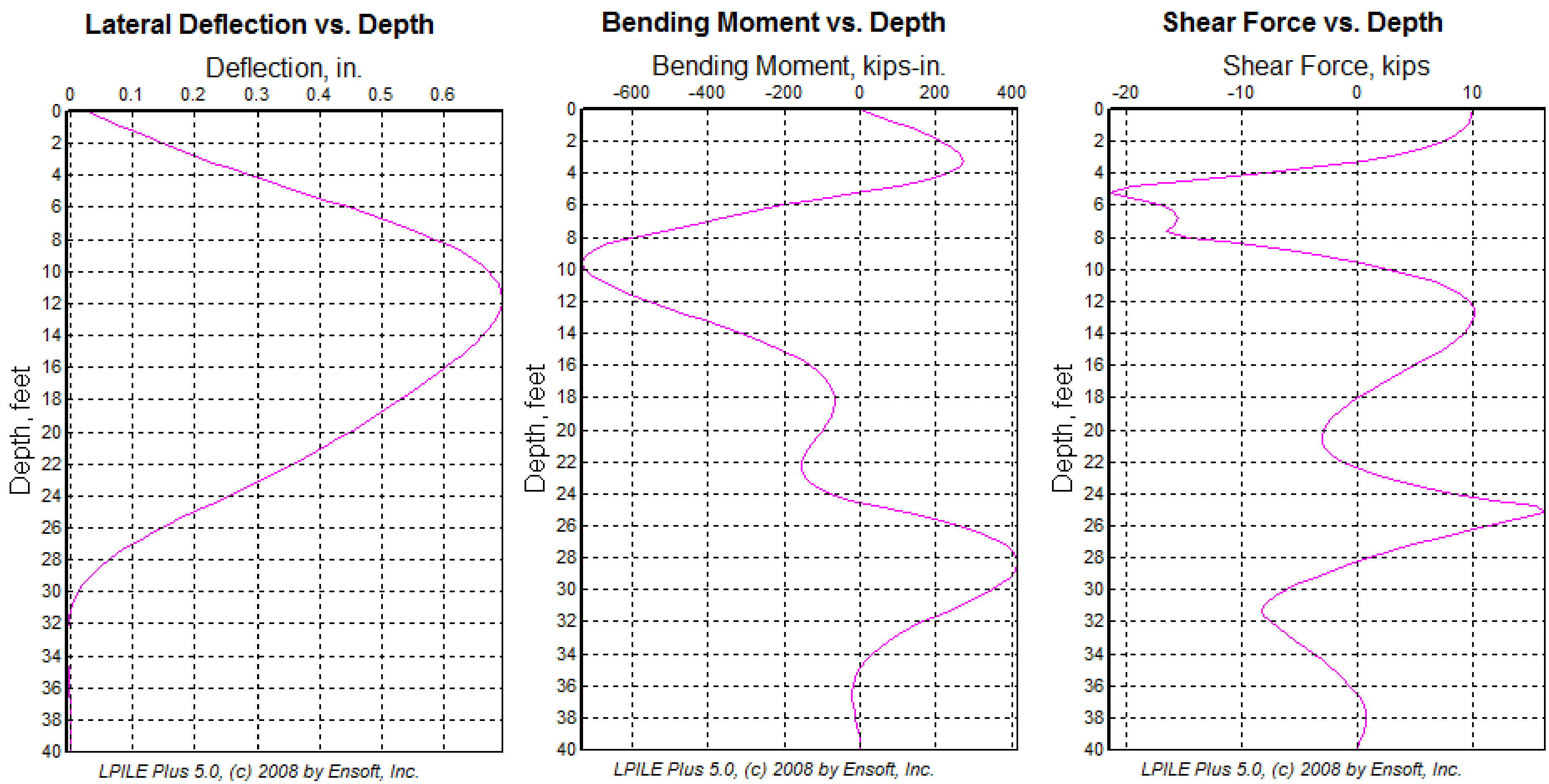

LPILE Analysis – North Approach
DSM Column Shear and Moment (Pseudo-static Conditions)
0.23g – ½ of design PGA

Airport Way South Viaduct over ARGO Railroad Yard project
Seattle, Washington

GeoEngineers

Figure 29

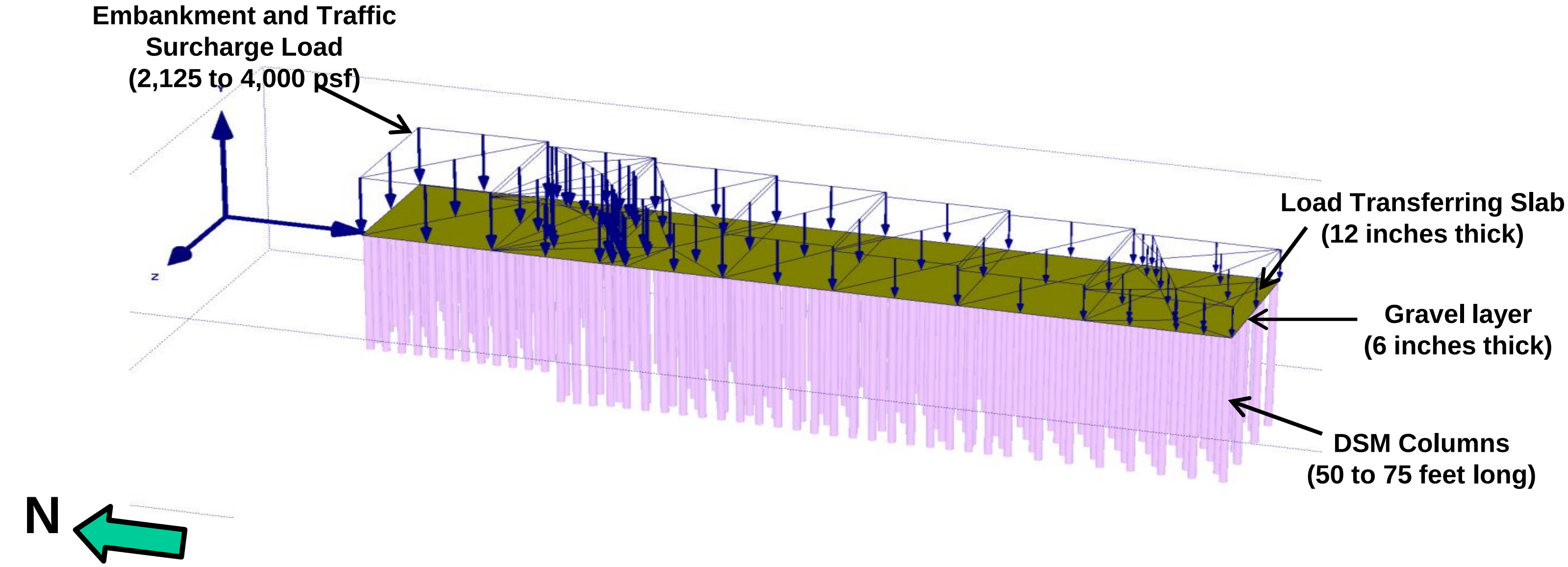

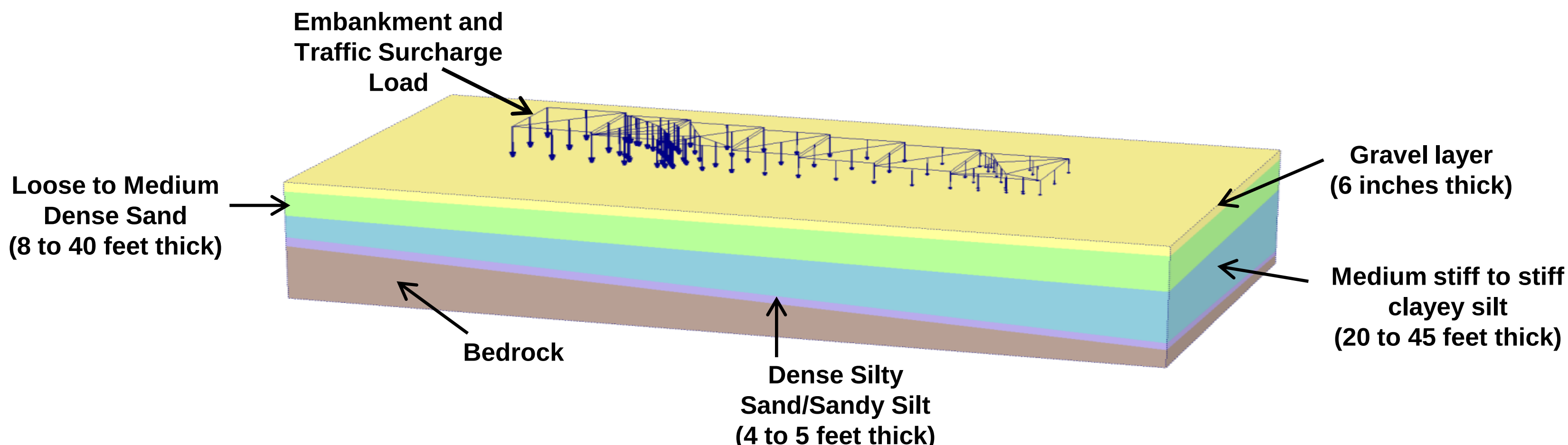

PLAXIS 3D Model – South Approach
(DSM Columns and Soil Profile)

Airport Way South Viaduct over Argo Railroad Yard Rehabilitation
Seattle, Washington

GeoEngineers

Figure 30

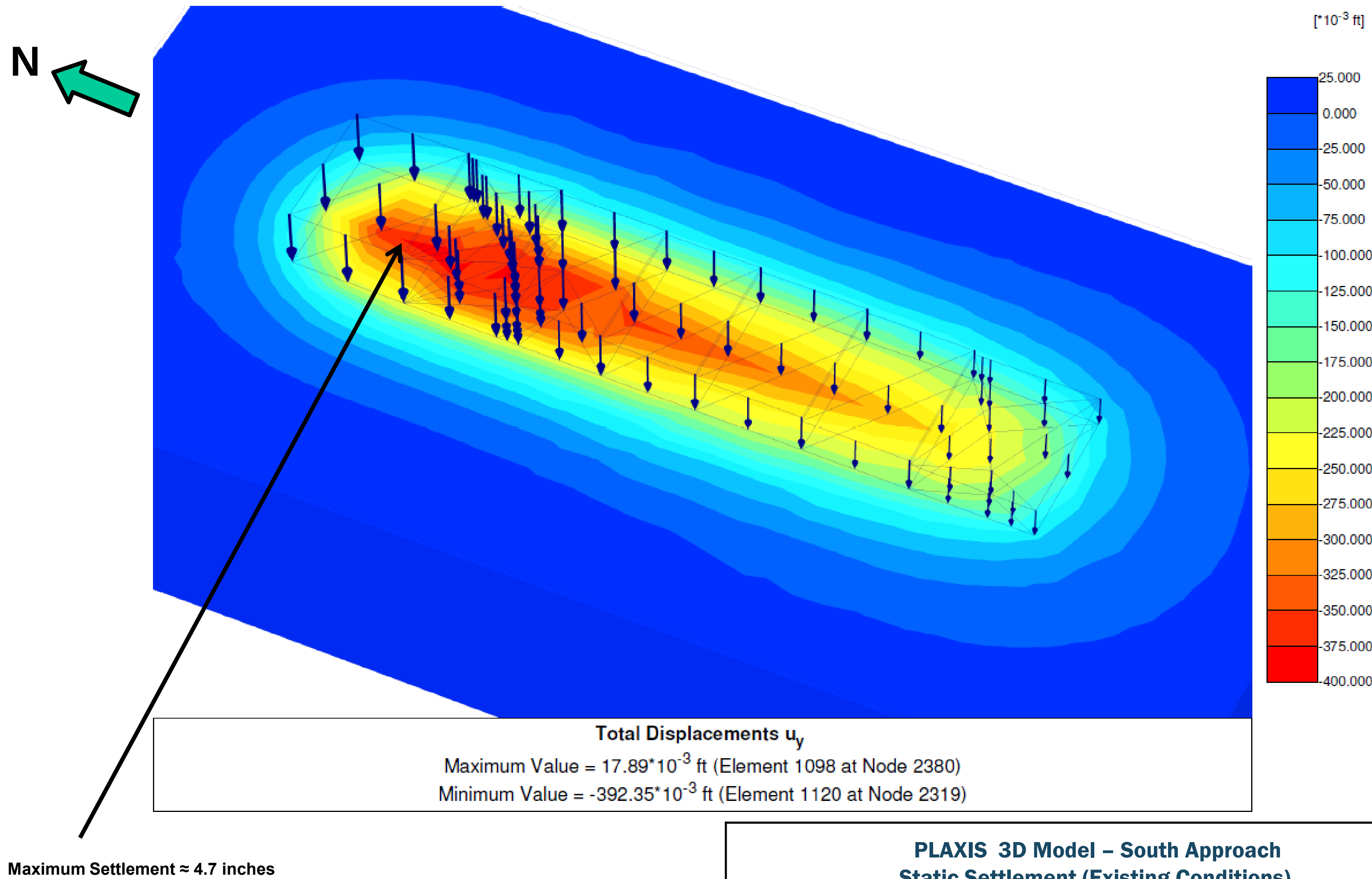

PLAXIS 3D Model – South Approach
Static Settlement (Existing Conditions)

Airport Way South Viaduct over ARGO Railroad Yard project
Seattle, Washington

GeoEngineers

Figure 31

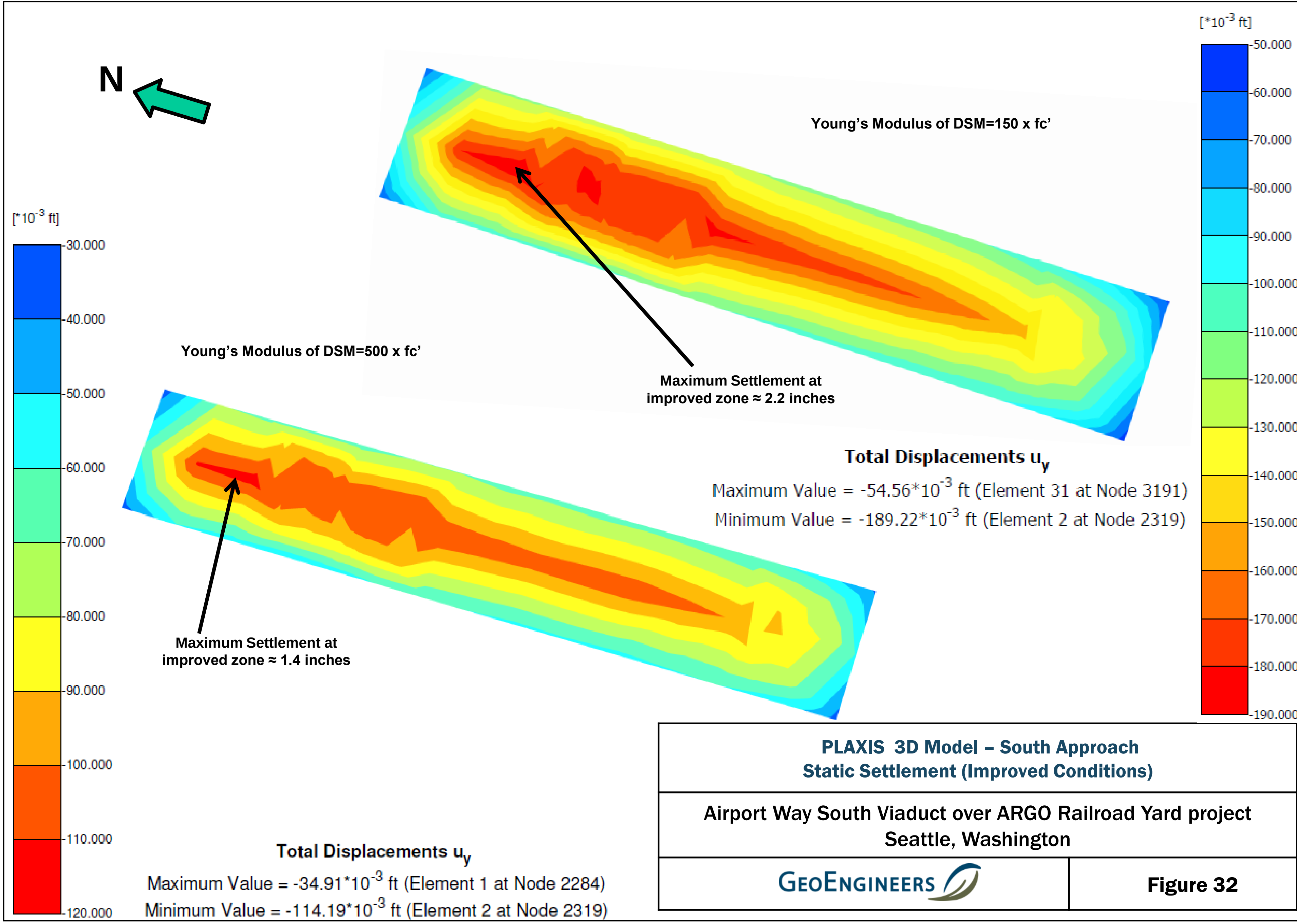

PLAXIS 3D Model – South Approach
Static Settlement (Improved Conditions)

Airport Way South Viaduct over ARGO Railroad Yard project
Seattle, Washington

GEOENGINEERS

Figure 32

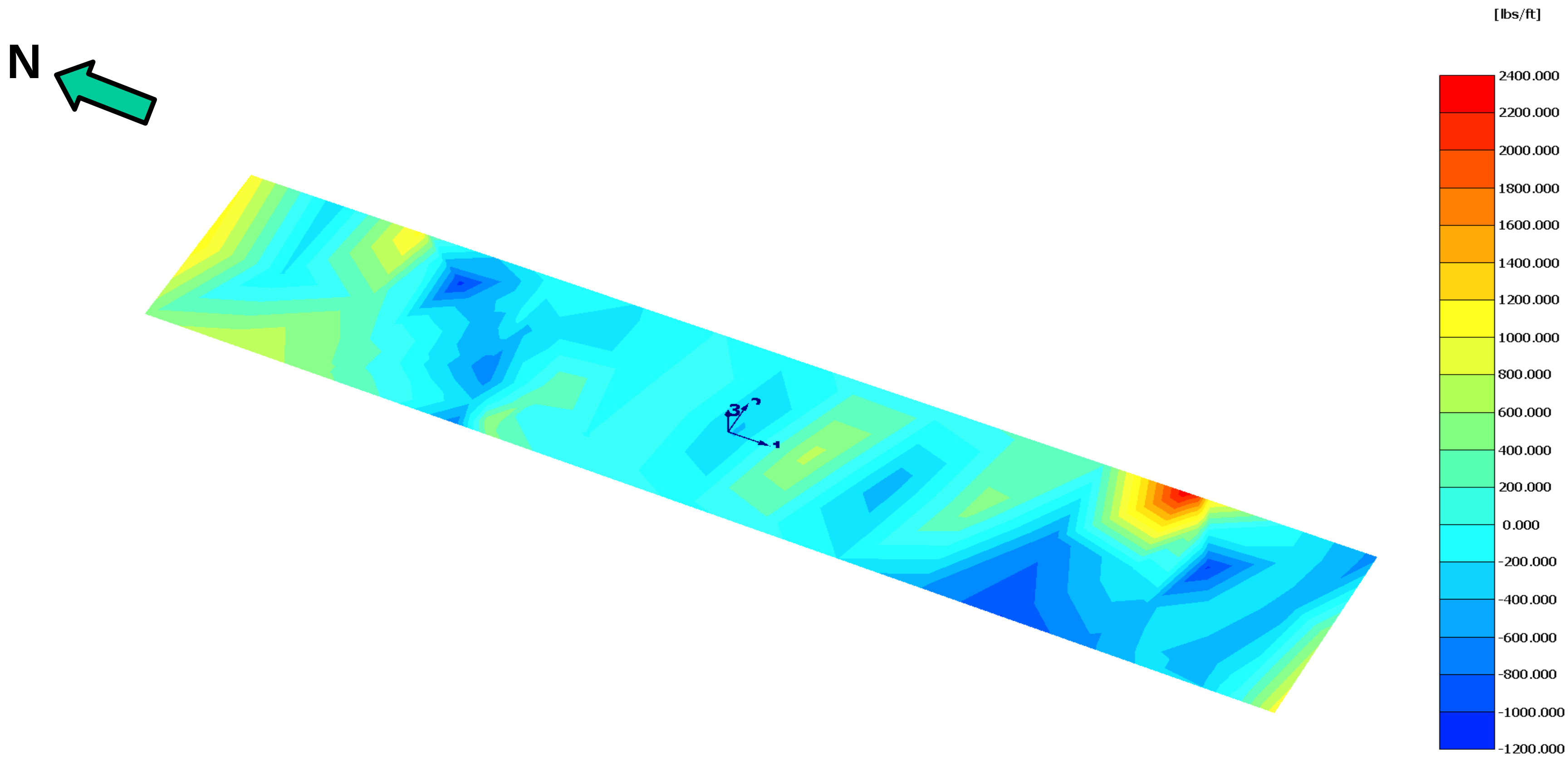

Shear Forces Q_{12}

Maximum Value = $2.37*10^3$ lbs/ft (Element 25 at Node 3046)

Minimum Value = $-1.06*10^3$ lbs/ft (Element 3 at Node 2385)

PLAXIS 3D Model – South Approach
Slab Forces (Static Conditions)

Airport Way South Viaduct over ARGO Railroad Yard project
Seattle, Washington

GEOENGINEERS

Figure 33

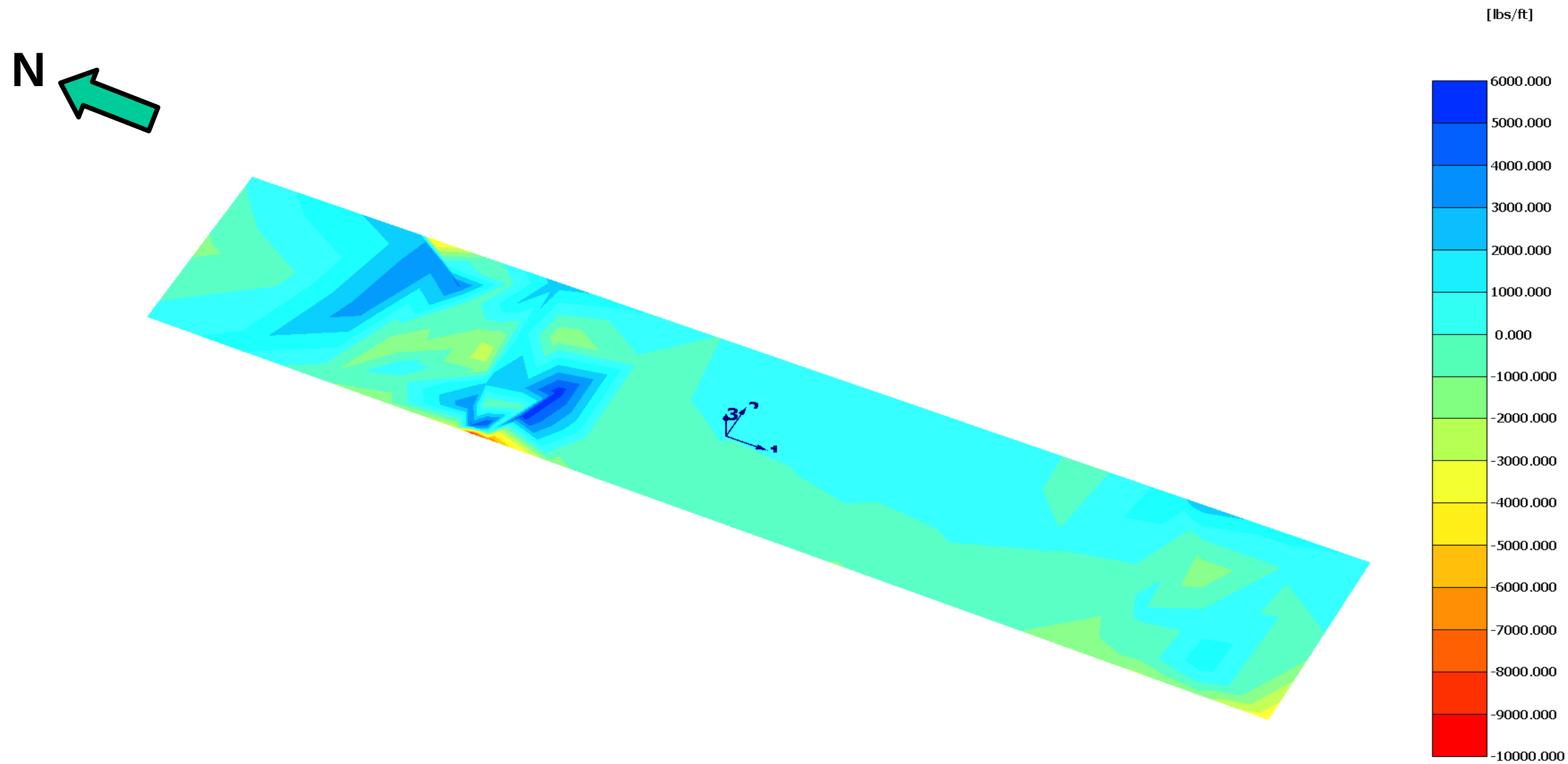

Shear Forces Q_{23}

Maximum Value = $5.58*10^{3}$ lbs/ft (Element 13 at Node 2618)

Minimum Value = $-9.33*10^{3}$ lbs/ft (Element 19 at Node 2593)

PLAXIS 3D Model – South Approach
Slab Forces (Static Conditions)

Airport Way South Viaduct over ARGO Railroad Yard project
Seattle, Washington

GeoEngineers

Figure 34

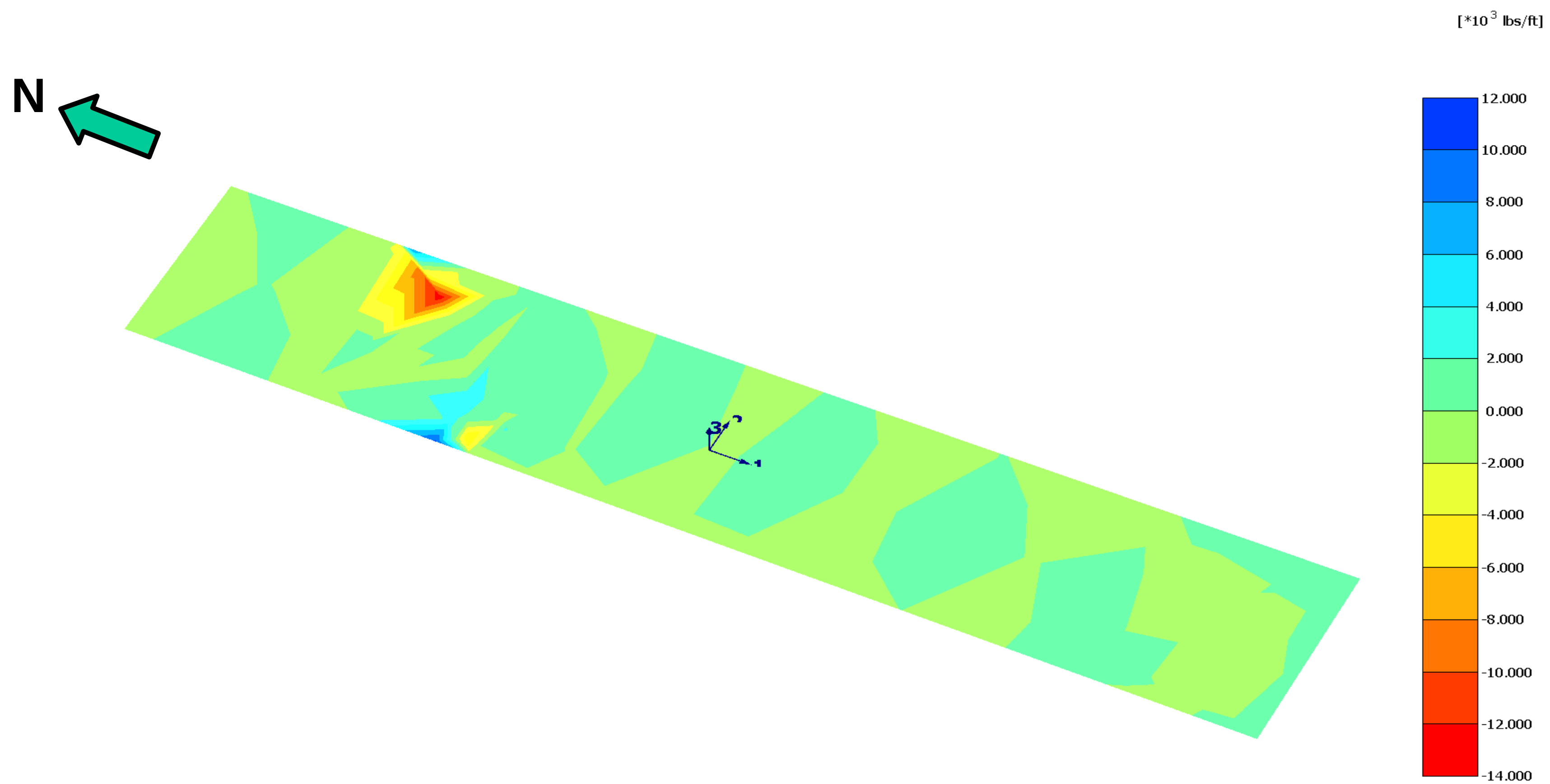

Shear Forces Q_{13}

Maximum Value = $10.41*10^3$ lbs/ft (Element 6 at Node 2592)

Minimum Value = $-13.02*10^3$ lbs/ft (Element 3 at Node 2385)

PLAXIS 3D Model – South Approach **Slab Forces (Static Conditions)**	
Airport Way South Viaduct over ARGO Railroad Yard project Seattle, Washington	
GeoEngineers	**Figure 35**

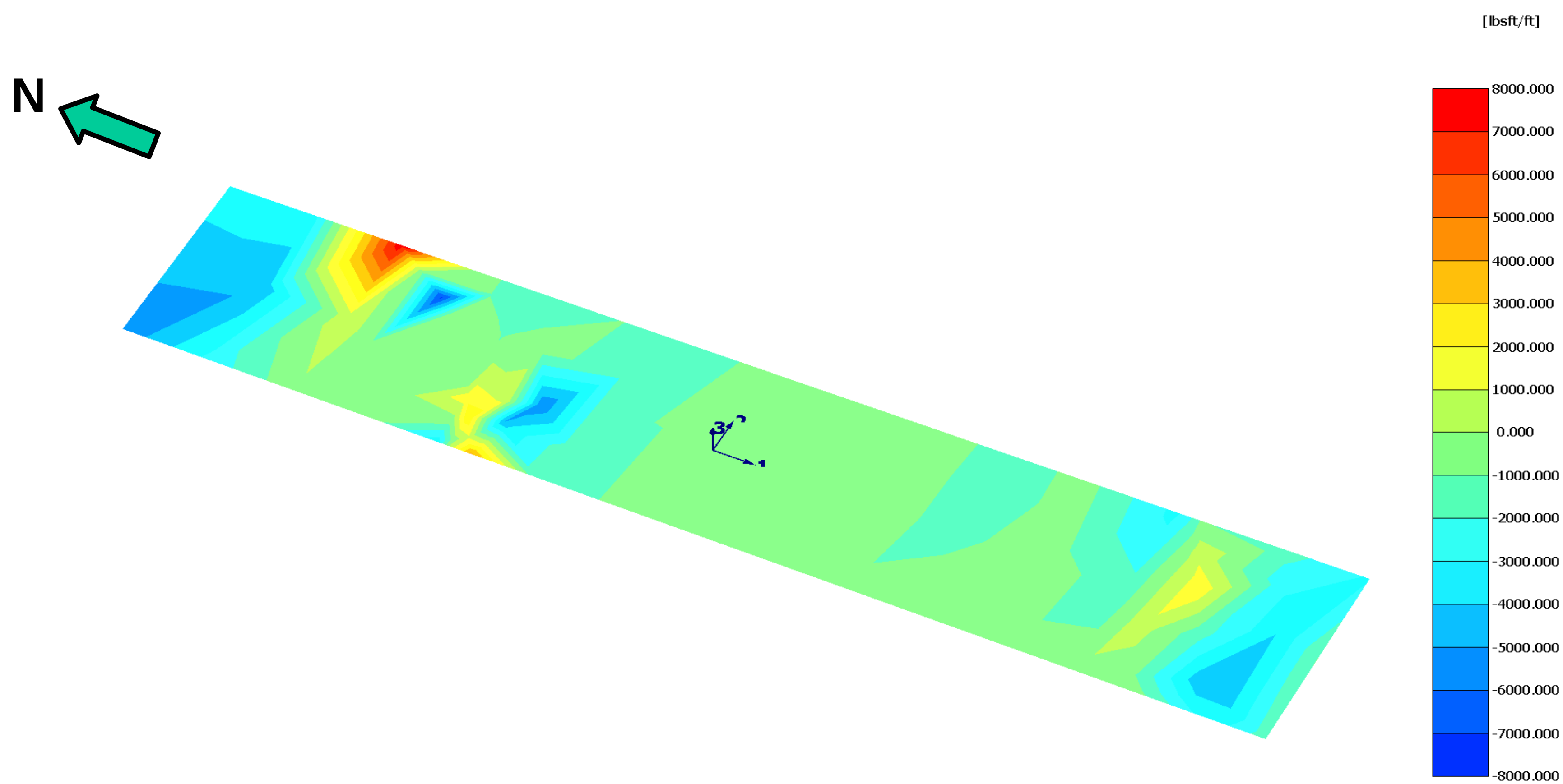

Bending Moments M_{11}

Maximum Value = 7.70×10^3 lbsft/ft (Element 3 at Node 2317)

Minimum Value = -7.16×10^3 lbsft/ft (Element 3 at Node 2385)

PLAXIS 3D Model – South Approach
Slab Forces (Static Conditions)

Airport Way South Viaduct over ARGO Railroad Yard project
Seattle, Washington

GeoEngineers

Figure 36

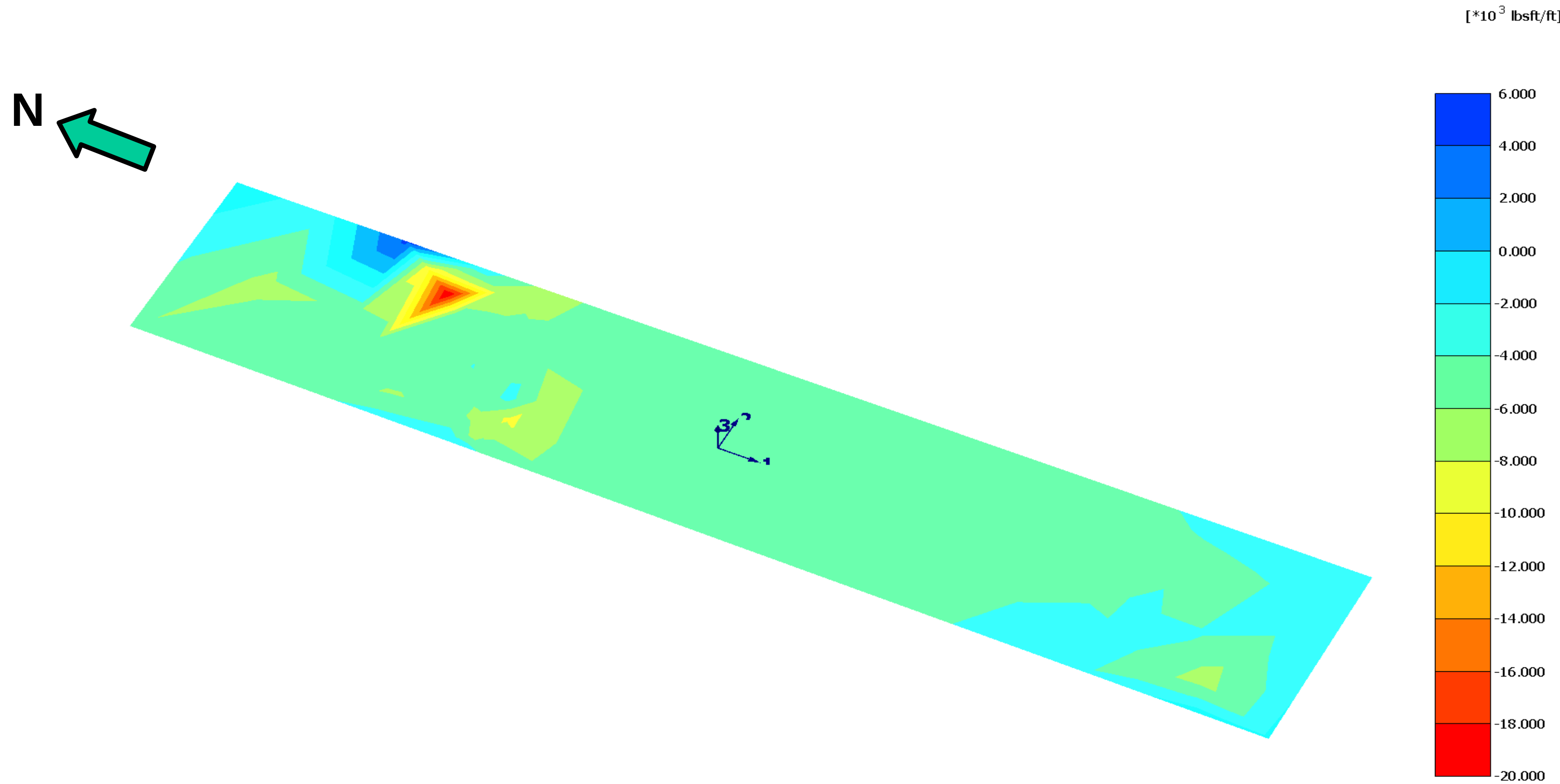

Bending Moments M_{22}

Maximum Value = $4.92*10^3$ lbsft/ft (Element 3 at Node 2317)

Minimum Value = $-19.74*10^3$ lbsft/ft (Element 3 at Node 2385)

PLAXIS 3D Model – South Approach
Slab Forces (Static Conditions)

Airport Way South Viaduct over ARGO Railroad Yard project
Seattle, Washington

GeoEngineers

Figure 37

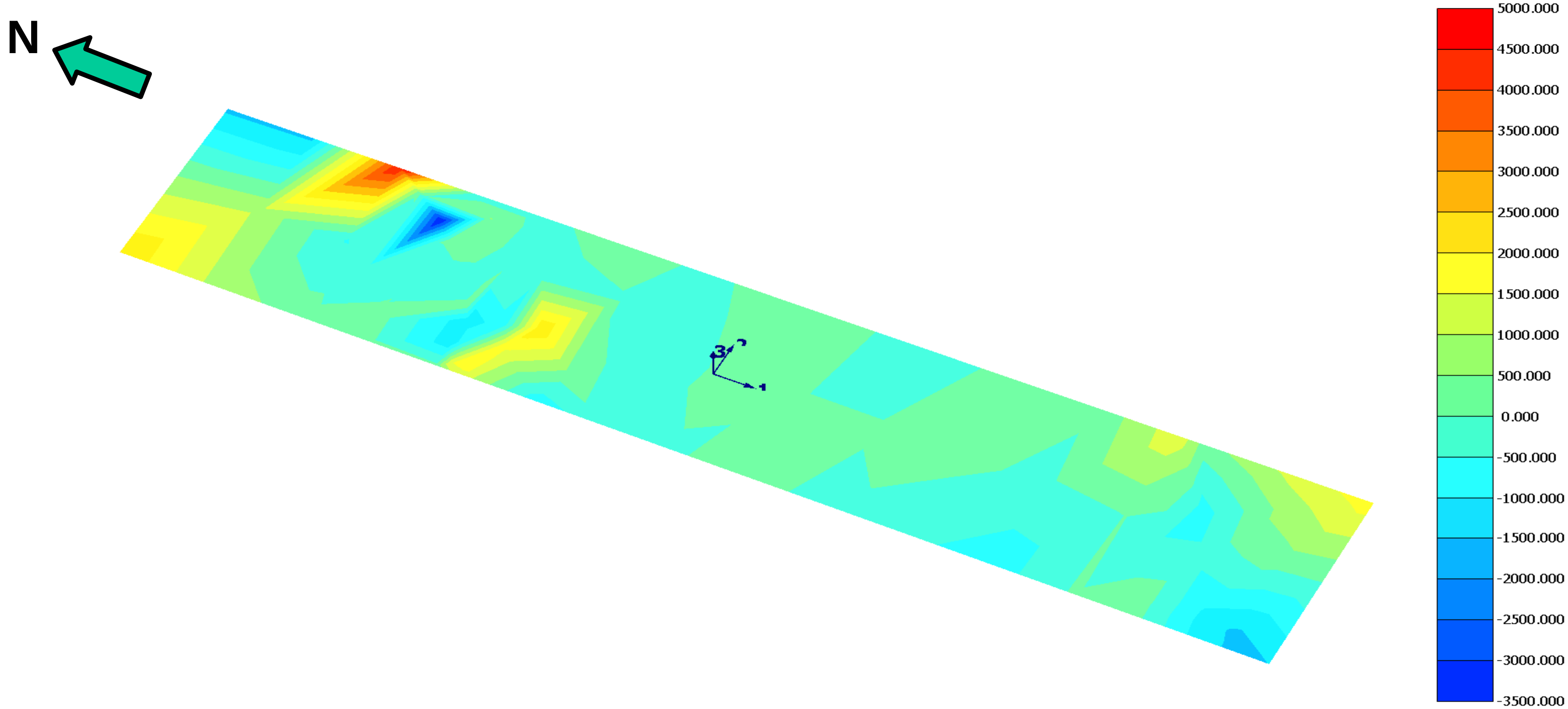

Torsion Moments M_{12}

Maximum Value = $4.65*10^3$ lbsft/ft (Element 3 at Node 2317)

Minimum Value = $-3.46*10^3$ lbsft/ft (Element 3 at Node 2385)

PLAXIS 3D Model – South Approach
Slab Forces (Static Conditions)

Airport Way South Viaduct over ARGO Railroad Yard project
Seattle, Washington

GeoEngineers

Figure 38

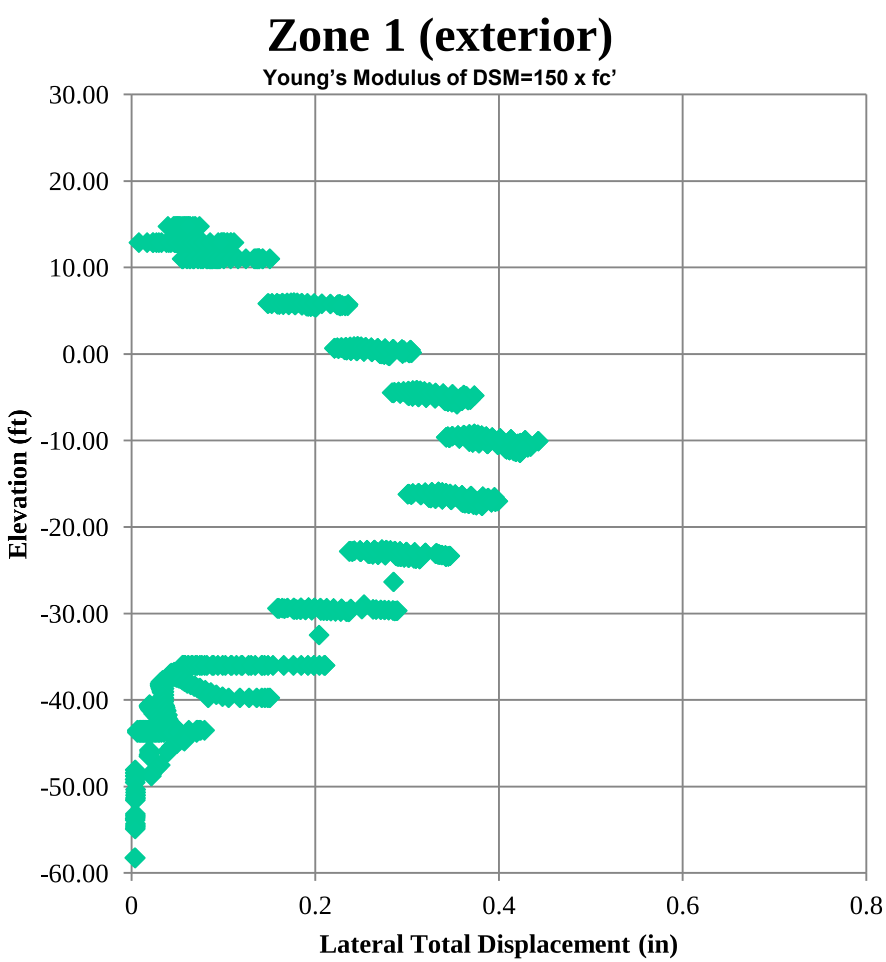

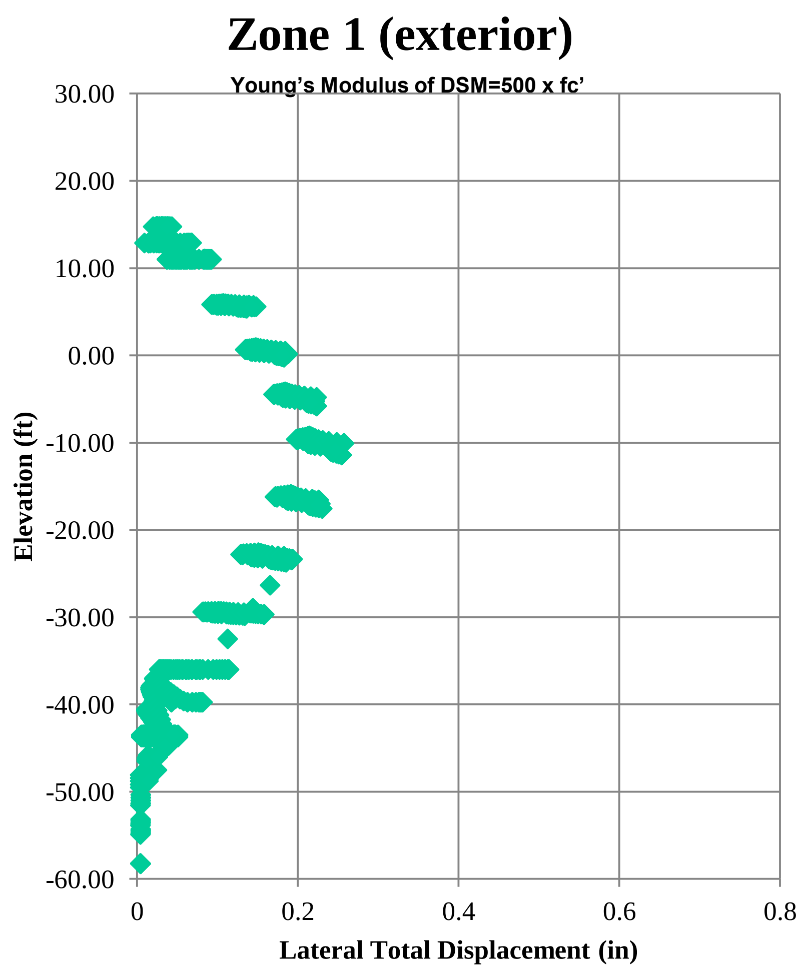

PLAXIS 3D Model – South Approach (Zone 1 Exterior)
DSM Lateral Displacement (Static Conditions)

Airport Way South Viaduct over ARGO Railroad Yard project
Seattle, Washington

GEOENGINEERS

Figure 39

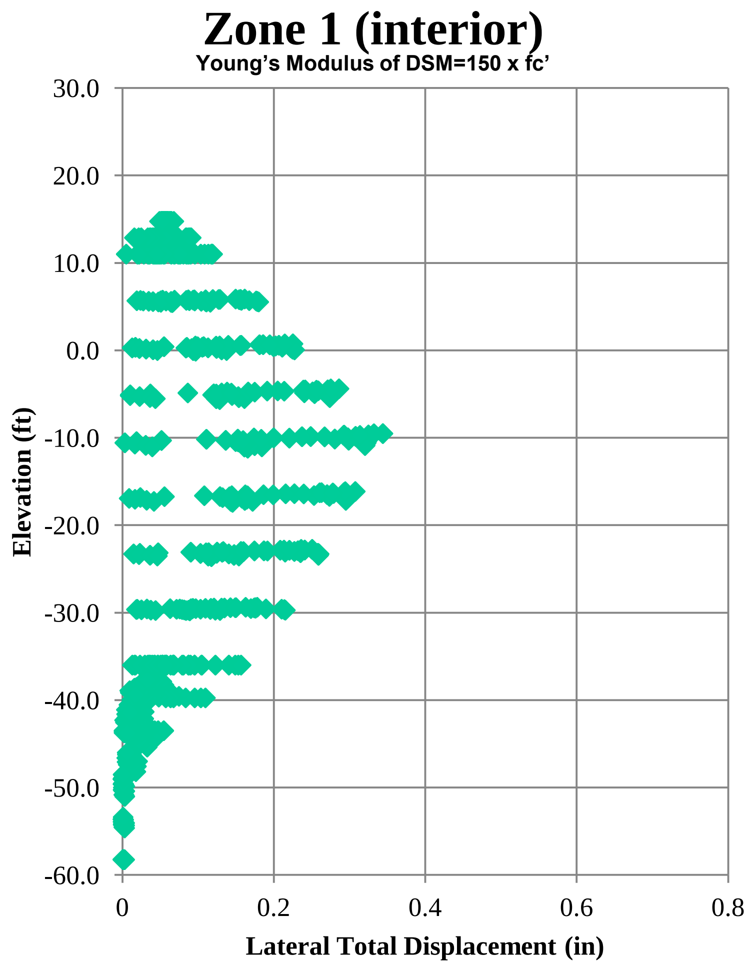

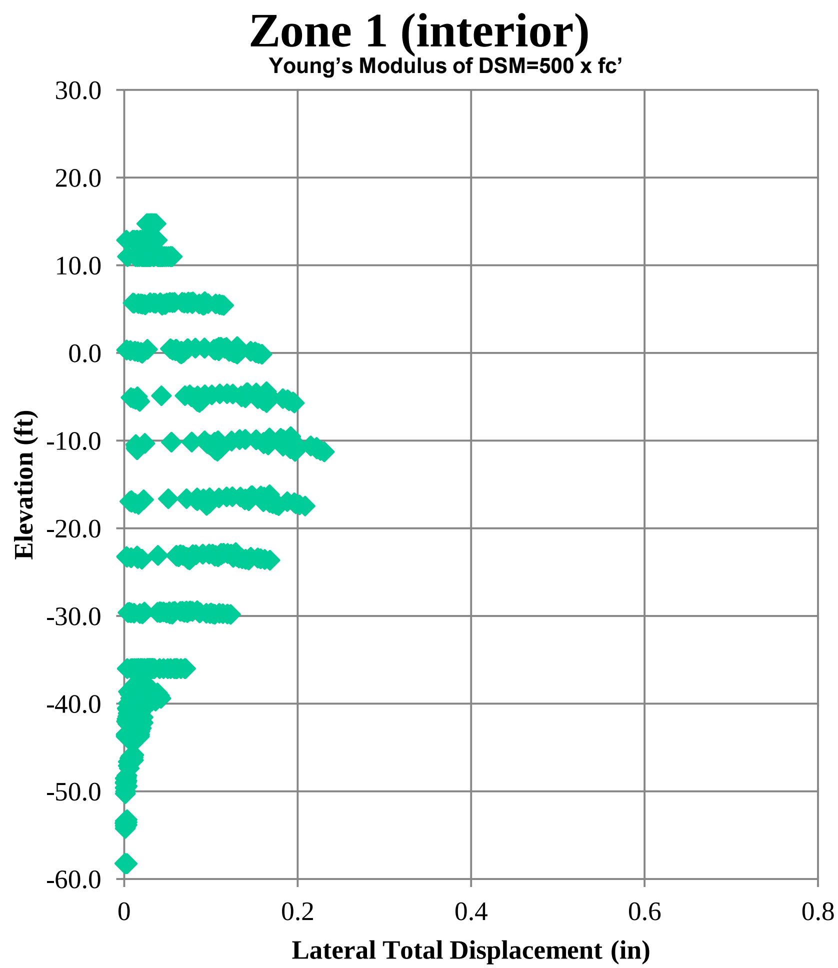

PLAXIS 3D Model – South Approach (Zone 1 Interior)
DSM Lateral Displacement (Static Conditions)

Airport Way South Viaduct over ARGO Railroad Yard project
Seattle, Washington

GEOENGINEERS

Figure 40

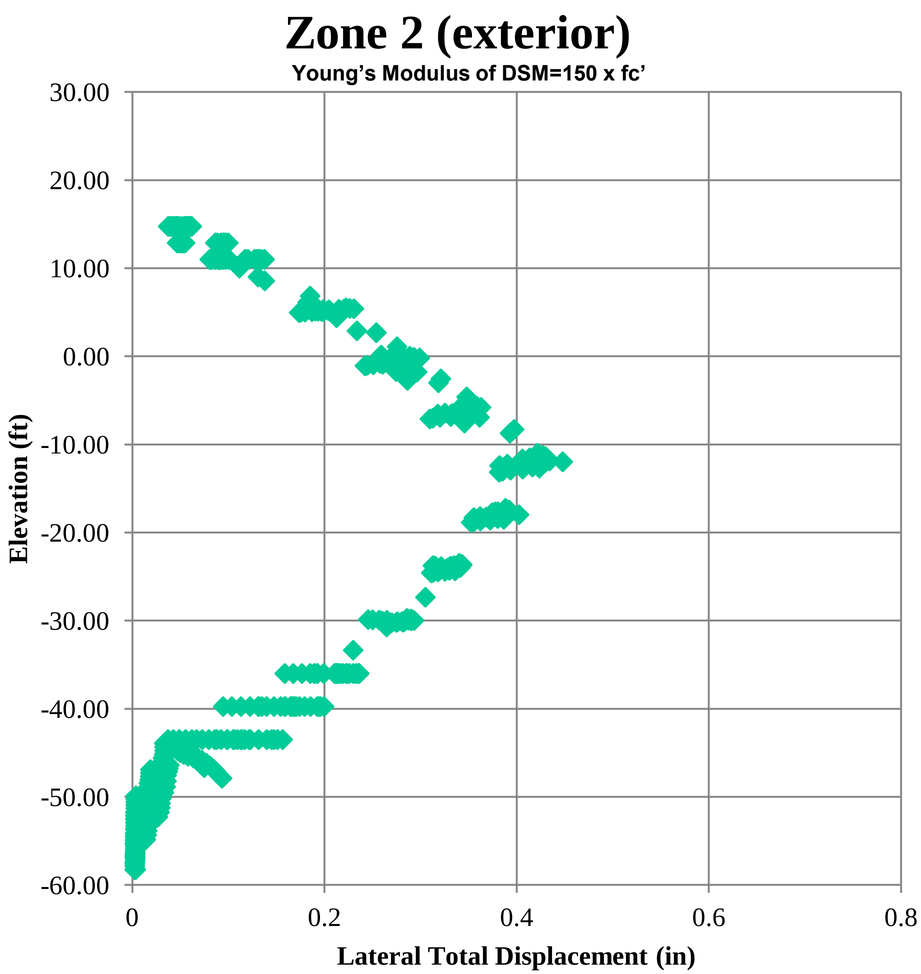

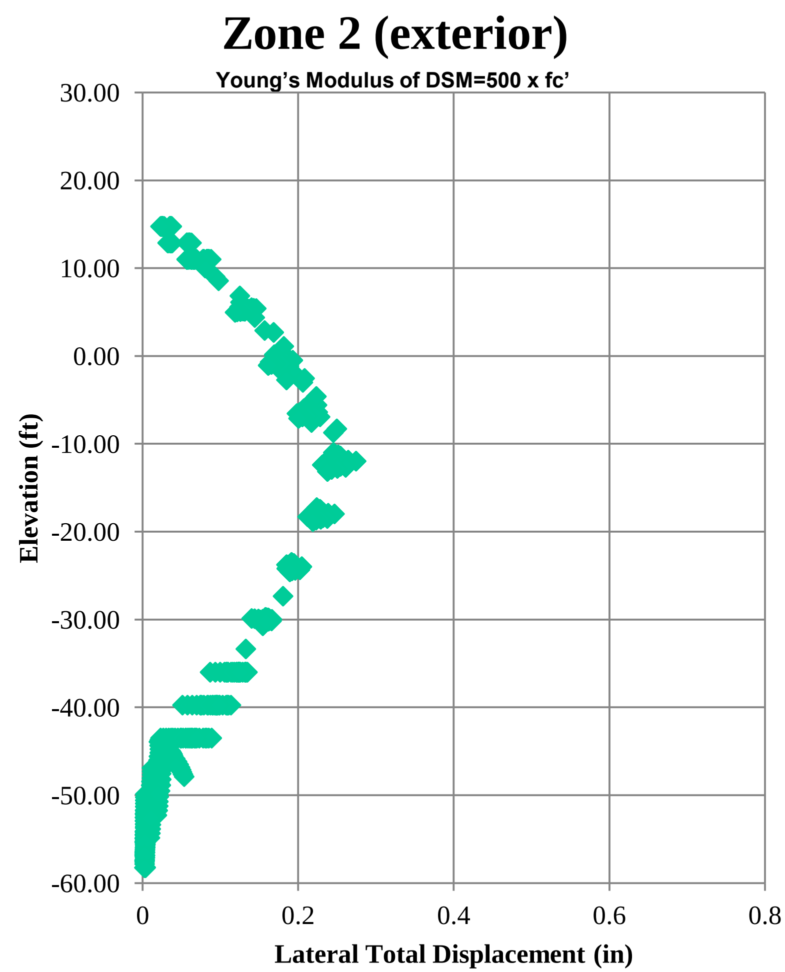

PLAXIS 3D Model – South Approach (Zone 2 Exterior)
DSM Lateral Displacement (Static Conditions)

Airport Way South Viaduct over ARGO Railroad Yard project
Seattle, Washington

GEOENGINEERS

Figure 41

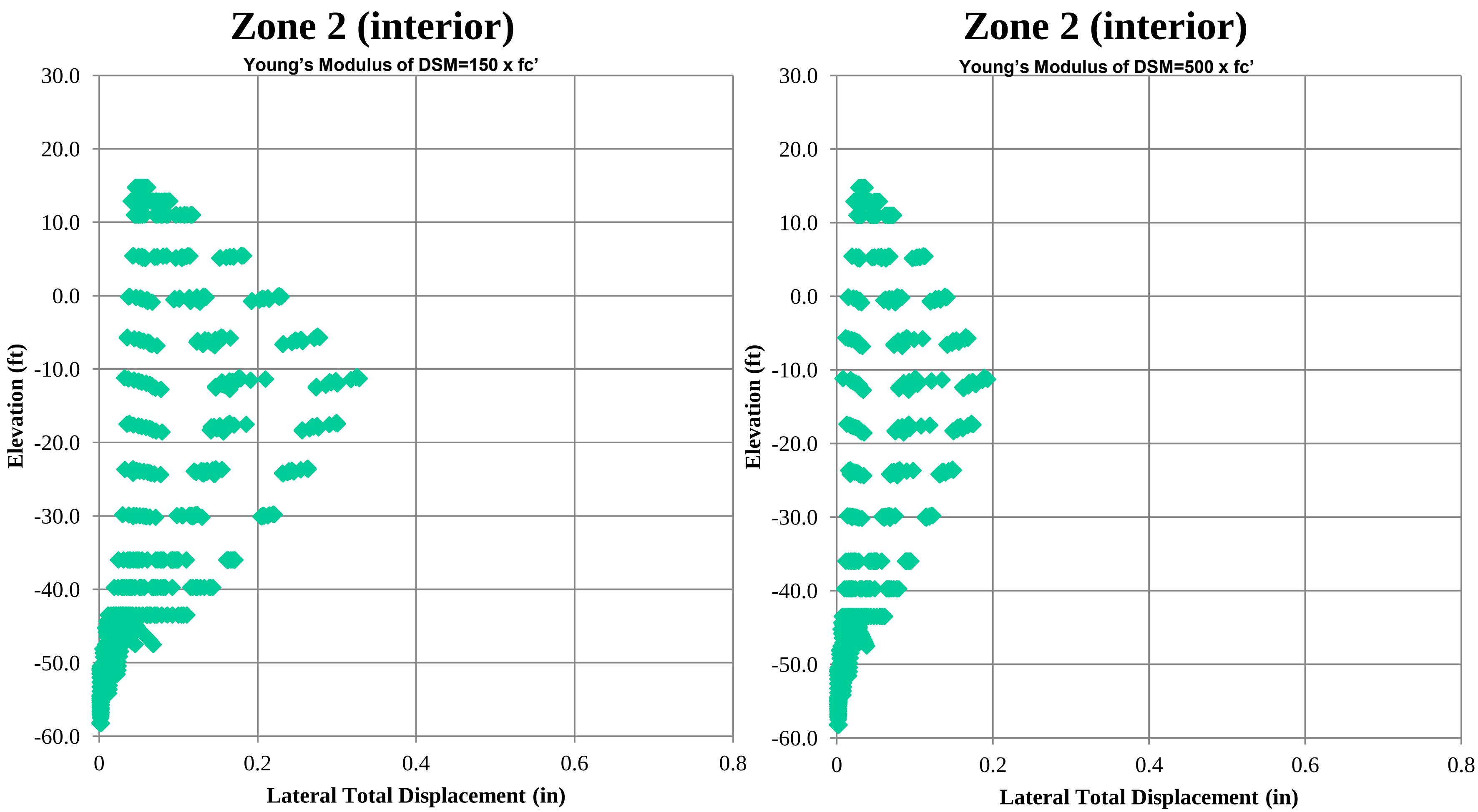

PLAXIS 3D Model – South Approach (Zone 2 Interior) DSM Lateral Displacement (Static Conditions)	
Airport Way South Viaduct over ARGO Railroad Yard project Seattle, Washington	
GEOENGINEERS	**Figure 42**

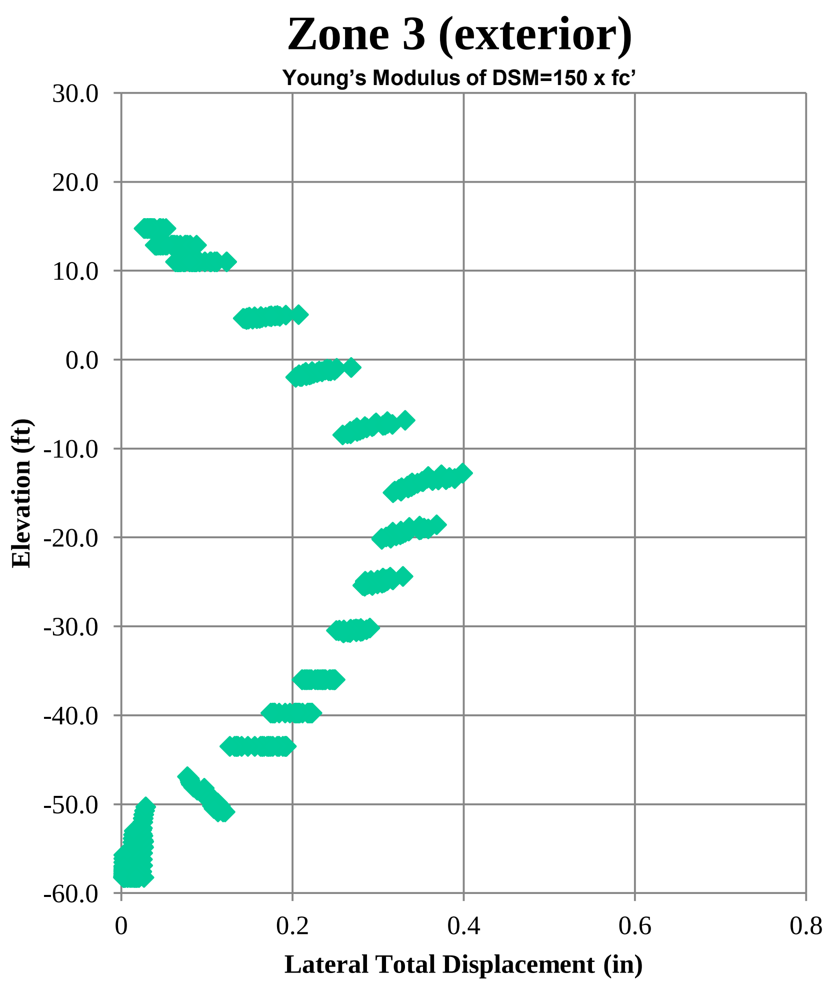

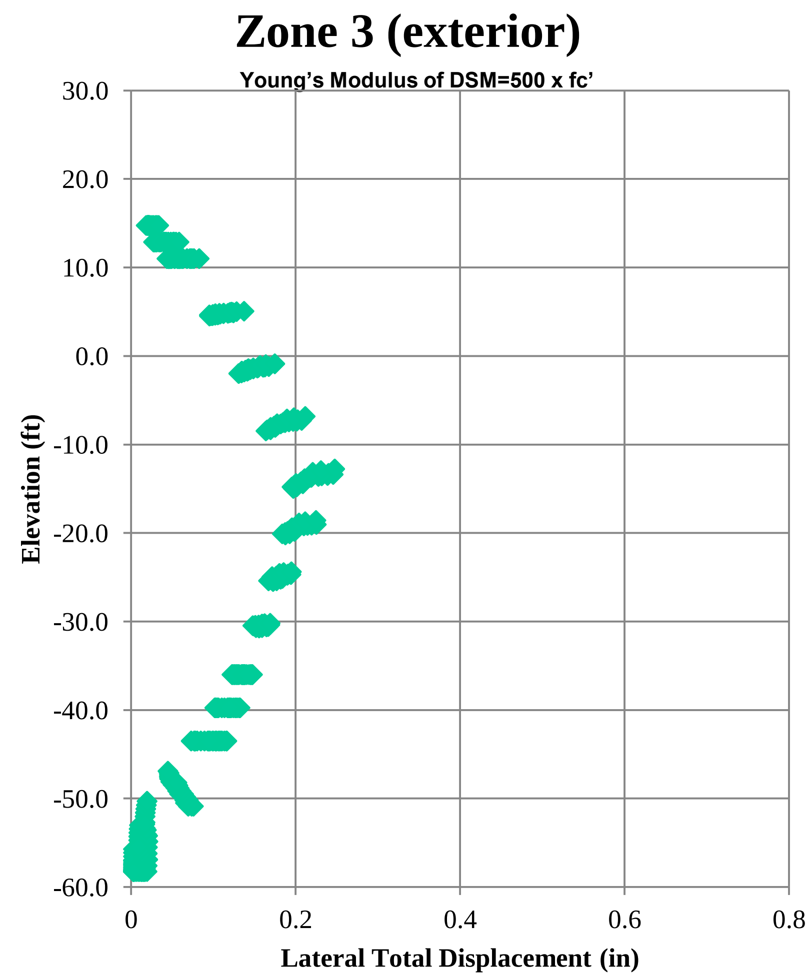

PLAXIS 3D Model – South Approach (Zone 3 Exterior) **DSM Lateral Displacement (Static Conditions)**	
Airport Way South Viaduct over ARGO Railroad Yard project Seattle, Washington	
GeoEngineers	**Figure 43**

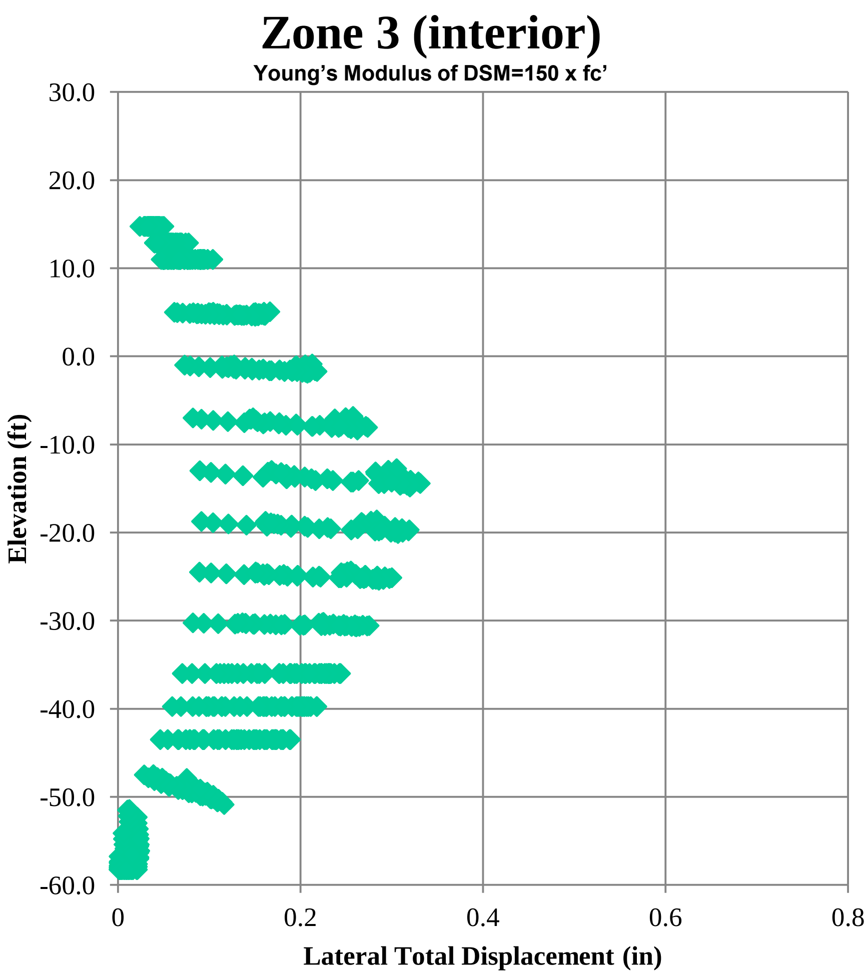

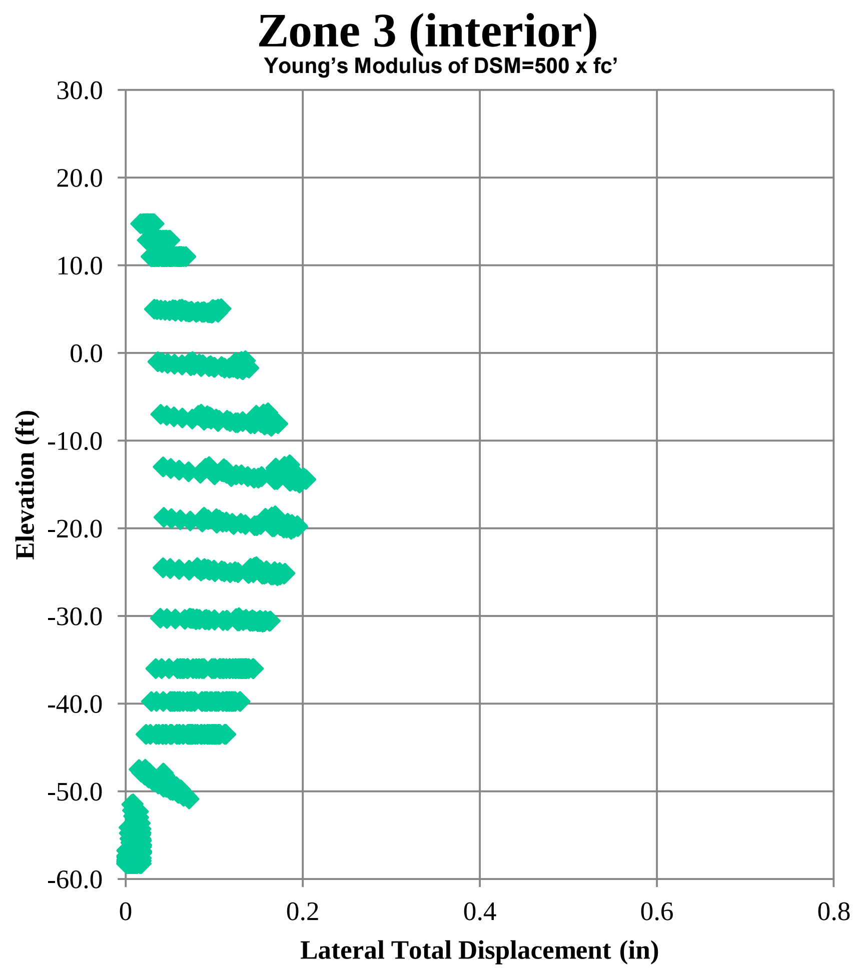

PLAXIS 3D Model – South Approach (Zone 3 Interior)
DSM Lateral Displacement (Static Conditions)

Airport Way South Viaduct over ARGO Railroad Yard project
Seattle, Washington

GeoEngineers

Figure 44

Young's Modulus of DSM=150 x fc'

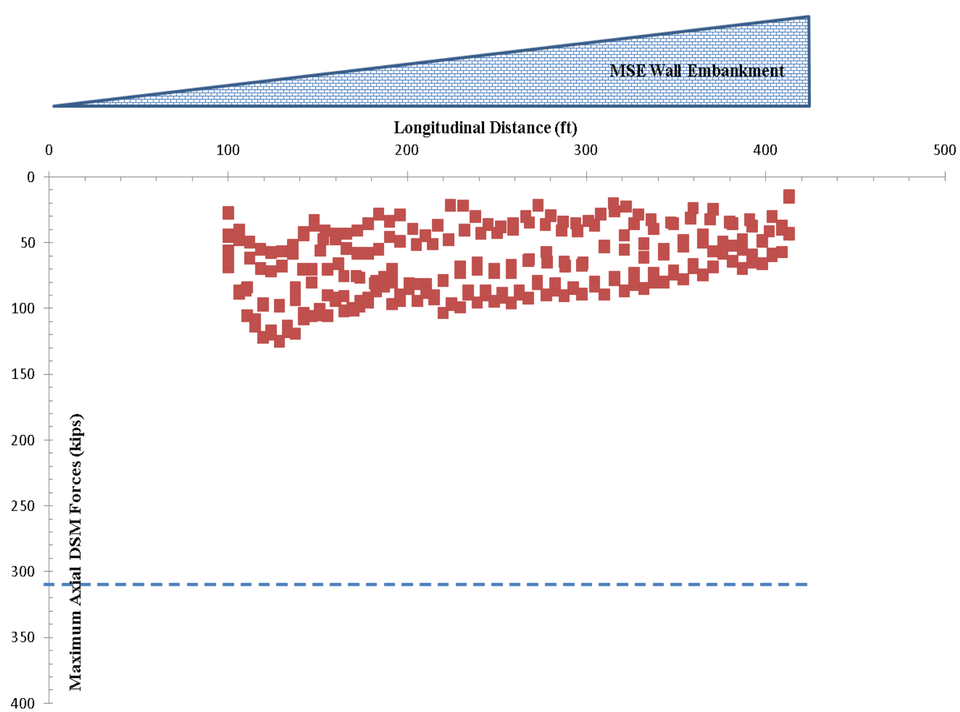

Young's Modulus of DSM=500 x fc'

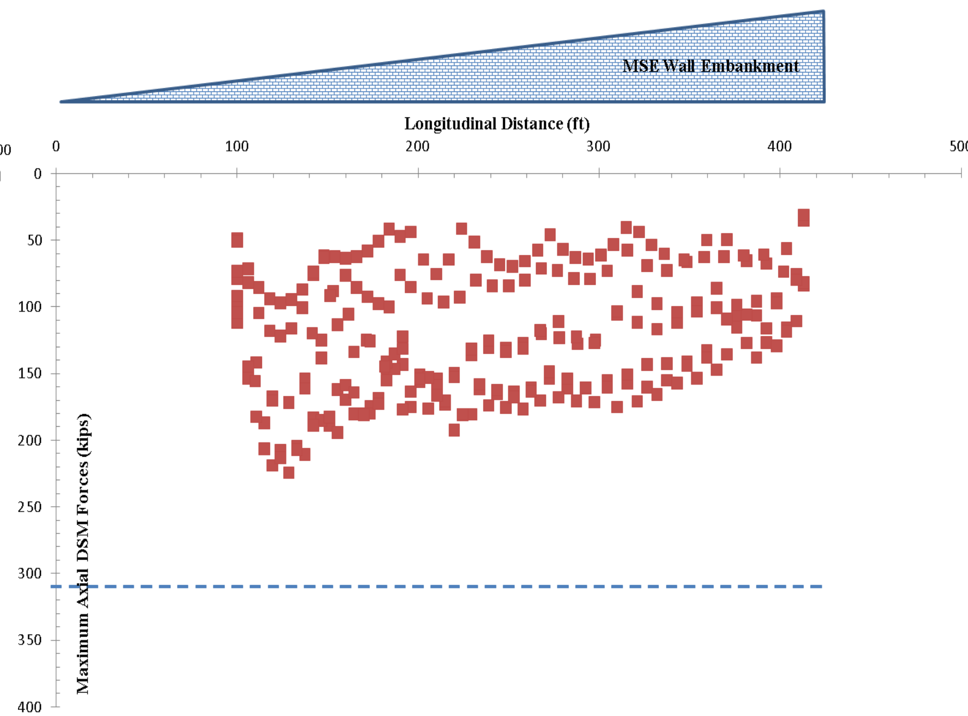

PLAXIS 3D Model – South Approach
DSM Maximum Axial Forces (Static Conditions)

Airport Way South Viaduct over ARGO Railroad Yard project
Seattle, Washington

GeoEngineers

Figure 45

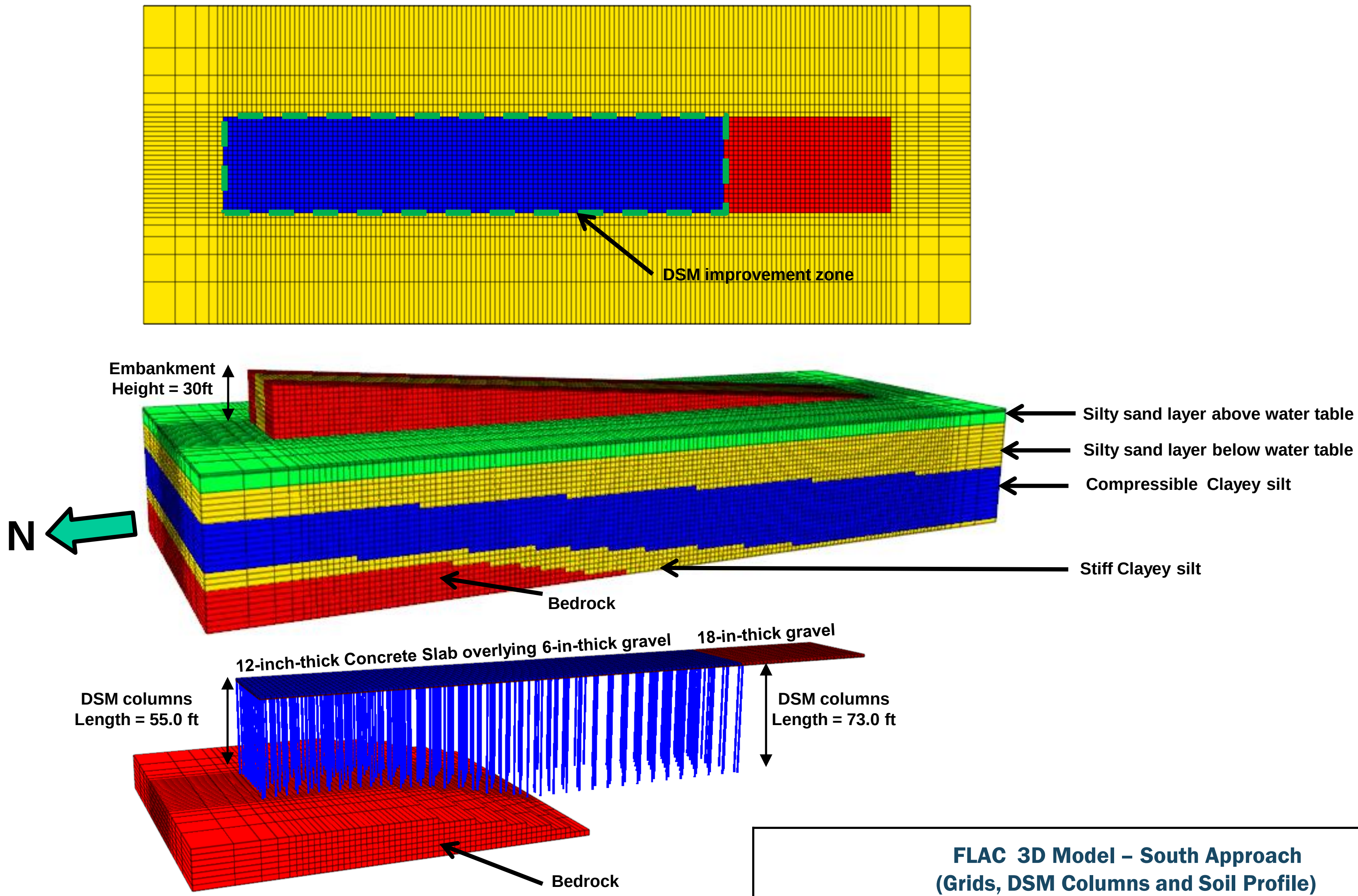

FLAC 3D Model – South Approach
(Grids, DSM Columns and Soil Profile)

Airport Way South Viaduct over ARGO Railroad Yard project
Seattle, Washington

GEOENGINEERS

Figure 46

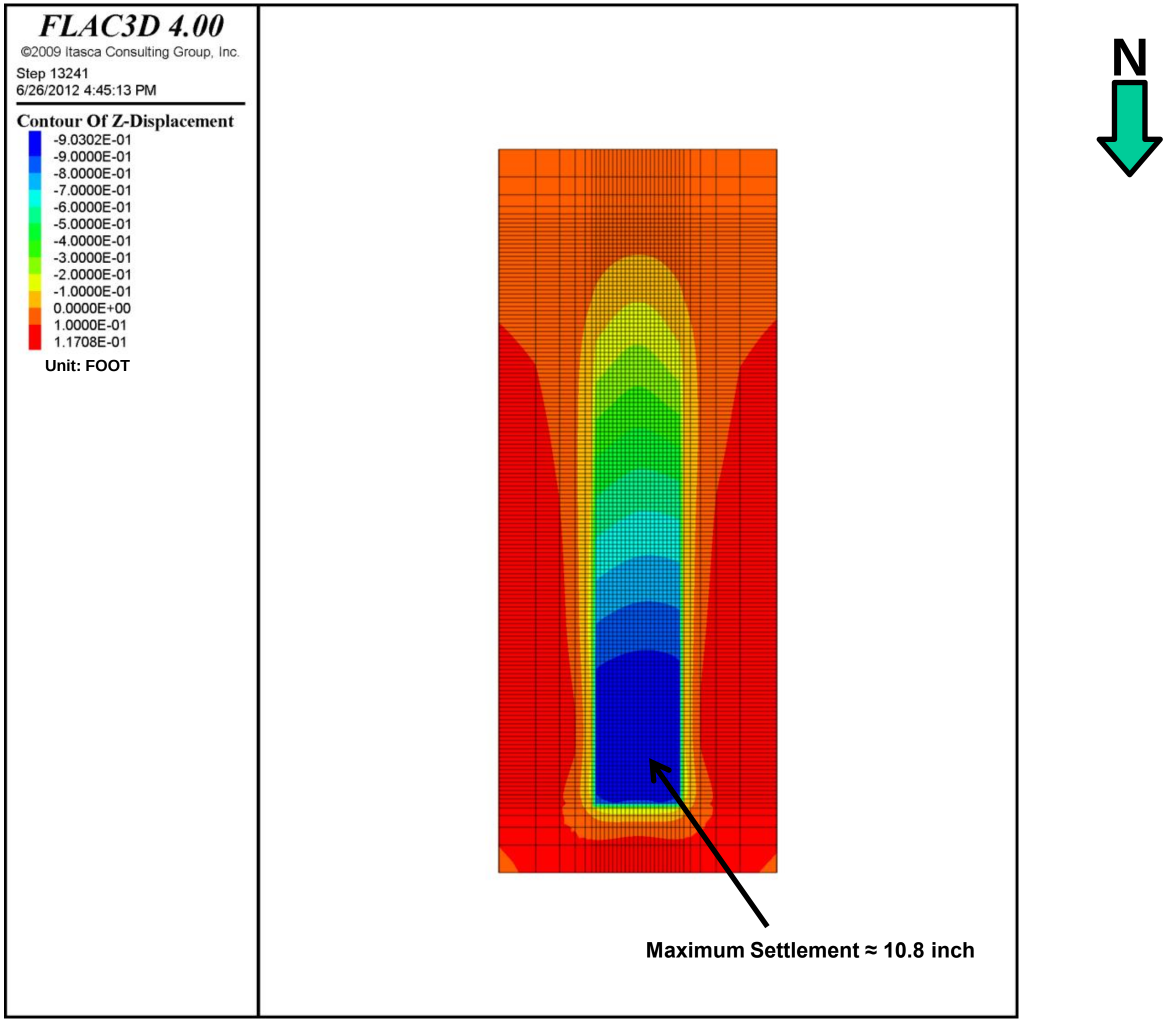

FLAC 3D Model – South Approach
Liquefaction-Induced Settlement (Existing Conditions)

Airport Way South Viaduct over ARGO Railroad Yard project
Seattle, Washington

GeoEngineers

Figure 47

N

Young's Modulus of DSM=150 x fc'

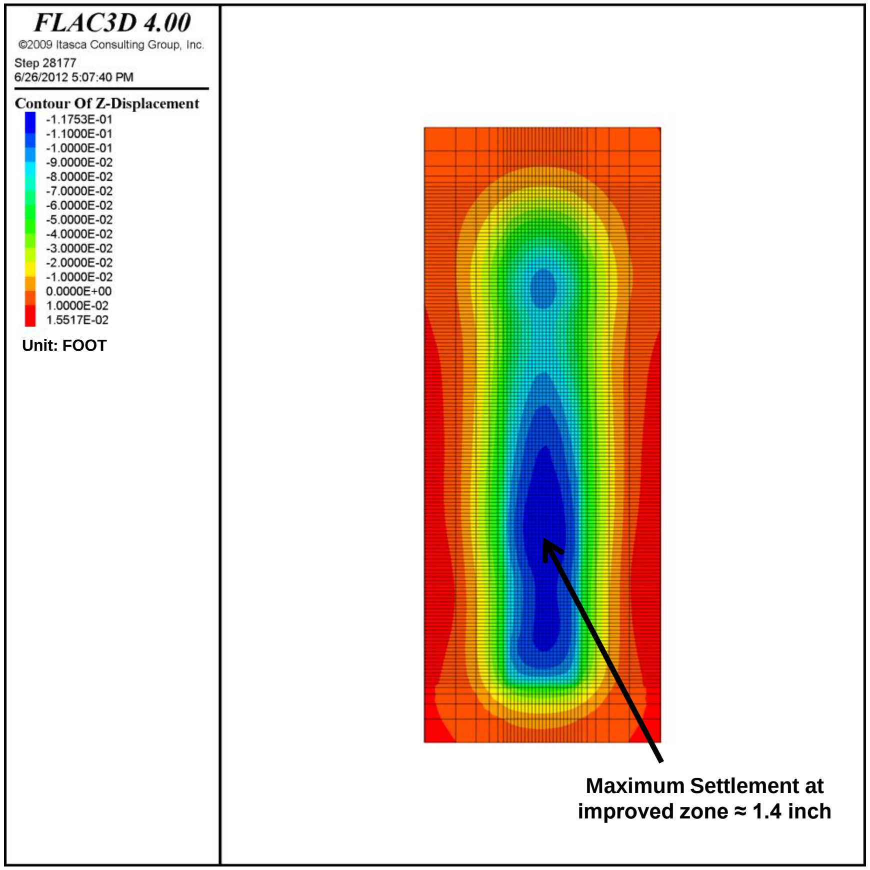

Young's Modulus of DSM=500 x fc'

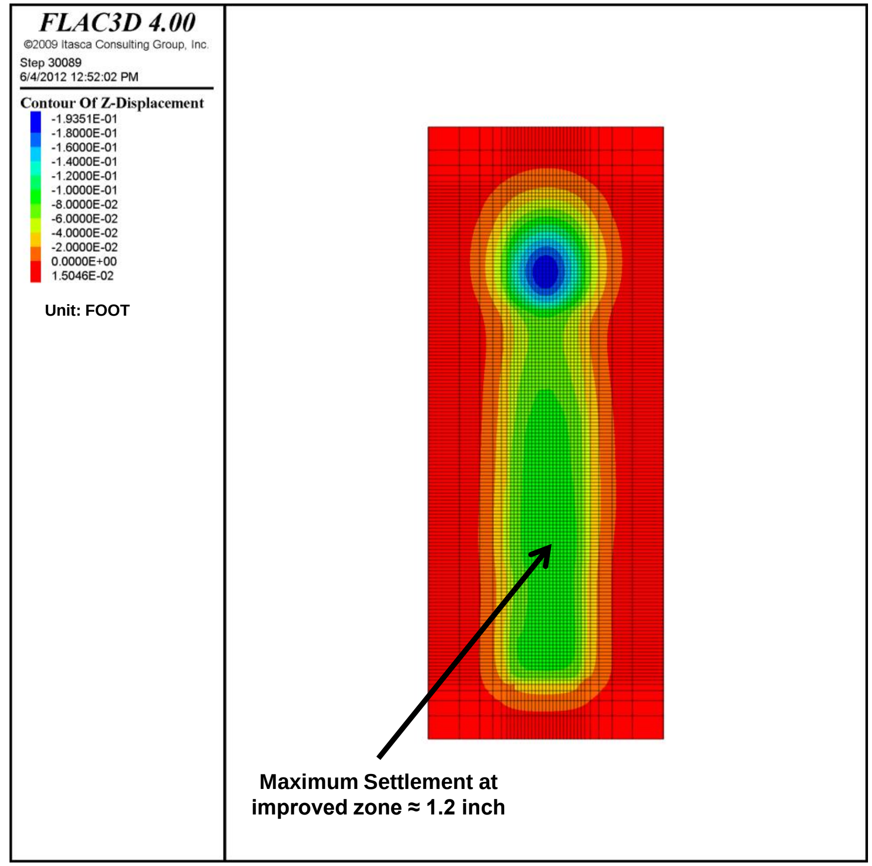

FLAC 3D Model – South Approach
Liquefaction-Induced Settlement (Improved Conditions)

Airport Way South Viaduct over ARGO Railroad Yard project
Seattle, Washington

GeoEngineers

Figure 48

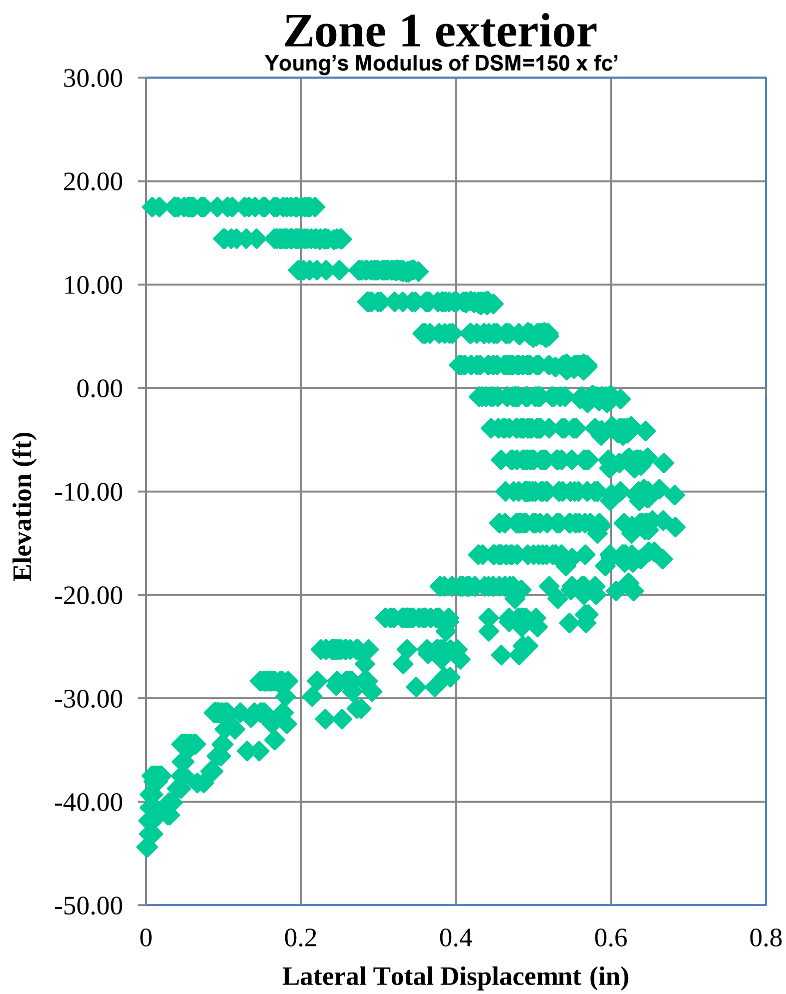

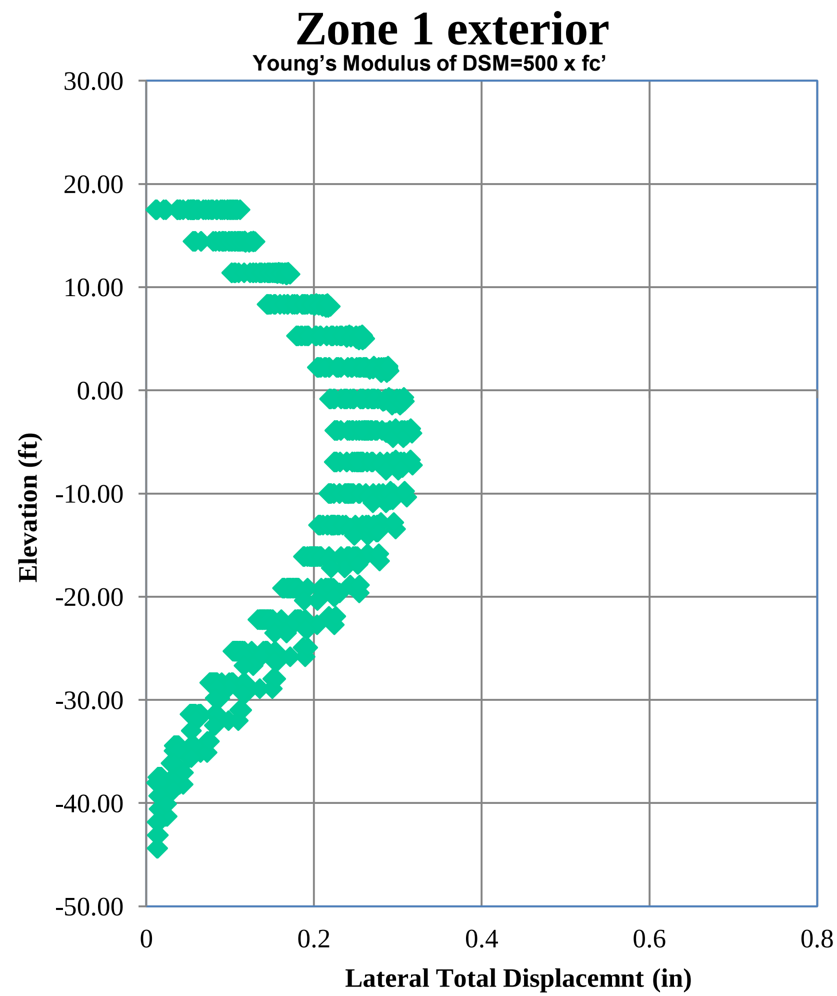

FLAC 3D Model – South Approach (Zone 1 Exterior)
DSM Lateral Displacement (Liquefied Conditions)

Airport Way South Viaduct over ARGO Railroad Yard project
Seattle, Washington

GeoEngineers

Figure 49

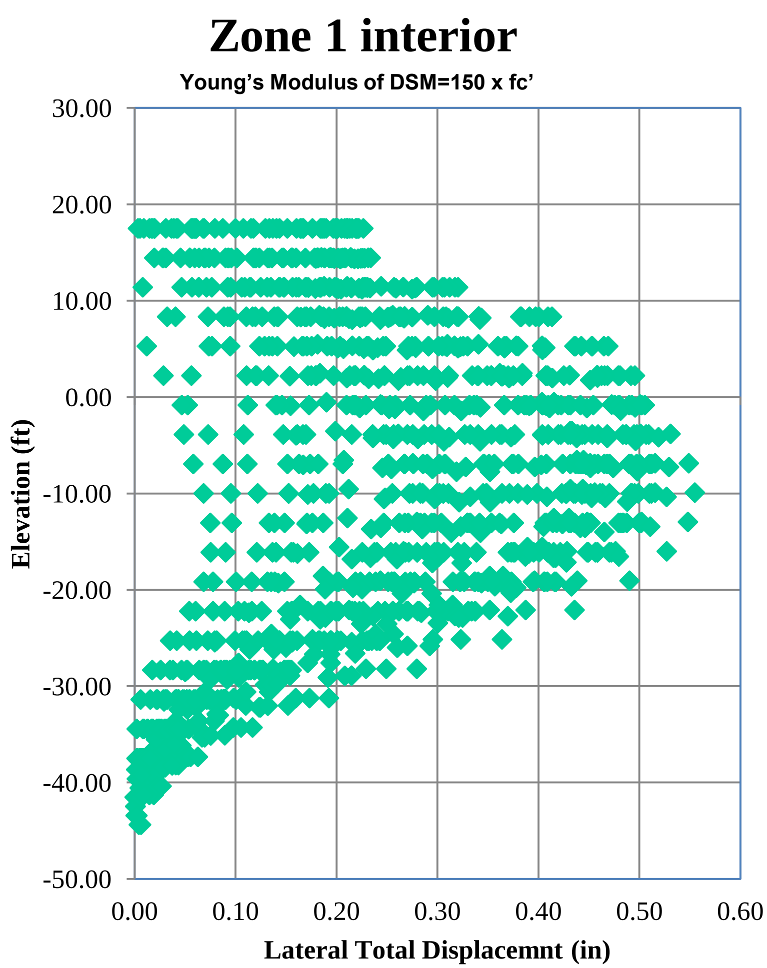

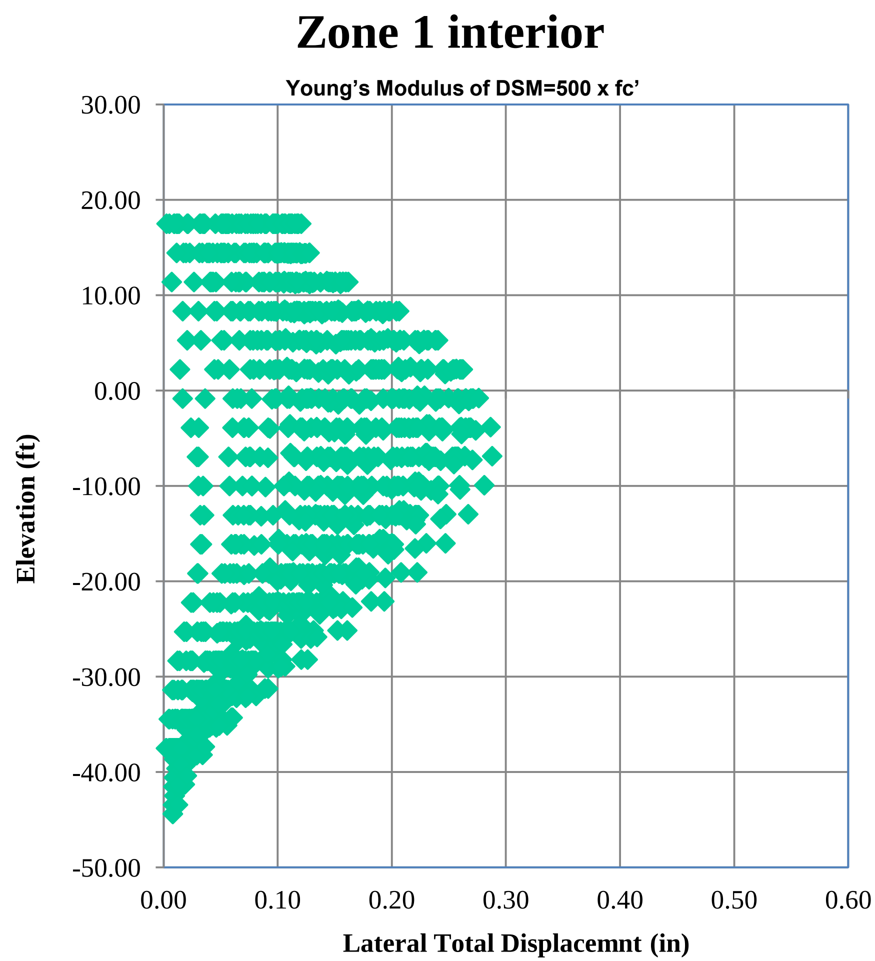

FLAC 3D Model – South Approach (Zone 1 Interior)
DSM Lateral Displacement (Liquefied Conditions)

Airport Way South Viaduct over ARGO Railroad Yard project
Seattle, Washington

GeoEngineers

Figure 50

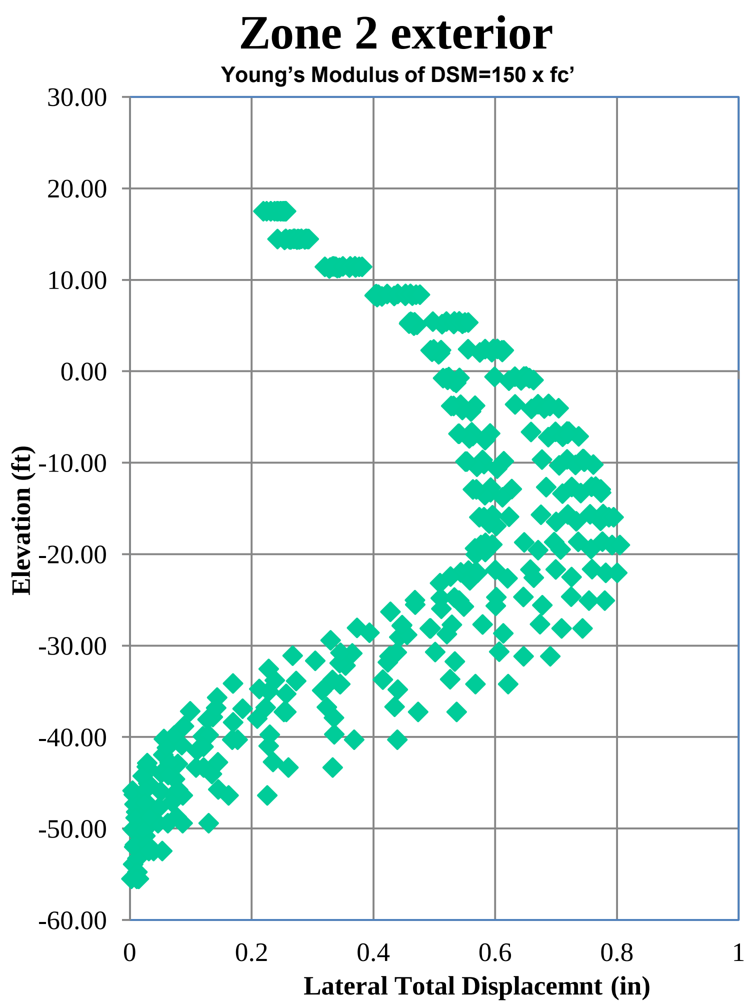

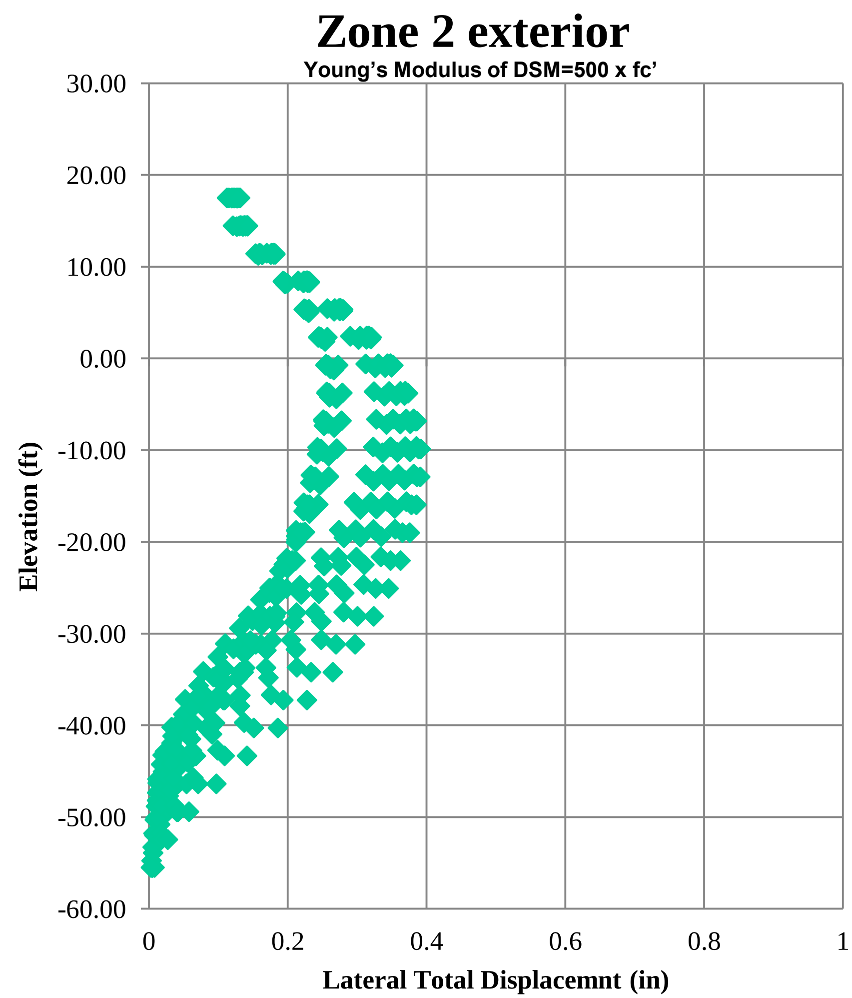

FLAC 3D Model – South Approach (Zone 2 Exterior)
DSM Lateral Displacement (Liquefied Conditions)

Airport Way South Viaduct over ARGO Railroad Yard project
Seattle, Washington

GEOENGINEERS

Figure 51

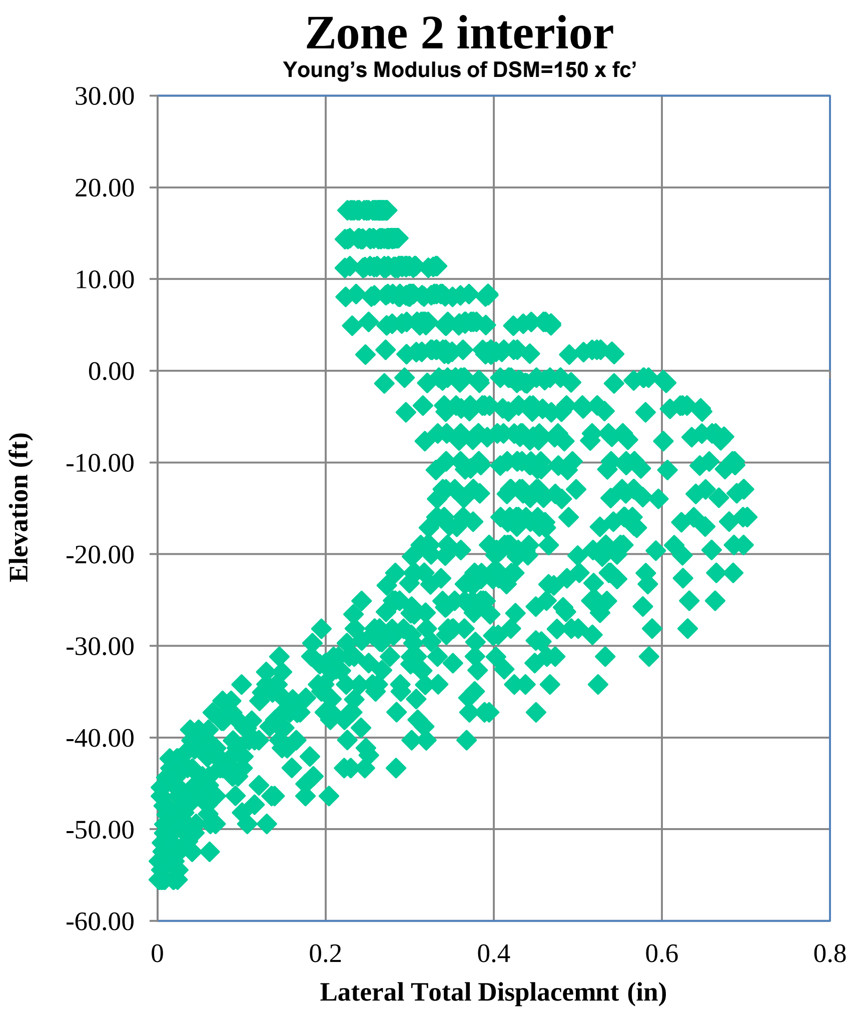

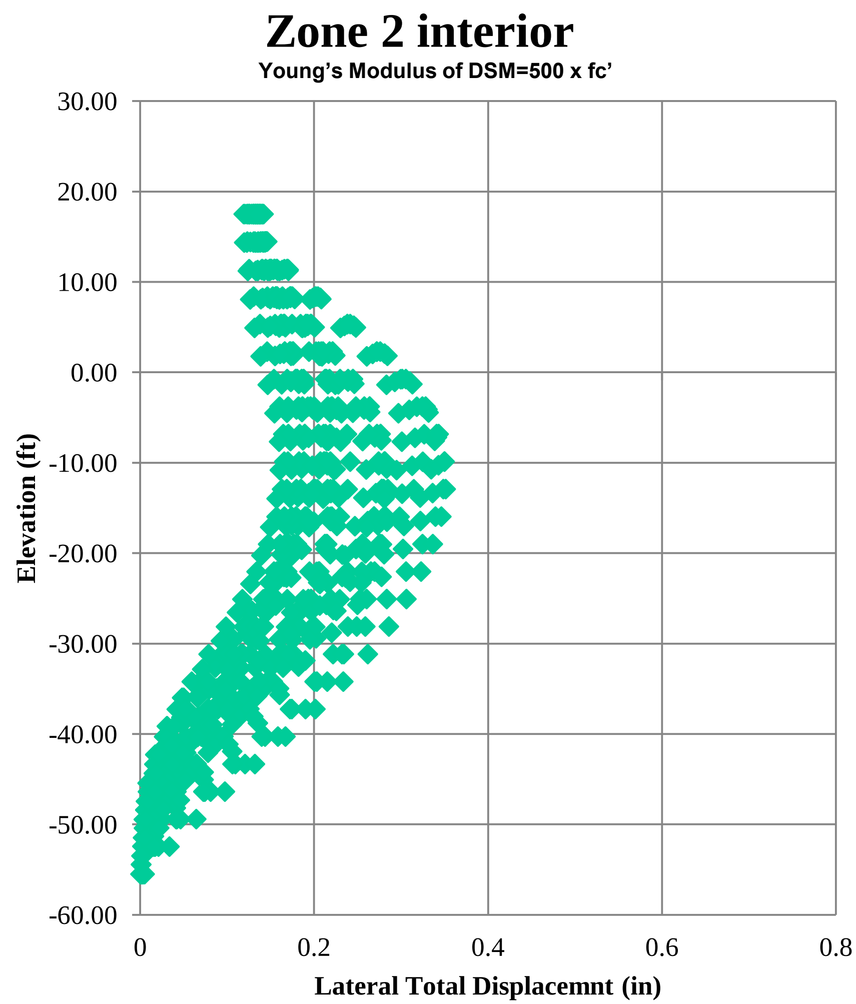

FLAC 3D Model – South Approach (Zone 2 Interior)
DSM Lateral Displacement (Liquefied Conditions)

Airport Way South Viaduct over ARGO Railroad Yard project
Seattle, Washington

GEOENGINEERS

Figure 52

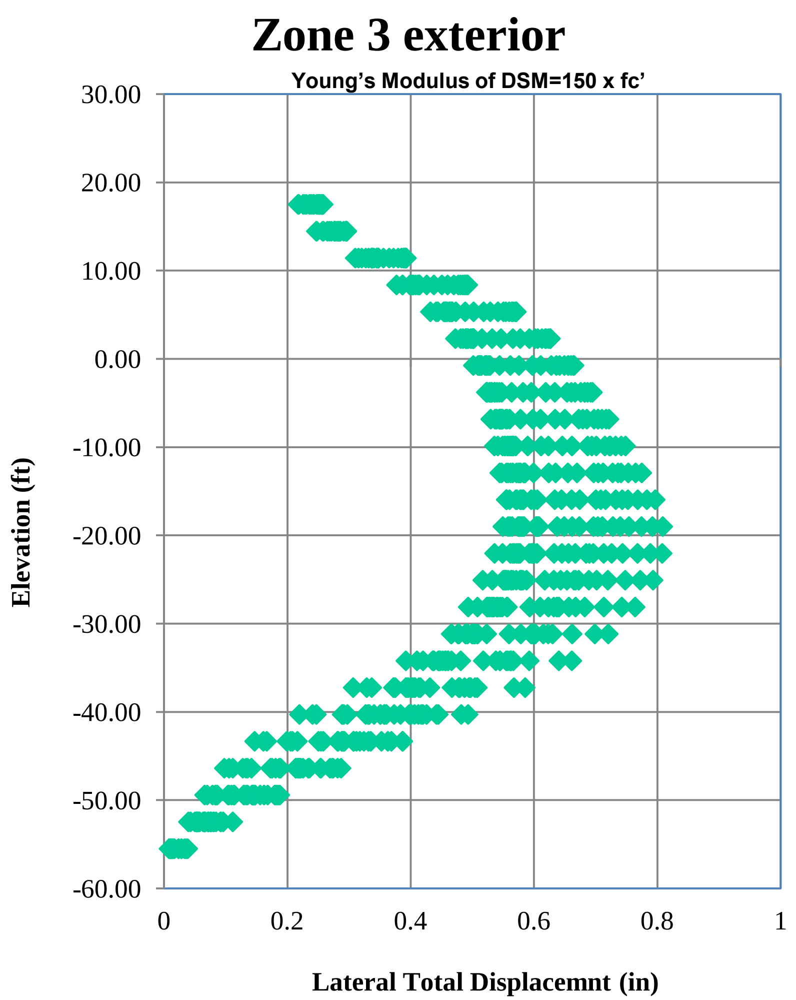

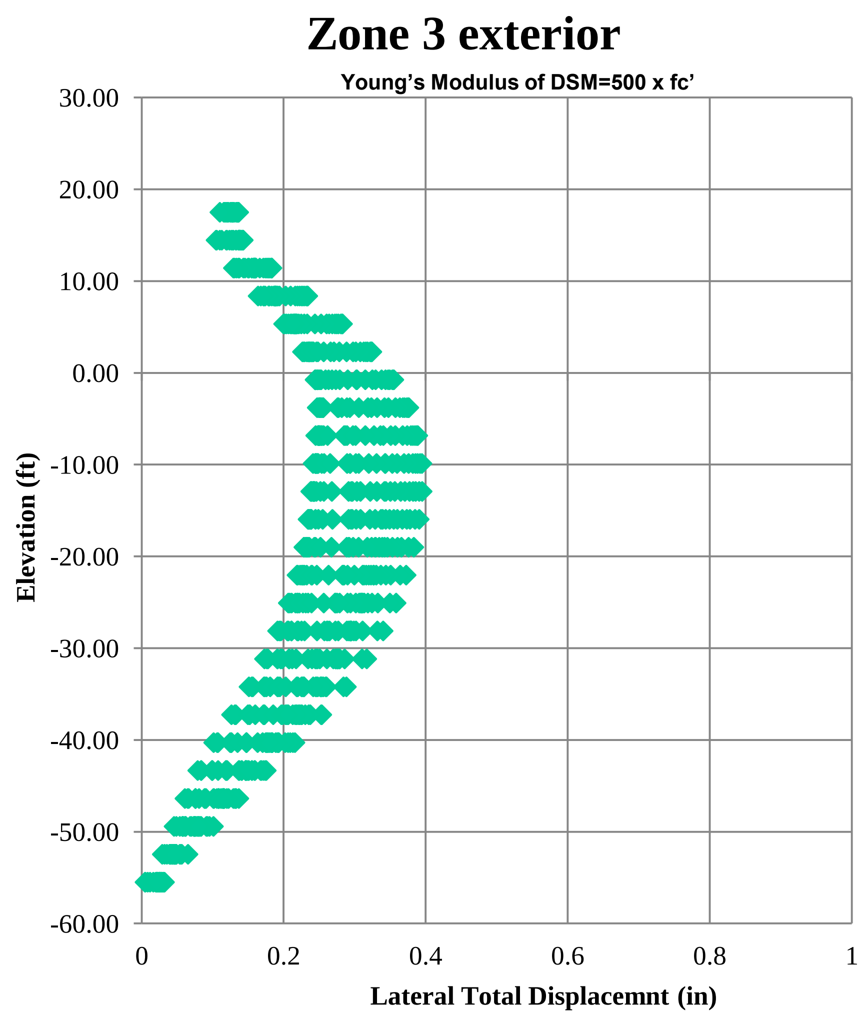

FLAC 3D Model – South Approach (Zone 3 Exterior)
DSM Lateral Displacement (Liquefied Conditions)

Airport Way South Viaduct over ARGO Railroad Yard project
Seattle, Washington

GeoEngineers

Figure 53

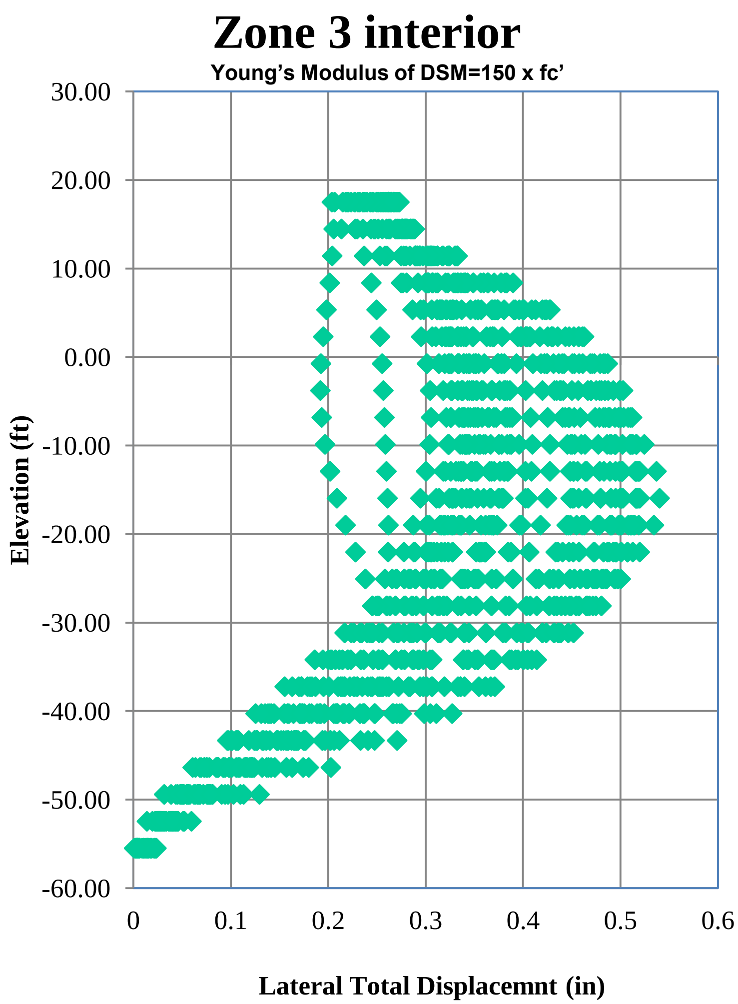

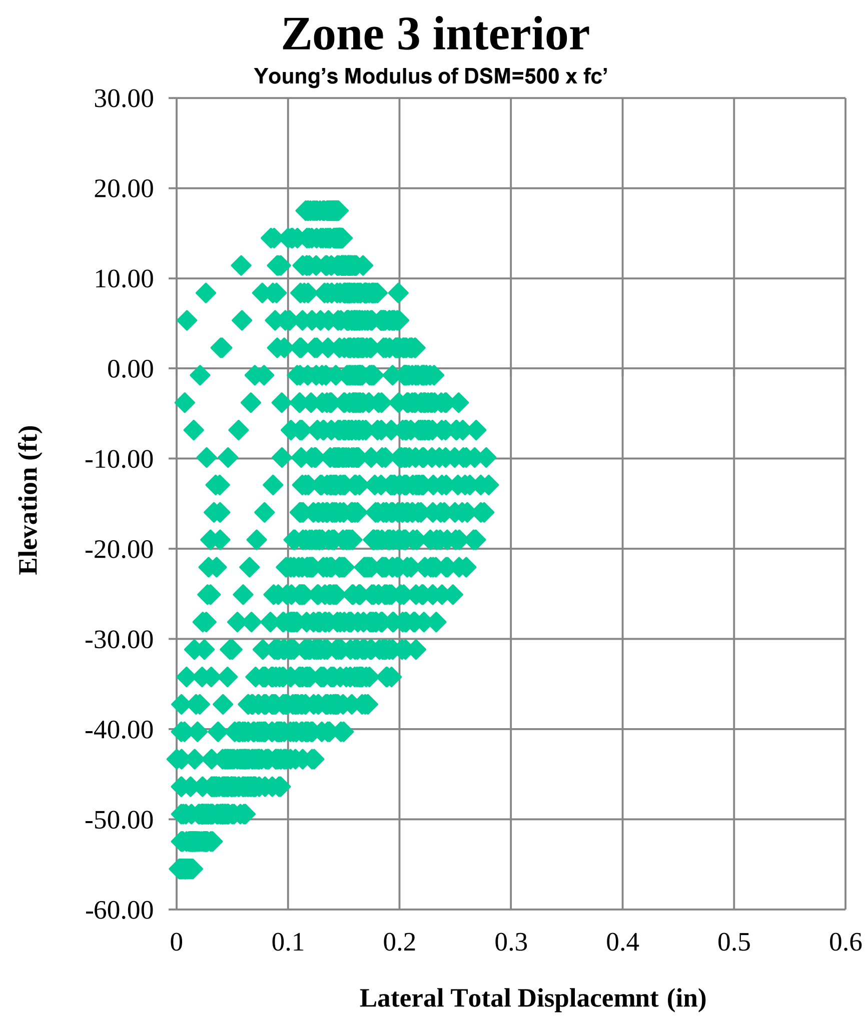

FLAC 3D Model – South Approach (Zone 3 Interior)
DSM Lateral Displacement (Liquefied Conditions)

Airport Way South Viaduct over ARGO Railroad Yard project
Seattle, Washington

GeoEngineers

Figure 54

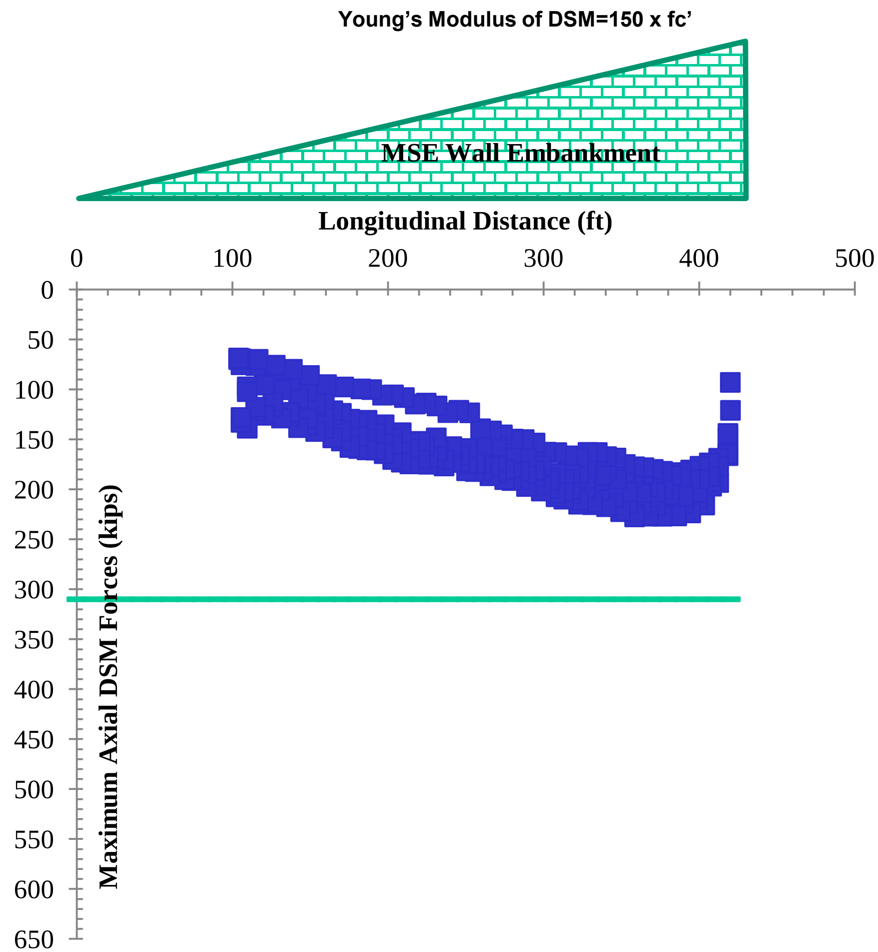

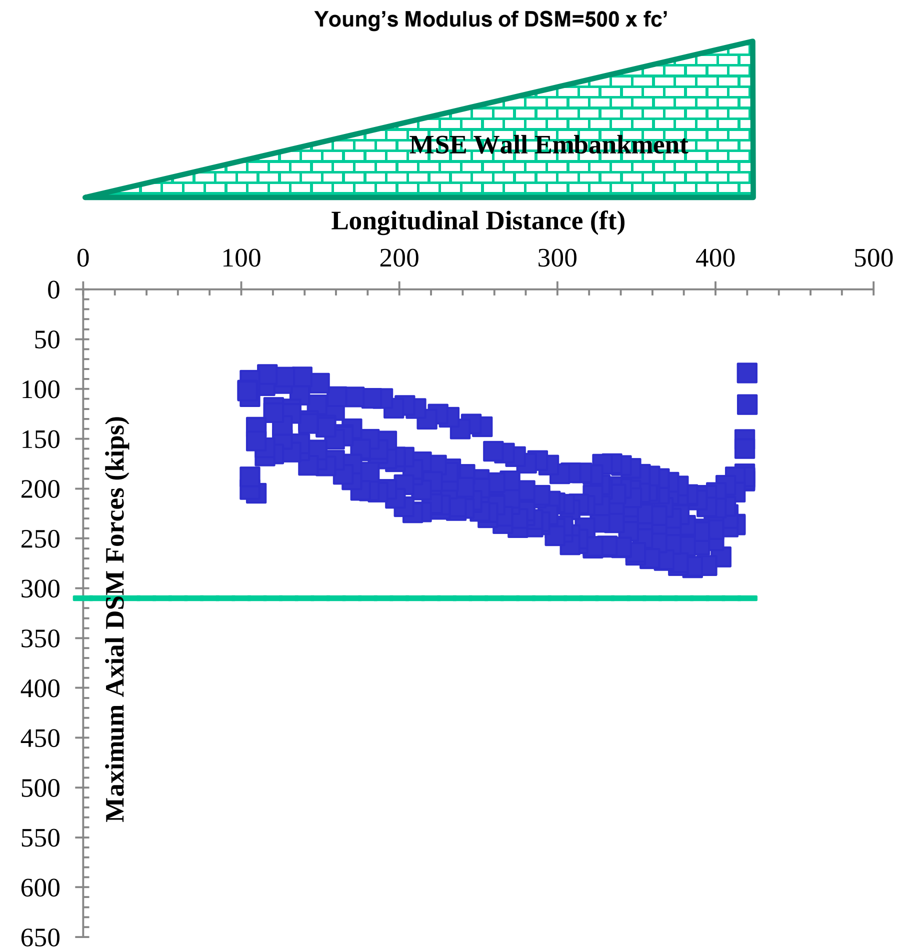

FLAC 3D Model – South Approach
DSM Maximum Axial Forces (Liquefied Conditions)

Airport Way South Viaduct over ARGO Railroad Yard project
Seattle, Washington

GEOENGINEERS

Figure 55

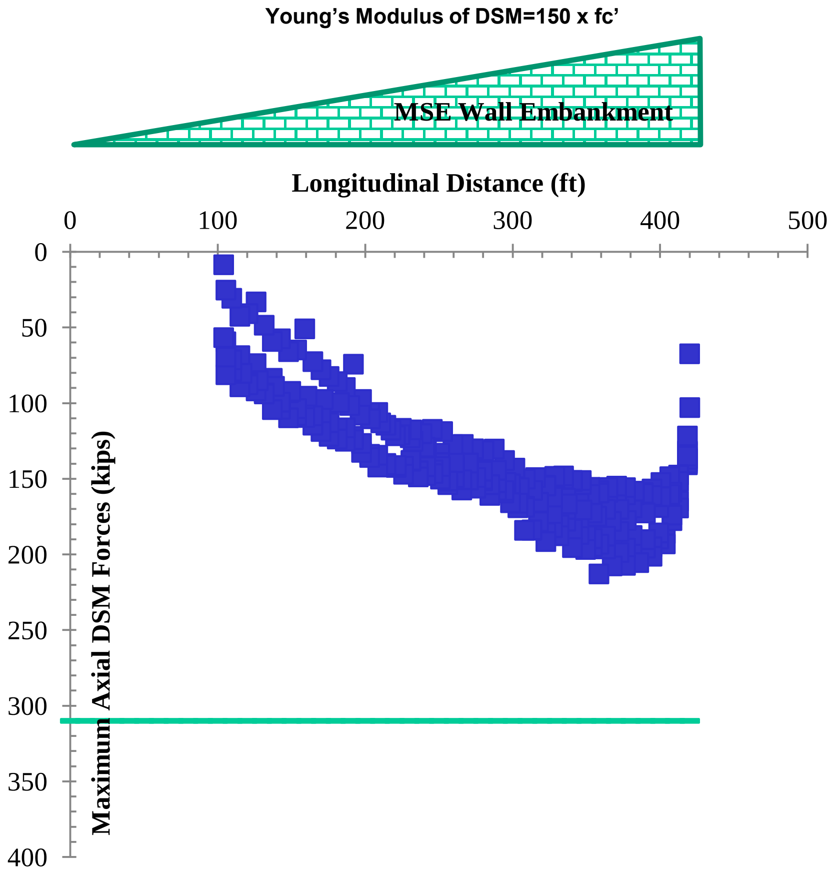

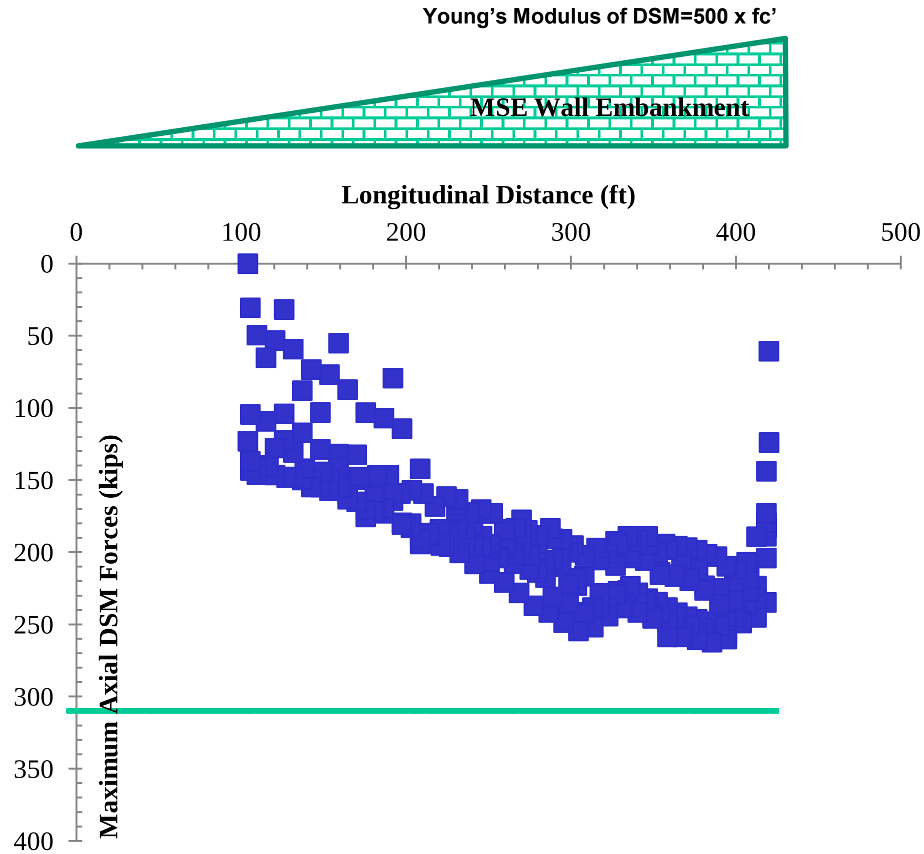

FLAC 3D Model – South Approach
DSM Maximum Axial Forces (Pseudo-static Conditions)
0.23g – ½ of design PGA

Airport Way South Viaduct over ARGO Railroad Yard project
Seattle, Washington

GeoEngineers

Figure 56

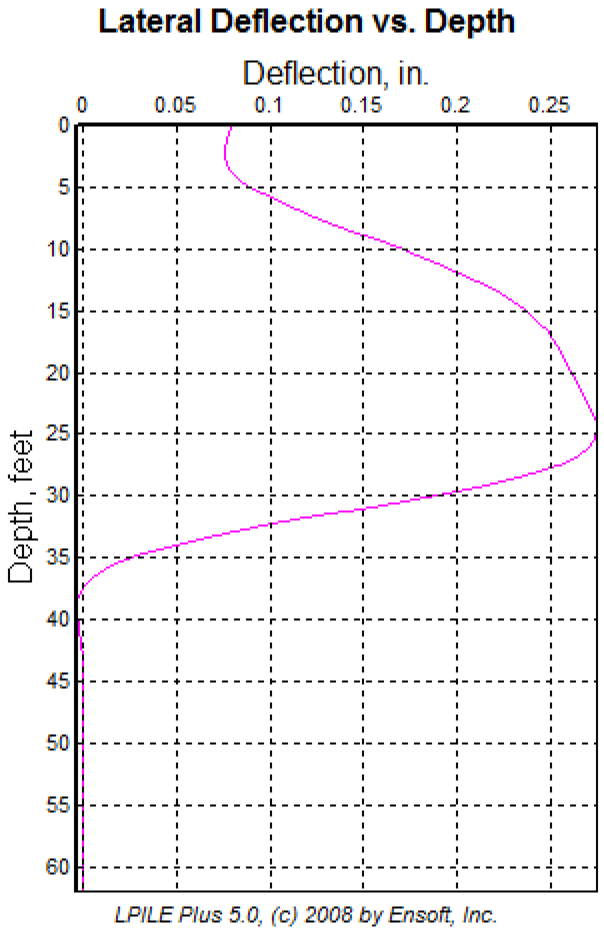

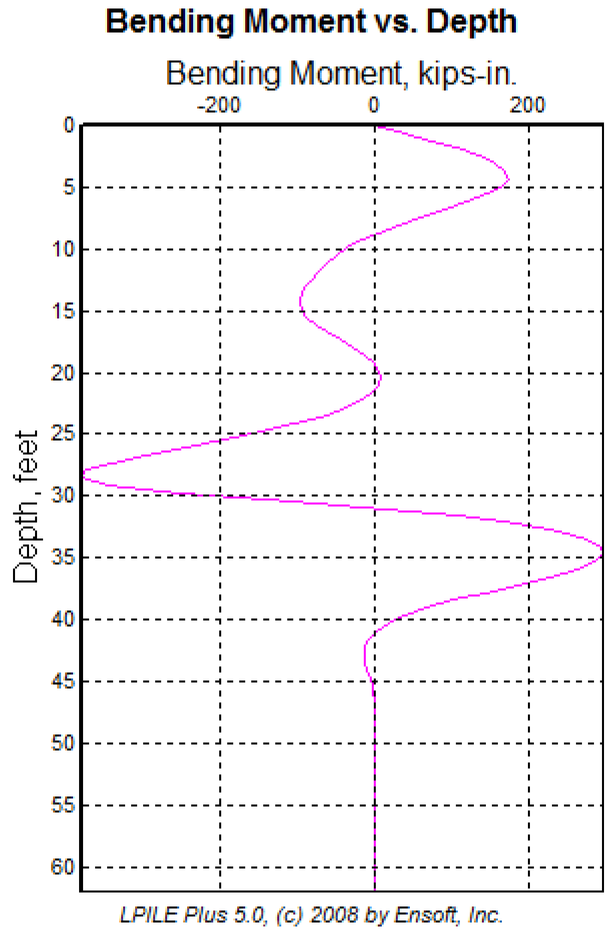

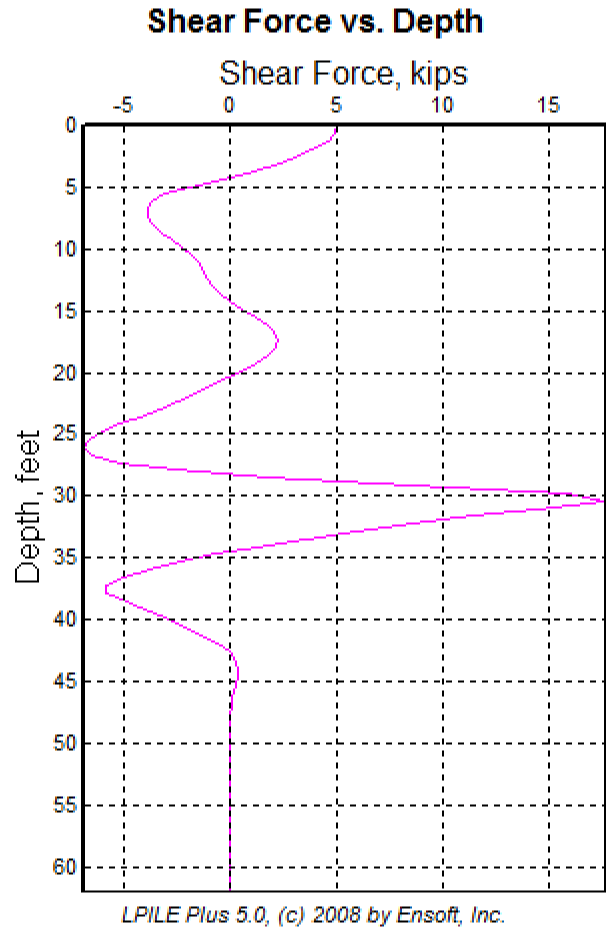

LPILE Analysis – South Approach
DSM Column Shear and Moment (Static Conditions)

Airport Way South Viaduct over ARGO Railroad Yard project
Seattle, Washington

GEOENGINEERS

Figure 57

http://projects/sites/0012914101/Draft\0129-141-01_DSM_Design_Figures.ppt WBH:hpd:khc:sds 07/5/2012

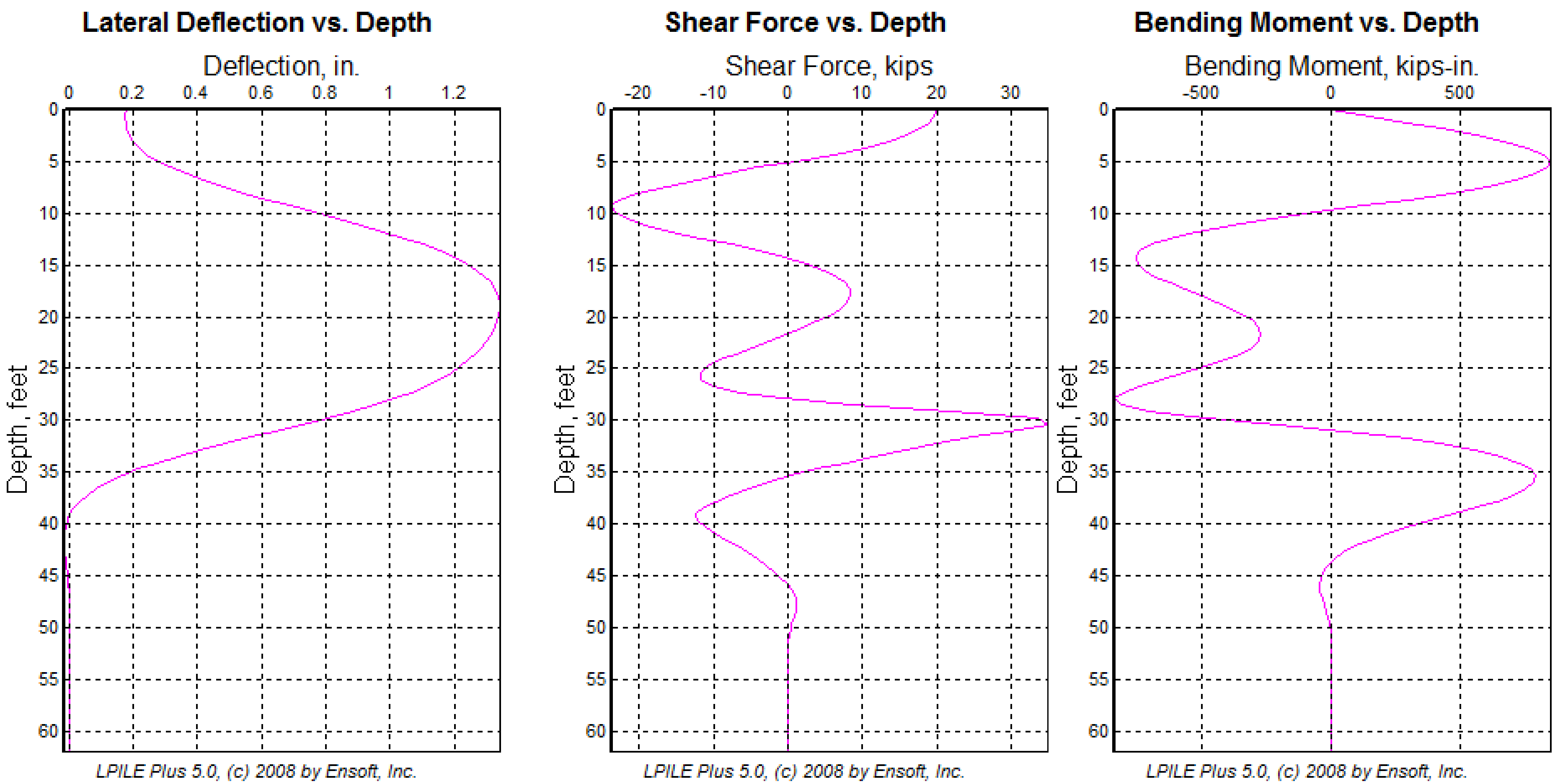

LPILE Analysis – South Approach
DSM Column Shear and Moment (Pseudo-static Conditions)
0.23g – ½ of design PGA

Airport Way South Viaduct over ARGO Railroad Yard project
Seattle, Washington

GeoEngineers

Figure 58

APPENDICES

APPENDIX A
Deep Soil Mixing Columns Design Criteria

APPENDIX A
DEEP SOIL MIXING COLUMNS DESIGN CRITERIA

1.0 Design Manuals and Guidelines

1.1 AASHTO Guide Specifications for LRFD Seismic Bridge Design, 2009

1.2 AASHTO LRFD Bridge Design Specifications, 4th Edition, with interims through 2009

1.3 Washington State Department of Transportation Geotechnical Design Manual, M 46-03.07, 2006

1.4 Federal Highway Administration, Ground Improvement Technical Summaries, FHWA Manual No. FHWA-SA-98-086, 1998

1.5 An Introduction to the Deep Soil Mixing Methods as Used in Geotechnical Applications, FHWA Technical Report No. FHWA-RD-99-138, 1999

2.0 Factor of Safety and Performance Criteria

2.1 Static conditions:

- 2.1.1 Approach embankment global stability factor of safety > 1.5 per AASHTO
- 2.1.2 Post-construction settlement of the approach embankment < 1 inch (design life = 75 years)
- 2.1.3 Load transfer slab:
  - 2.1.3.1 LRFD Design Specifications per AASHTO
- 2.1.4 DSM columns:
  - 2.1.4.1 Unconfined compressive strength factor of safety > 3.0
  - 2.1.4.2 Soil end bearing capacity factor of safety > 3.0

2.2 Seismic conditions:

- 2.2.1 Approach embankment global stability factor of safety > 1.1 with seismic coefficient = ½ PGA (peak ground acceleration) with non-liquefied soil conditions per AASHTO
- 2.2.2 Post earthquake global stability factor of safety > 1.1 with liquefied soil conditions
- 2.2.3 Post-earthquake settlement of the approach embankment < 1 inch
- 2.2.4 Load transfer slab:
  - 2.2.4.1 Plastic moment and cracked modulus will be used in the design analysis based on AASHTO
- 2.2.5 DSM columns:
  - 2.2.5.1 Unconfined compressive strength factor of safety > 2.0
  - 2.2.5.2 Soil end bearing capacity factor of safety > 2.0

3.0 Design Loading Conditions:

3.1 Static conditions:

- 3.1.1 Weight of the embankment, unit weight = 125 pcf
- 3.1.2 Traffic/temporary construction surcharge = 250 psf
- 3.1.3 Weight of load transfer slab, unit weight = 150 pcf
- 3.1.4 Weight of gravel layer, unit weight = 125 pcf

3.2 Seismic conditions:
- 3.2.1 AASHTO design earthquake (7 percent probability of exceedance in 75 years, 1,000-year return period)
- 3.2.2 Design PGA = 0.45g, earthquake magnitude = 6.8 per S&W GT Report
- 3.2.3 Live load will not be included in the design based on low ADT on the roadway

3.3 Post earthquake conditions:
- 3.3.1 Weight of the embankment, unit weight = 125 pcf

4.0 QA/QC Items to Check During design

4.1 DSM columns:
- 4.1.1 Column shear capacity
- 4.1.2 Column buckling
- 4.1.3 Downdrag force induced by soil liquefaction
- 4.1.4 Settlement
- 4.1.5 Load distribution to transfer slab for varying top of column elevation
- 4.1.6 Check on temporary construction surcharge

4.2 Transfer slab:
- 4.2.1 Beam shear
- 4.2.2 Punching shear
- 4.2.3 Bending
- 4.2.4 Deflection tolerance
- 4.2.5 Load distribution variances for varying top of DSM column elevation
- 4.2.6 Check on temporary construction surcharge

APPENDIX B
Report Limitations and Guidelines for Use

APPENDIX B
REPORT LIMITATIONS AND GUIDELINES FOR USE[1]

This appendix provides information to help you manage your risks with respect to the use of this report.

Geotechnical Services Are Performed for Specific Purposes, Persons and Projects

This final report has been prepared for the exclusive use of the City of Seattle Department of Transportation, HNTB, and their authorized agents. This report is not intended for use by others, and the information contained herein is not applicable to other sites.

GeoEngineers structures our services to meet the specific needs of our clients. For example, a geotechnical or geologic study conducted for a civil engineer or architect may not fulfill the needs of a construction contractor or even another civil engineer or architect that are involved in the same project. Because each geotechnical or geologic study is unique, each geotechnical engineering or geologic report is unique, prepared solely for the specific client and project site. Our report is prepared for the exclusive use of our Client. No other party may rely on the product of our services unless we agree in advance to such reliance in writing. This is to provide our firm with reasonable protection against open-ended liability claims by third parties with whom there would otherwise be no contractual limits to their actions. Within the limitations of scope, schedule and budget, our services have been executed in accordance with our Agreement with the Client and generally accepted geotechnical practices in this area at the time this report was prepared. This report should not be applied for any purpose or project except the one originally contemplated.

A Geotechnical Engineering or Geologic Report Is Based on a Unique Set of Project-Specific Factors

This final report has been prepared for the Airport Way South Viaduct over ARGO Railroad Yard project. GeoEngineers considered a number of unique, project-specific factors when establishing the scope of services for this project and report. Unless GeoEngineers specifically indicates otherwise, do not rely on this report if it was:

- not prepared for you,
- not prepared for your project,
- not prepared for the specific site explored, or
- completed before important project changes were made.

[1] Developed based on material provided by ASFE, Professional Firms Practicing in the Geosciences; www.asfe.org .

For example, changes that can affect the applicability of this report include those that affect:

- the function of the proposed structure;
- elevation, configuration, location, orientation or weight of the proposed structure;
- composition of the design team; or
- project ownership.

If important changes are made after the date of this report, GeoEngineers should be given the opportunity to review our interpretations and recommendations and provide written modifications or confirmation, as appropriate.

Subsurface Conditions Can Change

This geotechnical or geologic report is based on conditions that existed at the time the study was performed. The findings and conclusions of this report may be affected by the passage of time, by manmade events such as construction on or adjacent to the site, or by natural events such as floods, earthquakes, slope instability or groundwater fluctuations. Always contact GeoEngineers before applying a report to determine if it remains applicable.

Most Geotechnical and Geologic Findings Are Professional Opinions

Our interpretations of subsurface conditions are based on field observations from widely spaced sampling locations at the site. Site exploration identifies subsurface conditions only at those points where subsurface tests are conducted or samples are taken. GeoEngineers reviewed field and laboratory data and then applied our professional judgment to render an opinion about subsurface conditions throughout the site. Actual subsurface conditions may differ, sometimes significantly, from those indicated in this report. Our report, conclusions and interpretations should not be construed as a warranty of the subsurface conditions.

Geotechnical Engineering Report Recommendations Are Not Final

Do not over-rely on the preliminary construction recommendations included in this report. These recommendations are not final, because they were developed principally from GeoEngineers' professional judgment and opinion. GeoEngineers' recommendations can be finalized only by observing actual subsurface conditions revealed during construction. GeoEngineers cannot assume responsibility or liability for this report's recommendations if we do not perform construction observation.

Sufficient monitoring, testing and consultation by GeoEngineers should be provided during construction to confirm that the conditions encountered are consistent with those indicated by the explorations, to provide recommendations for design changes should the conditions revealed during the work differ from those anticipated, and to evaluate whether or not earthwork activities are completed in accordance with our recommendations. Retaining GeoEngineers for construction observation for this project is the most effective method of managing the risks associated with unanticipated conditions.

A Geotechnical Engineering or Geologic Report Could Be Subject To Misinterpretation

Misinterpretation of this report by other design team members can result in costly problems. You could lower that risk by having GeoEngineers confer with appropriate members of the design team after submitting the report. Also retain GeoEngineers to review pertinent elements of the design team's plans and specifications. Contractors can also misinterpret a geotechnical engineering or geologic report. Reduce that risk by having GeoEngineers participate in pre-bid and preconstruction conferences, and by providing construction observation.

Do Not Redraw the Exploration Logs

Geotechnical engineers and geologists prepare final boring and testing logs based upon their interpretation of field logs and laboratory data. To prevent errors or omissions, the logs included in a geotechnical engineering or geologic report should never be redrawn for inclusion in architectural or other design drawings. Only photographic or electronic reproduction is acceptable, but recognize that separating logs from the report can elevate risk.

Give Contractors a Complete Report and Guidance

Some owners and design professionals believe they can make contractors liable for unanticipated subsurface conditions by limiting what they provide for bid preparation. To help prevent costly problems, give contractors the complete geotechnical engineering or geologic report, but preface it with a clearly written letter of transmittal. In that letter, advise contractors that the report was not prepared for purposes of bid development and that the report's accuracy is limited; encourage them to confer with GeoEngineers and/or to conduct additional study to obtain the specific types of information they need or prefer. A pre-bid conference can also be valuable. Be sure contractors have sufficient time to perform additional study. Only then might an owner be in a position to give contractors the best information available, while requiring them to at least share the financial responsibilities stemming from unanticipated conditions. Further, a contingency for unanticipated conditions should be included in your project budget and schedule.

Contractors Are Responsible for Site Safety on Their Own Construction Projects

Our geotechnical recommendations are not intended to direct the contractor’s procedures, methods, schedule or management of the work site. The contractor is solely responsible for job site safety and for managing construction operations to minimize risks to on-site personnel and to adjacent properties.

Read These Provisions Closely

Some clients, design professionals and contractors may not recognize that the geoscience practices (geotechnical engineering or geology) are far less exact than other engineering and natural science disciplines. This lack of understanding can create unrealistic expectations that could lead to disappointments, claims and disputes. GeoEngineers includes these explanatory “limitations” provisions in our reports to help reduce such risks. Please confer with GeoEngineers if you are unclear how these “Report Limitations and Guidelines for Use” apply to your project or site.

Geotechnical, Geologic and Environmental Reports Should Not Be Interchanged

The equipment, techniques and personnel used to perform an environmental study differ significantly from those used to perform a geotechnical or geologic study and vice versa. For that reason, a geotechnical engineering or geologic report does not usually relate any environmental findings, conclusions or recommendations; e.g., about the likelihood of encountering underground storage tanks or regulated contaminants. Similarly, environmental reports are not used to address geotechnical or geologic concerns regarding a specific project.

Biological Pollutants

GeoEngineers' Scope of Work specifically excludes the investigation, detection, prevention or assessment of the presence of Biological Pollutants. Accordingly, this report does not include any interpretations, recommendations, findings, or conclusions regarding the detecting, assessing, preventing or abating of Biological Pollutants and no conclusions or inferences should be drawn regarding Biological Pollutants, as they may relate to this project. The term "Biological Pollutants" includes, but is not limited to, molds, fungi, spores, bacteria, and viruses, and/or any of their byproducts.

If Client desires these specialized services, they should be obtained from a consultant who offers services in this specialized field.

Have we delivered World Class Client Service?

Please let us know by visiting **www. geoengineers.com/feedback**.

GeoEngineers